PTK7 signaling complexes in neural crest cell migration

Dissertation

zur Erlangung des

Doktorgrades der Naturwissenschaften (Dr. rer. nat.)

dem Fachbereich Biologie

der Philipps-Universität Marburg

vorgelegt von

Anita Grund

geboren in Hagenow

Marburg an der Lahn, August 2019

Vom Fachbereich Biologie der Philipps-Universität Marburg als Dissertation angenommen am: 29.10.2019

Erstgutachterin: Frau Prof. Dr. Annette Borchers
Zweitgutachter: Herr Prof. Dr. Ralf Jacob

Tag der mündlichen Prüfung am: 13.11.2019

List of publication

Maj, E., Künneke, L., Loresch, E., **Grund, A.**, Melchert, J., Pieler, T., Aspelmeier, T., Borchers, A. (2016). Controlled levels of canonical Wnt signaling are required for neural crest migration. Developmental Biology, 417:77-90.

Podleschny, M.*, **Grund, A.***, Berger, H., Rollwitz, E., Borchers, A. (2015). A PTK7/Ror2 Co-Receptor Complex Affects *Xenopus* Neural Crest Migration. Plos One, 10:e0145169.
* These authors contributed equally to this work.

Zusammenfassung

Zellmigration ist ein bedeutender Prozess während der Embryonal-Entwicklung und wird stark von äußeren Signalen, chemische als auch mechanische, reguliert. Neuralleistenzellen (NLZ) sind hoch migratorische Zellen, welche sich auf Grund ihrer Ähnlichkeiten zu Krebszellen hervorragend zur Analyse von Zellmigration eignen. NLZ werden an der Grenzregion der Neuralfalten induziert und migrieren entlang der anterioren-posterioren Achse durch den Embryo. Die NLZ besitzen die Fähigkeit mesenchymales und ektodermales Gewebe zu durchdringen, um jedoch nicht andere NLZ zu überlaufen, setzt der sogenannte Prozess der Kontaktinhibierung der Lokomotion ein (*contact inhibition of locomotion*, CIL). CIL beschreibt den Prozess, in dem aufeinandertreffende Zellen nach dem Zell-Zell-Kontakt ihre Migrationsrichtung ändern. Dabei spielt der nicht-kanonische Wnt Signalweg eine wichtige Rolle. Bei der Aktivierung des nicht-kanonischen Wnt Signalweges wird das cytoplasmatische Protein Dishevelled durch den Rezeptor Frizzled an die Membran rekrutiert. Dies führt zur Aktivierung von kleinen GTPasen und zur Reorganisation des Aktin-Zytoskeletts. Das Transmembranprotein PTK7 (*protein tyrosine kinase 7*) ist ein Aktivator des nicht-kanonischen Wnt Signalweges und in NLZ exprimiert. Diese Arbeit zeigt, dass in migrierenden NLZ PTK7, vermittelt über dessen extrazelluläre Domäne, an Zell-Zell-Kontakten akkumuliert. Ein Funktionsverlust von PTK7 in *Xenopus* führt zu einer Inhibierung der NLZ-migration. In dieser Arbeit konnte gezeigt werden, dass ein Funktionsverlust von PTK7 zu einer Veränderung der Zellmorphologie von NLZ und damit Inhibierung der NLZ-migration führt. Über den PTK7 Signalweg während der NLZ-migration ist nicht viel bekannt. Während dieser Arbeit konnte jedoch gezeigt werden, dass eine Überexpression von Dishevelled den Funktionsverlust von PTK7 während der NLZ-migration kompensiert. Außerdem konnte ein neuer Interaktionspartner identifiziert werden. Der Rho-Guaninnukleotid-Austauschfaktor Trio interagiert mit PTK7, zudem ko-lokalisiert Trio mit PTK7 in NLZ und eine Überexpression von Trio rettet den Funktionsverlust von PTK7 in der NLZ-migration. Zusammenfassend konnte diese Arbeit weiteren Aufschluss über den PTK7 Signalweg während der NLZ-migration geben.

Abstract

Cell migration is an important process during embryonic development and is strongly regulated by external signals, both chemical and mechanical. Neural crest (NC) cells are highly migratory cells, which are ideal for analyzing cell migration due to their high similarities to cancer cells. NC cells are induced at the border region of the neural folds and migrate along the anterior-posterior axis through the embryo. The NC cells have the ability to penetrate mesenchymal and ectodermal tissue but do not penetrate other NC cells, regulated by a process called contact inhibition of locomotion (CIL). CIL describes the process in which cells change their migration direction after contact with another cell. The non-canonical Wnt pathway is important for this process. Upon activation of the non-canonical Wnt pathway, the Frizzled receptor recruits the cytoplasmic protein Dishevelled to the membrane. This leads to activation of small GTPases and reorganization of the actin cytoskeleton. The transmembrane protein PTK7 (protein tyrosine kinase 7) is an activator of the non-canonical Wnt signaling pathway and expressed in NC cells. This study shows that in migrating NC cells PTK7, mediated by its extracellular domain, accumulates at cell-cell contact sites. A loss of function of PTK7 in *Xenopus* leads to an inhibition of NC cell migration. However, the role of PTK7 signaling during NC cell migration remains to be analyzed. During this study it has been shown that PTK7 loss of function leads to alteration of NC cell morphology and thereby inhibition of NC cell migration. This NC cell migration defects can be rescued by overexpression of Dishevelled. In addition, a new interaction partner was identified. The Rho guanine nucleotide exchanging factor Trio interacts with PTK7, co-localizes with PTK7 in NC cells and an overexpression of Trio rescues PTK7 loss of function defects in NC cell migration. In summary, this work has provided further insight into the PTK7 signaling pathway during NC cell migration.

Table of Contents

Abbreviations

APC	adenomatous polyposis coli
Arp	actin-related protein
BMP	bone morphogenetic protein
C3a	complement component factor 3a
cdc42	cell division control protein 42 homolog
CIL	contact inhibition of locomotion
CK1	casein kinase 1
Co-IP	co-immunoprecipitation
DEP	Dishevelled, Egl-10 and Pleckstrin
Dgo	Diego
DIX	Dishevelled-Axin
Dsh	Dishevelled
EMT	epithelial-to-mesenchymal transition
F-actin	filamentous actin
FGF	fibroblast growth factor
Fmi	Flamingo
Fz	Frizzled
G-actin	globular actin
GAP	GTPase activating factor
GEF	Rho guanine nucleotide exchanging factor
GR	Glucocorticoid-receptor
GSK3	glycogen synthase kinase 3
Ig	immunoglobulin domain
kDA	kilo Dalton
LEF	lymphoid-enhancing factor
LIM	Lin11, Isl-1, Mec-3
LIMK	LIM Kinase
LRP	low-density lipoprotein receptor-related protein
mDia	mouse Diaphanous related formin
MO	Morpholino oligonucleotides
NC	neural crest
Par3	partition defective 3 homologue
PAK	p21-activated kinase 3
PCP	planar cell polarity
PDZ	Post synaptic density protein, Disc large tumor suppressor, Zonula occludens-1 protein

Pk	Prickle
PKCδ1	Protein Kinase C Delta 1
PTK7	protein tyrosine kinase 7
Rac1	Ras-related C3 botulinum toxin substrate 1
RACK1	Receptor of Activated protein Kinase C 1
Rho GDI	Rho guanine nucleotide dissociation inhibitor
RhoA	Ras homolog gene family, member A
ROCK	Rho-associated kinase
Ror2	receptor tyrosine kinase like orphan receptor 2
Sdf1	stromal cell-derived factor 1
s.e.m.	standard error of the mean/median
TCF	T-cell factor
Vangl	VanGogh-like
WASP	Wiskott-Aldrich syndrome protein
WAVE	WASP-family verprolin-homologous protein
Wnt	Wingless/Integrated

1. Introduction

Cell migration and cell communication play a crucial role during embryonic development and in adult organisms. Tissue formation during morphogenesis, tissue homeostasis, wound repair and immune responses all require migration of cells in response to external signals (Friedl and Gilmour, 2009). Defective cell behavior can lead to various diseases like an open neural tube (craniorachischisis) and cancer (Kuriyama and Mayor, 2008; Nikolopoulou et al., 2017). Neural crest (NC) cells are a highly migratory pluripotent cell population that behave in a similar way to invasive tumor cells and are ideal for analyzing cell migration (Kuriyama and Mayor, 2008; Mayor and Theveneau, 2013; Szabó and Mayor, 2018). NC cells can differentiate into a variety of cell types including neurons, skeletal and connective tissues, smooth muscle cells and pigment cells (reviewed in (Dupin et al., 2006; Etchevers et al., 2019; Minoux and Rijli, 2010; Shyamala et al., 2015)). Due to the possibility to differentiate into a variety of different cell types, the NC is proposed to be referred to as the fourth germ layer (Hall, 2000; Shyamala et al., 2015). Defects in NC cell migration cause so called neurocristopathies. Craniofacial and cardiac defects as well as mental retardation and pigmentation defects are frequent in neurocristopathies (reviewed in (Etchevers et al., 2019)).

1.1 Neural crest induction and delamination

NC cells are induced at the border region of the neural folds between the neuroepithelium and the ectoderm along the anterior-posterior axis of the embryo. A combination of BMP (bone morphogenetic protein), Notch, FGF (fibroblast growth factor) and Wnt signaling in the neural plate, surrounding epidermis and underlying mesoderm leads to the activation of a genetic cascade in the neural folds which induces NC cells (reviewed in (Groves and LaBonne, 2014; Milet and Monsoro-Burq, 2012; Pla and Monsoro-Burq, 2018; Prasad et al., 2019; Sauka-Spengler and Bronner-Fraser, 2008)). After induction, NC cells delaminate from the neuroepithelium and migrate in distinct streams within the embryo. Based on their location in the embryo, NC cells are categorized into cranial/cephalic, cardiac, vagal, sacral and trunk NC cells (Aybar and Mayor, 2002). In the following, only the migration of cranial NC cells will be described.

In *Xenopus*, delamination of NC cells occurs prior to neural tube closure and epithelial-to-mesenchymal transition (EMT) commences before neural tube closure. Here, EMT is suggested as partial EMT because EMT is not completed after the onset of migration (fig. 1) (reviewed in (Alfandari et al., 2010; Taneyhill and Schiffmacher, 2017; Theveneau et al., 2010)). During EMT, the NC cells are decreasing their cell adhesion, lose their apical-basal polarity, undergo cytoskeletal rearrangement and gain migratory properties (fig. 1 B). An important step during EMT in *Xenopus* is a switch from E- to N-Cadherin

(Scarpa et al., 2015). There is not a complete Cadherin exchange since E-Cadherin transcripts are still present in migrating NC cells (Huang et al., 2016). Moreover, the extracellular domain of E-Cadherin seems to be necessary for proper NC cell migration.

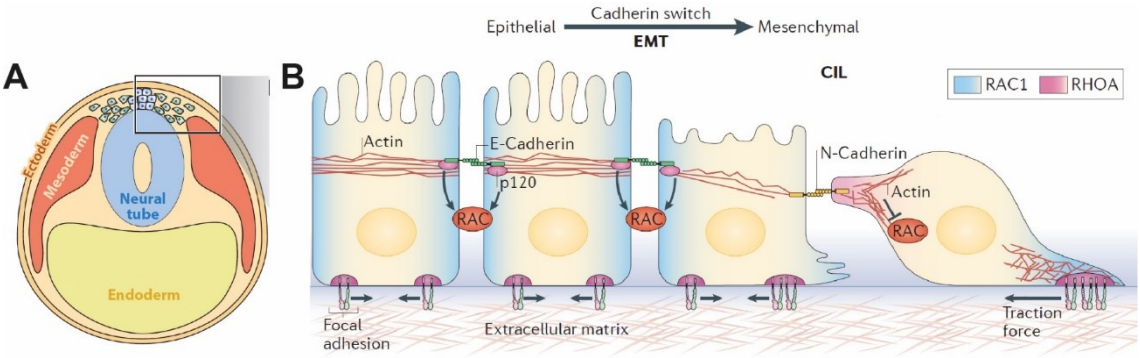

Fig. 1: Cellular changes during NC delamination. A Schematic section through a *Xenopus* embryo during NC delamination (modified after (Szabó and Mayor, 2018)). **B** Cadherin switching in the regulation of EMT and contact inhibition of locomotion (CIL). Switch from E-Cadherin to N-Cadherin allows NC cells to undergo EMT while gaining a capacity for CIL. E-Cadherin suppresses EMT by, among others, p120 catenin which polarizes Rac1 to cell-cell junctions. N-Cadherin promotes Rac1 activity towards the leading edge of cells allowing asymmetric traction stresses for directed migration away from neighboring cells (Stramer and Mayor, 2017).

Recent findings indicate that EMT of NC cells is initiated by the stiffness of the underlying mesoderm (Barriga et al., 2018). NC cells detect the stiffness of the mesoderm caused by the convergent extension movement during gastrulation. The increasing stiffness of the mesoderm leads to EMT of the NC cells and triggers their migration (Barriga et al., 2018). This shows that not only molecular but also mechanical interactions between the NC cells and their environment are essential for NC cell migration.

1.2 Keeping NC cells on track

For collective NC cell migration, cell communication between NC cells and the surrounding tissues is necessary (fig. 2). While chemoattractions and –repellents keep NC cells in distinct streams, contact inhibition of locomotion (CIL), where cells change the direction of migration after contact with another cell (Abercrombie, 1979), and NC co-attraction promote the dispersion of NC cells but at the same time prevent the complete dispersion of single NC cells (reviewed in (Shellard and Mayor, 2019; Szabó and Mayor, 2018)).

The best investigated chemoattractant is the chemokine Sdf1 (stromal cell-derived factor 1) secreted by placodal cells (fig. 2 C), which binds to Cxcr4 expressed by the NC cells (Theveneau et al., 2010). Sdf1/Cxcr4 signaling in NC cells increases the activity of the small GTPase Rac1 which stabilizes cell protrusions and promotes migration (Ridley et

al., 2003; Shellard et al., 2018; Theveneau et al., 2010). However, in order to respond well to the Sdf1 source NC cells have to be in contact with other NC cells. It has been shown that single cells respond in a less directional manner than a group of NC cells (Theveneau et al., 2010).

In order to delimit the migration routes of the NC cells, a set of negative regulators need to be expressed in the prospective NC-free area. Two classes of molecules have been identified as negative guidance cues: ephrins and their corresponding Eph receptor as well as class3-semaphorins and their neuropilin/plexin receptors (Kuriyama and Mayor, 2008; Theveneau and Mayor, 2012a; Theveneau and Mayor, 2012b). These molecules induce the collapse of cell protrusions of the NC cells by inhibiting Rac1 so that the NC cells do not migrate towards this area (Bajanca et al., 2019; Gammill et al., 2007; Koestner et al., 2008). Interestingly, the effect of semaphorins is temporal and at later stages Sdf1 drives NC entry into semaphorin-positive tissue (Bajanca et al., 2019; Gammill et al., 2007).

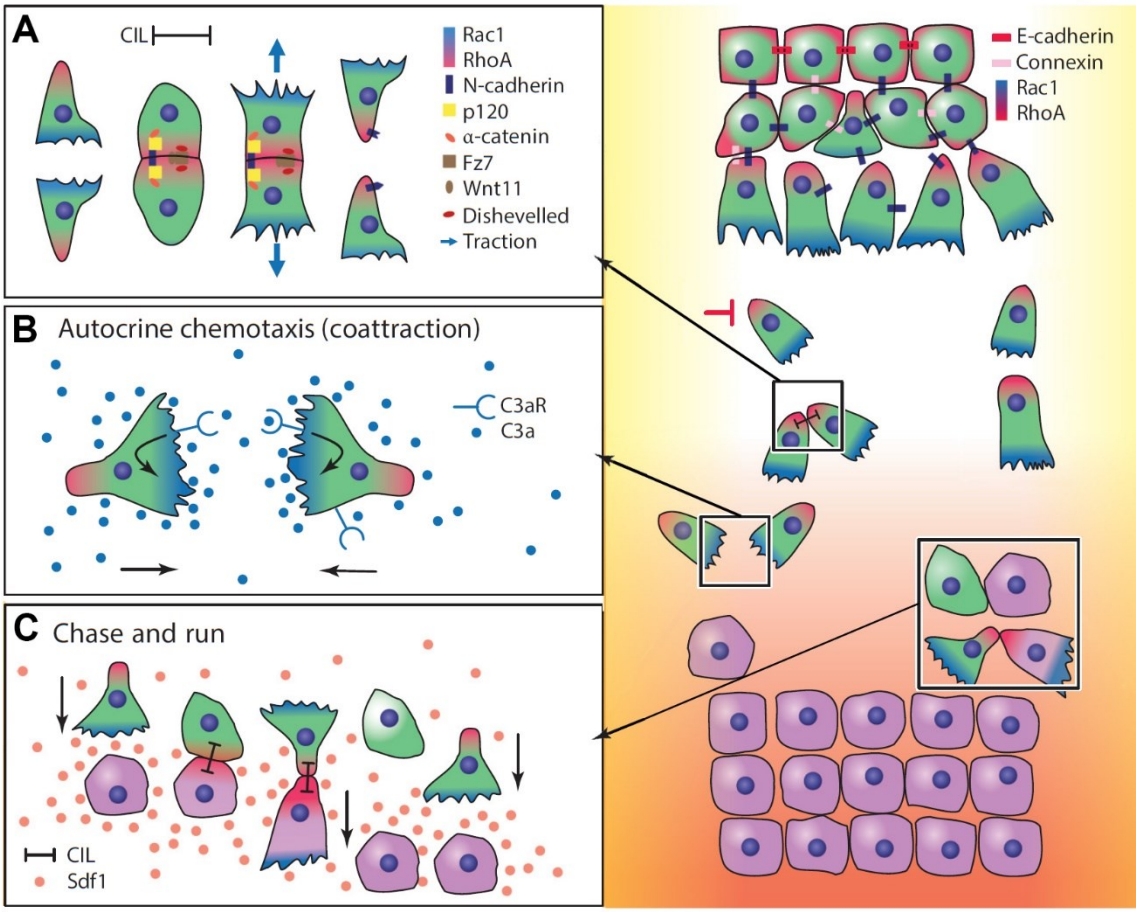

Fig. 2: Control of collective NC cell migration. A Contact inhibition of locomotion (CIL) polarizes colliding cells. **B** Autocrine chemotaxis helps maintain collectiveness. **C** The chase-and-run mechanism between NC cells and placodes directs NC migration and coordinates the migration between NC cells and placodes. Across the panels, colors differentiate the Rac1 (blue) and RhoA (red) activity of NC cells (green) and placodal cells (magenta) (modified after (Szabó and Mayor, 2018)).

As already mentioned, a NC cell responds better to a Sdf1 source when it is in contact with other NC cells, indicating a collective migration behavior of NC cells. Indeed, NC cells secret the chemokine C3a (complement component factor 3a), and express its receptor C3aR at the same time, to prevent the complete dispersion of single cells (fig. 2 B) (Carmona-Fontaine et al., 2011). C3a/C3aR signaling activates Rac1 which stabilizes cell protrusions so that the dispersed NC cell migrates back to the cell group, which has a higher concentration of C3a.

If a NC cell than gets in contact with another NC cell, NC cells undergo CIL (fig. 2 A) (Carmona-Fontaine et al., 2008b). The process of CIL prevents NC cells from invading each other without losing the ability to penetrate mesenchymal and ectodermal cells and also promote the dispersion of the NC cells. Four main steps occur during CIL: 1. cell-cell contact, 2. inhibition of cell protrusion at the site of contact, 3. contraction of protrusion at cell contact and generation of new protrusion, 4. migration away from collision. Repolarization and cell separation may not occur in all cases after collision. It is furthermore affected by the geometry of the collision for example lamellae-to-lamellae versus lamellae-to-rear (Desai et al., 2013; Stramer and Mayor, 2017).

Taken together, NC cells migrate towards the chemoattractant Sdf1, the area in which the cells migrate is determined by negative guidance guess in the NC-free areas, dispersion of the cells is promoted by CIL but to prevent complete cell dispersion, NC cells secrete the chemokine C3a and its receptor C3aR.

1.3 PCP signaling leads to cell polarization

In order for CIL to take place, the non-canonical Wnt pathway has to be activated at cell-cell contact sites (Carmona-Fontaine et al., 2008b). The non-canonical or β-catenin-independent Wnt pathway is also known as the PCP (planar cell polarity) signaling pathway. PCP describes the coordinated orientation of cells and cellular structures within the plane of an epithelium. PCP has been first described in *Drosophila* where it could be shown that the planar polarization of epithelial cells is necessary for the orientation of wing hairs (reviewed in (Klein and Mlodzik, 2005)). The planar polarization plays an equally important role in tissue polarity and cell movements in vertebrates (Guo et al., 2004; Heisenberg et al., 2000; Jessen et al., 2002; Mitchell et al., 2009; Wallingford et al., 2000). Loss of function of core PCP proteins can lead to defects in convergent extension movement, neural tube closure and disoriented inner ear hair cells (see review (Wallingford, 2012)). The core PCP proteins are the transmembrane proteins Frizzled (Fz), VanGogh-like (Vangl) and Flamingo (Fmi) and the cytoplasmic proteins Dishevelled (Dsh), Prickle (Pk) and Diego (Dgo) (reviewed in (Yang and Mlodzik, 2015)). Further studies show that Fz, Dsh and Dgo are localized together at one side of a cell while Vangl

and Pk are localized at the opposite sides (fig. 3 A). Fmi is localized at both sides. The cell polarization is established due to the interaction of the protein complexes in the cell as well as across the cell membrane. Fmi interacts with Fz and Vangl and is able to form homodimers across the cell (Chen et al., 2008; Usui et al., 1999). In presence of Fmi, Fz and Vangl are capable to recruit each other to the cell membrane (fig. 3 A) (Chen et al., 2008; Wu and Mlodzik, 2008). There is a contradictory view of how this mutual recruitment takes place (see review (Peng and Axelrod, 2012)). However, stabilization of PCP complexes across the membrane by Fmi is important to propagate PCP from cell to cell (Struhl et al., 2012; Strutt, 2001; Strutt and Strutt, 2008; Usui et al., 1999). To stabilize planar polarization within the cell, an inhibitory feedback loop with Dsh and Pk takes place. Fz recruits Dsh to the membrane and by the binding of Dsh to Dgo, Dgo is also localized at the cell membrane with Dsh and Fz (fig. 3 A) (Axelrod, 2001; Axelrod et al., 1998; Jenny et al., 2005). On the opposite side, Vangl interacts with Pk (Jenny et al., 2003). Vangl is also able to interact with Dsh but it is proposed that Vangl has a stronger affinity to interact with Pk than with Dsh (Das et al., 2004; Jenny et al., 2003). Pk is also able to interact with Dsh and Dgo but the Pk-Dsh interaction is inhibited in presence of Dgo leading to an intracellular inhibitory feedback loop to establish PCP (fig. 3 A) (Das et al., 2004; Jenny et al., 2003; Jenny et al., 2005; Tree et al., 2002).

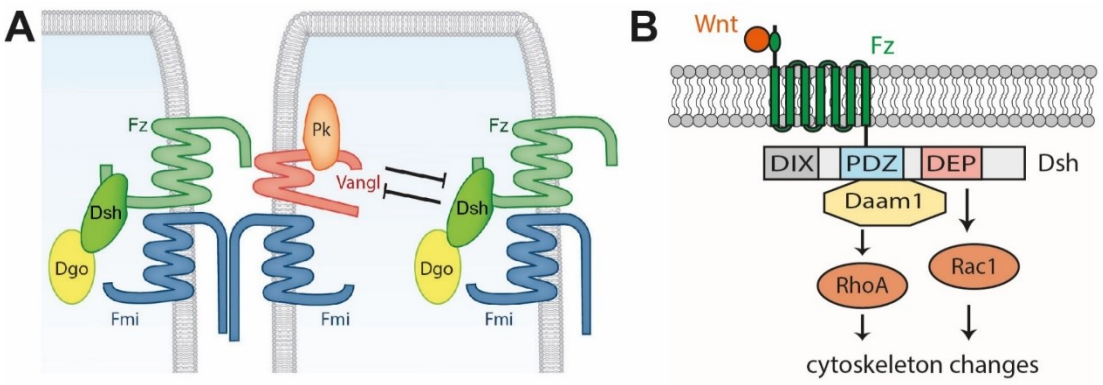

Fig. 3: Schematic model of PCP signaling. A Core PCP protein interaction across cells (modified after (Yang and Mlodzik, 2015)). **B** Activation of PCP signaling leads to cytoskeleton changes by activation of the small GTPases RhoA or Rac1 (based on (Wallingford and Habas, 2005)).

The activation of PCP signaling targets the small GTPases and affects changes in the cytoskeleton (fig. 3 B) (reviewed in (Braga, 2002)). The Fz receptor recruits Dsh to the membrane activating the small GTPases (Axelrod et al., 1998; Habas et al., 2003). Dsh is a scaffold protein and consists of three important domains, the N-terminal DIX, central PDZ and C-terminal DEP domains (fig. 3 B). It has been shown that the DIX domain functions in the canonical Wnt pathway and the DEP domain is important for PCP signaling (reviewed in (Mlodzik, 2015; Sharma et al., 2018)). The PDZ domain can be

part of the canonical pathway as well as the PCP pathway. In the PCP signaling pathway Dsh can activate the small GTPase RhoA or Rac1 (Čajánek et al., 2013; Habas et al., 2001; Habas et al., 2003). Active RhoA leads to the formation of actin stress fibers (Paterson et al., 1990; Totsukawa et al., 2000). However, activation of Rac1 leads to actin cytoskeleton rearrangements and also to the activation of JNK which causes the expression of specific genes important for cell polarity and migration (Boutros et al., 1998; Kjøller and Hall, 1999; Kraynov et al., 2000; Yamanaka et al., 2002).

In migrating NC cells, PCP signaling is activated at cell-cell contact sites, indicated by the recruitment of Dsh to Fz (Carmona-Fontaine et al., 2008b). Fz/Dsh signaling leads to an activation of RhoA at the contact area which leads to filopodia collapse (Carmona-Fontaine et al., 2008b; Theveneau et al., 2010). RhoA-mediated contraction of filopodia is initiated by inhibition of Rac1 but also by actomyosin assembly (Kadir et al., 2011; Moore et al., 2013; Scarpa et al., 2015).

1.4 Small GTPases regulate the actin cytoskeleton

Migrating cells are polarized with a leading edge, in which a lamellipodium, which consists of branched actin filaments, is formed and a back side with actomyosin stress fibers (fig. 4). During migration, the actin nucleation in the lamellipodia pushes the cell membrane forward (Keren et al., 2008; Mogilner, 2009). Orientation of the lamellipodium is controlled by filopodia. Filopodia are thin, actin-rich structures which function to reinforce adherence to the extracellular matrix and guide towards chemoattractants (Bornschlögl, 2013; Johnson et al., 2015; Mattila and Lappalainen, 2008; Miki et al., 1998).

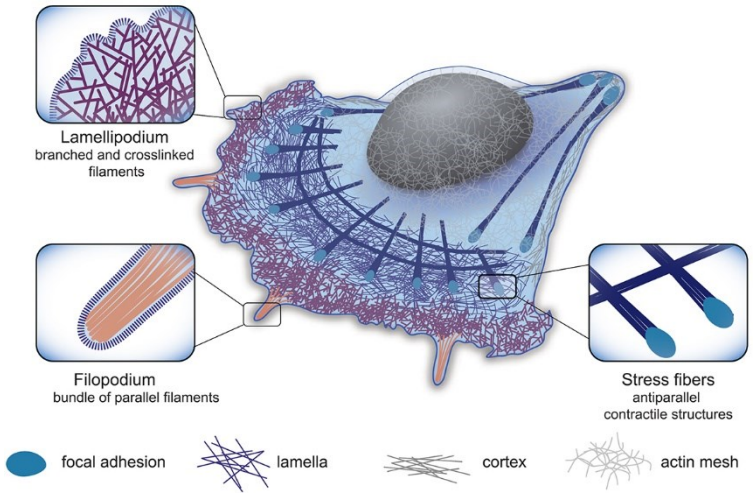

Fig. 4: Cellular actin network during cell migration. Schematic representation of the three main actin structures found in the cell: 1. Lamellipodium: dense, branched network involved in cell protrusion. 2. Filopodium: a finger-like structure located at the leading edge of the motile cell. 3. Contractile structure: dynamic structure made of antiparallel and/or mixed-polarity actin filaments. Zoomed regions highlight the specific actin organization of the different cellular actin structures (Letort et al., 2015).

Filamentous actin (F-actin) networks are highly dynamic structures assembled by globular actin (G-actin), the actin monomer. F-actin structures are polarized with a barbed end (or plus end, near the cell membrane) and a pointed end (or minus end). Elongation occurs at the barbed end, in which the monomer binding protein Profilin binds to the barbed end and delivers ATP-bond G-actin (fig. 5) (reviewed in (Pollard, 2017; Skruber et al., 2018)). Profilin is able to exchange ADP for ATP of G-actin to maintain the reserve of free actin necessary for actin nucleation (reviewed in (Coumans et al., 2018; Skruber et al., 2018)). To inhibit uncontrolled actin polymerization, capping proteins bind to the barbed ends and block G-actin addition (Isenberg et al., 1980). Restricting filament length by capping proteins can increase actin branching (Blanchoin et al., 2000). Actin branching occurs by the Arp2/3 complex, which is activated by WASP or WAVE complex. The Arp2/3 complex acts as a linker protein and binds to the so called mother filament (fig. 5). There, the Arp2/3 complex becomes the first subunit of the new filament (Rouiller et al., 2008). This is followed by association of additional actin monomers which generates a daughter filament branch. De-polymerization of actin filaments occurs at the pointed end by the actin-severing proteins of the ADF/cofilin family. Cofilin in its active (not phosphorylated) state depolymerizes or severs F-actin near the pointed end leading to increased concentration of ADP-bound G-actin which is captured by Profilin (fig. 5) (reviewed in (Coumans et al., 2018; Pollard, 2017)). Cofilin can be inhibited by phosphorylation due to LIM Kinase (LIMK), which leads to actin stabilization (Dang et al., 2013; Delorme et al., 2007; Pollard and Borisy, 2003).

F-actin can also bind to myosin II to form actomyosin stress fibers (reviewed in (Vincente-Manzanares et al., 2009)). In an active (phosphorylated) state, myosin II filaments bind to actin and link actin filaments together forming actomyosin stress fibers. Due to its enzymatic Mg^{2+}-ATPase motor domain (Vincente-Manzanares et al., 2009), myosin II can “walk” along the actin filament leading to contraction of the stress fibers.

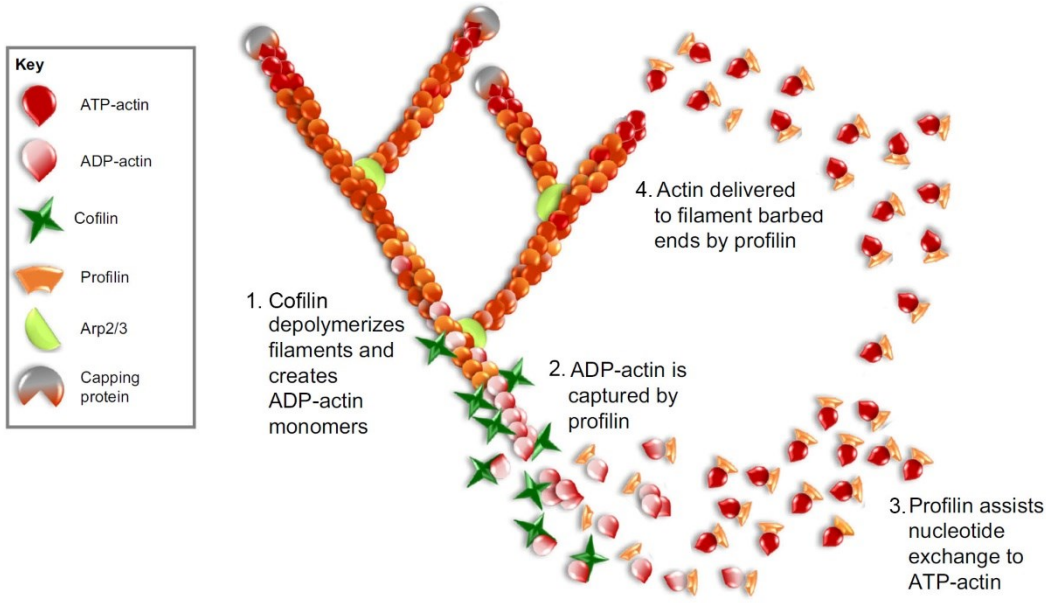

Fig. 5: Actin nucleation. F-actin consists of ATP-actin at its barbed ends and ADP-actin at its pointed end. Cofilin depolymerizes F-actin at the pointed end leading to monomeric ADP-G-actin. Profilin binds to G-actin and assists nucleotide exchange to ATP-actin and delivers it to actin barbed ends. There it assembles the F-actin strand. Capping proteins prevent actin assembly. Arp2/3 binds to filamentous actin to initiate branched actin formation (modified after (Skruber et al., 2018)).

As mentioned earlier, Rho GTPases regulate actin cytoskeleton rearrangements. Live-cell imaging shows that active Rac1 is localized in forming cell protrusions and photo-activation of Rac1 initiates lamellipodia formation (Kraynov et al., 2000; Wu et al., 2009). Rac1 regulates branched actin filaments by the activation of WAVE and Arp2/3 complex (fig. 6 A). In addition, Rac1 is also able to activate LIMK by activation of PAKs (p21-activated kinase) (Dang et al., 2013; Delorme et al., 2007; Pollard and Borisy, 2003). Such a Rac1 activation at the front of a cell leads to actin nucleation, stabilization and branching which results in lamellipodia formation. Cdc42 shares similar functions with Rac1. Cdc42 is also localized at the front of the cell and leads to inactivation of cofilin by PAKs and LIMK (reviewed in (Bishop and Hall, 2000). But unlike Rac1, Cdc42 activates Arp2/3 by activation of WASP (fig. 6 A). Overexpression of Cdc42 and WASP lead to thin, actin-rich structures (filopodia) (Miki et al., 1998). In conclusion, active Rac1 and Cdc42 in the cell leads to protrusion formation by actin elongation and branching.

Rac1 is able to inhibit RhoA activity by its downstream effector PAK, which phosphorylates and inactivates RhoA-specific activators (Zenke et al., 2004), leading to inhibition of RhoA-dependent stress fibers.

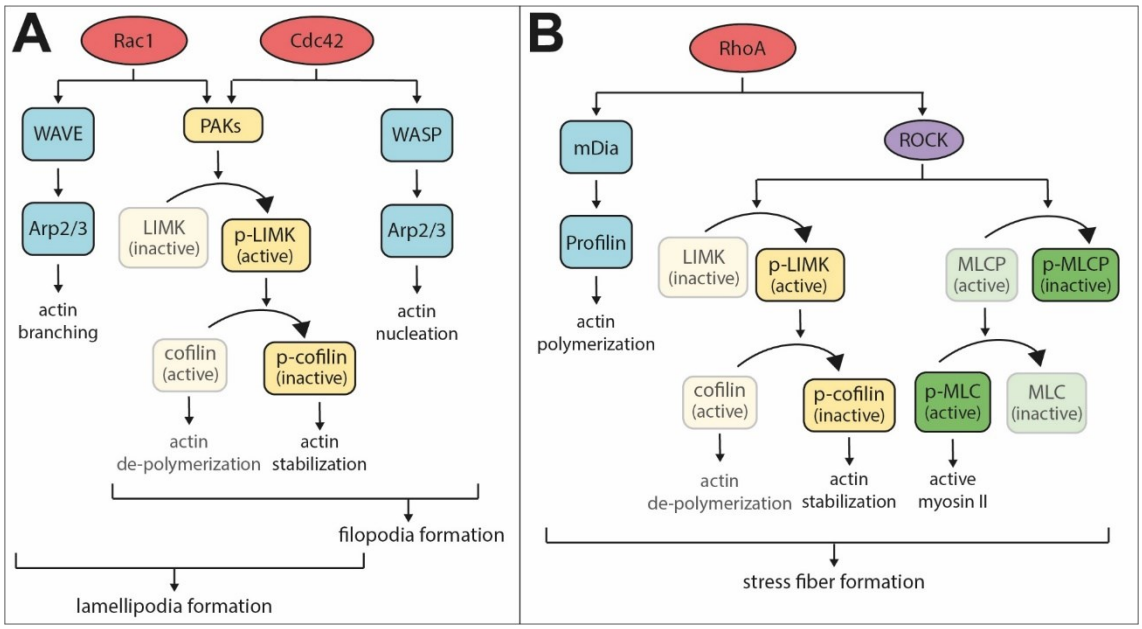

Fig. 6: Downstream effectors of active Rac1, Cdc42 and RhoA. A Activated Rac1 and Cdc42 leads to actin remodeling resulting in lamellipodia and filopodia formation. **B** Activation of RhoA leads to actomyosin stress fibers formation (own illustration).

Active RhoA induces actin assembly and stress fiber formation, which leads to cell contraction. RhoA promotes actin polymerization by activation of mDia and Profilin (fig. 6 B) (Watanabe et al., 1997). RhoA stabilizes existing actin filaments by Profilin activation and inhibition of Cofilin. Cofilin is inhibited by activation of LIMK but in contrast to Rac1, RhoA-mediated LIMK activation is arranged by ROCK (Rho-associated kinase) (fig. 6 B) (Maekawa et al., 1999). ROCK also activates myosin II directly or by inhibiting the myosin light chain phosphatase (MLCP), mediating actin stress fiber formation (Bresnick, 1999; Sellers, 1991; Vincente-Manzanares et al., 2009). Taken together, active RhoA initiates actomyosin stress fiber formation by stabilizing F-actin and myosin II binding to F-actin. RhoA is also capable to suppress Rac1 activity by activation of Rac1-specific inhibitors (Bryne et al., 2016; Ohta et al., 2006). The mutual inhibition of RhoA and Rac1 results in active RhoA being at the rear of the cell and active Rac1 at the front of the cell.

Cell blebbing is another form of cell migration, whereby cell uses spherical protrusions called blebs instead of lamellipodia and filopodia (reviewed in (Fackler and Grosse, 2008)). This form of cell motility is used by amoebae and mammalian tumor cells. Blebbing starts with dissociation of the membrane from the actin cytoskeleton and flow of the cytosol into the bleb expanses the blebs. Rapid reformation of actin filaments under the bleb membrane stops bleb expansion. Myosin accumulates to actin filaments and the actomyosin network leads to retraction of membrane bleb (Charras and Paluch, 2008; Charras et al., 2006). Rho-ROCK-myosin is important for blebbing dynamics. But

blebbing by Rho activation can also occur indirectly by activation of Rac GTPase since Rac and Rho activity is tightly balanced. It was shown that alteration of Rac activity (suppression or over-activation) can also stimulate membrane blebbing (Ohta et al., 2006; Schwartz et al., 1998; Vidali et al., 2006).

1.5 Trio – a GEF for Rac1 and RhoA

Small GTPases have an inactive GDP-bound and an active GTP-bound state (fig. 7). In their inactive state Rho GTPases are mainly localized in the cytosol and bound to Rho guanine nucleotide dissociation inhibitors (Rho GDI), which keeps them in the inactive state and prevents them from re-activation and degradation (DerMardirossian and Bokoch, 2005). GTPases are activated by Rho guanine nucleotide exchanging factors (GEFs). GEFs stimulate the release of GDP, allowing GTP to bind. For inactivation, GTPase activating proteins (GAPs) catalyze GTP hydrolysis which results in GDP-bound conformation of GTPases (fig. 7).

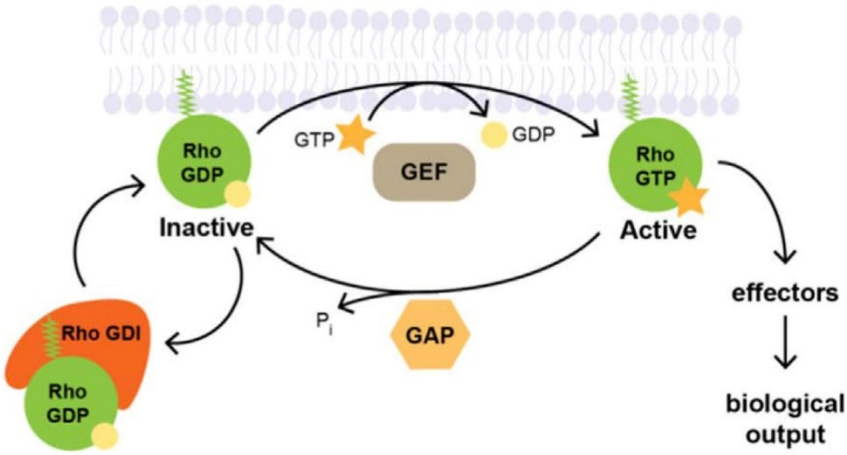

Fig. 7: Small GTPase cycle between inactive GDP- and active GTP-bound state. In the inactive state, GTPases are bound to GDP, which is exchanged for GTP by GEF. Inactivation occurs by GTP hydrolysis initiated by GAP. Rho-GDI binds GDP-bound Rho to keep Rho GTPases in the cytosol and prevents them from degradation (Arnold et al., 2017).

One known Rho-GEF protein is the ~ 340 kDa large protein Trio. Trio was named after its three enzymatic activity domains, the two Dbl-homology-Pleckstrin-homology (DH-PH) Rho-GEF units and a C-terminal serine/threonine kinase domain (fig. 8). In addition, Trio consists of an N-terminal putative lipid-transfer Sec14 motif, several spectrin-like repeats, two Src-homology 3 (SH3) domains and an immunoglobulin like (Ig) domain (fig. 8).

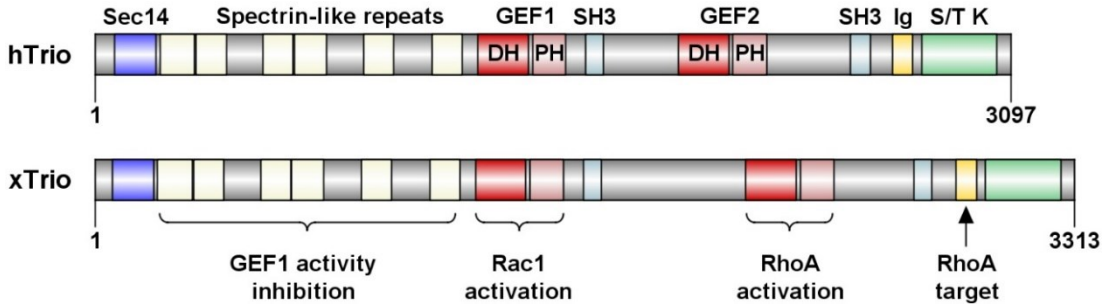

Fig. 8: Structure and function of Rho-GEF Trio. The Trio protein consists of a Sec14 and spectrin-like repeats at the N-terminus. It expresses two Dbl-homology (DH)- Pleckstrin-homology (PH) units (GEF). Trio also includes two SH3-domains, an immunoglobulin-like (Ig) domain and a serine/threonine kinase (S/T K) domain. Protein representation of human and *X. laevis* Trio and number at the ends indicate number of amino acids. Trio GEF1 domain leads the activation of Rac1 activation. The spectrin-like repeats can inhibit the GEF1 catalytical activity. Trio GEF2 domain activates RhoA. RhoA-GTP binds to Trio Ig domain (own illustration).

Trio functions as a GEF for the small GTPase Rac1 as well as RhoA. The Trio N-terminal GEF1 domain activates Rac1 (Bellanger et al., 1998; Debant et al., 1996; Maier et al., 2018). Rac1 activation by GEF1 in turn induces JNK activation and actin cytoskeleton remodeling (Bellanger et al., 1998; Bellanger et al., 2000; Bellanger et al., 2003; Seipel et al., 1999). Interestingly, the activity of GEF1 is inhibited by binding of the spectrin-like repeats to the GEF1 domain (Chen et al., 2011). Binding of proteins, e. g. DISC1, to the spectrin-like repeats can abolish the intramolecular inhibition of GEF1 and activates Rac1 (Chen et al., 2011). On the other hand, the C-terminal GEF2 domain activates RhoA and also leads to actin cytoskeleton remodeling (Backer et al., 2018; Debant et al., 1996; Seipel et al., 1999). However, Trio does not only activate RhoA but active RhoA binds to Trio Ig domain and alters Trio localization effecting the cell morphology (Medley et al., 2000).

Several Trio isoforms have been identified which are largely expressed in the brain and nervous system whereas full-length Trio can be ubiquitously found (reviewed in (Schmidt and Debant, 2014; van Rijssel and van Buul, 2012)). Trio is also expressed in *Xenopus* NC cells (Kratzer et al., 2019) and recent studies show that Trio is important for NC cell migration (Kashef et al., 2009; Moore et al., 2013). Trio interacts with the classical cadherin adhesion molecule Cadherin-11 and acts as a Rac1 activator to mediate protrusion activity (Kashef et al., 2009; Li et al., 2011). In addition, Trio interacts with the polarity protein Par3 (Landin Malt et al., 2019; Moore et al., 2013). In the inner ear hair cells Par3 activates Rac1 by Trio and thereby regulating microtubule dynamics (Landin Malt et al., 2019). In NC cells, Trio activates Rac1, which leads to microtubule polymerization. Interaction of Par3 with Trio leads to Trio inhibition, decrease in Rac1 activity and thus to microtubule catastrophe, which leads to CIL respond of migrating NC

cells (Moore et al., 2013). Since Trio is localized at the cell membrane of NC cells (Moore et al., 2013), it has to be investigated, if Trio possible functions in different signaling processes in different subcellular areas of migrating NC cells.

1.6 PTK7: Regulator of the Wnt pathway

1.6.1 PTK7 domain structure

Another protein which is differently localized at the membrane of NC cells is the Wnt receptor protein tyrosine kinase 7 (PTK7) (Podleschny et al., 2015). PTK7 is an evolutionary conserved transmembrane protein. It was first identified in normal melanocytes and full-length PTK7 could be first isolated out of colon carcinoma cells (hence named as colon carcinoma kinase 4, CCK-4) (Lee et al., 1993; Mossie et al., 1995). Orthologues of PTK7/CCK-4 can be found in mouse, chicken (known as Kinase-like gene) and *Xenopus* as well as in the invertebrates *Drosophila* (known as Off-track) and *Hydra* (alias Lemon) (Chou and Hayman, 1991; Jung et al., 2004; Lu et al., 2004; Miller and Steele, 2000; Mossie et al., 1995; Pulido et al., 1992; Winberg et al., 2001). However, PTK7 was detected as an upregulated gene in colon carcinoma cells and also in gastric and esophageal cancer (Kim et al., 2014; Lin et al., 2012; Mossie et al., 1995; Saha et al., 2001; Shin et al., 2013). Recent studies show that PTK7 can also be downregulated in other cancers like lung squamous cell carcinoma and epithelial ovarian cancer (Kim et al., 2014; Wang et al., 2015a). This suggests that PTK7 may have dual effects (up- or downregulation), depending on specific tissues or tumors.

PTK7 consists of extracellular seven Ig domains, a transmembrane and an intracellular kinase homology domain (fig. 9) (Mossie et al., 1995; Park et al., 1996). The kinase domain exhibits the structure of a catalytic domain of tyrosine kinases, however, the DFG triplet, which is necessary for kinase activity (Moran et al., 1988), is mutated resulting in a catalytic inactive kinase (Park et al., 1996).

Analysis in human cell lines shows that PTK7 can be cleaved by MT1-MMP (membrane type-1 matrix metalloproteinase) in Ig7 and also by ADAMs, e.g. ADAM17, between Ig7

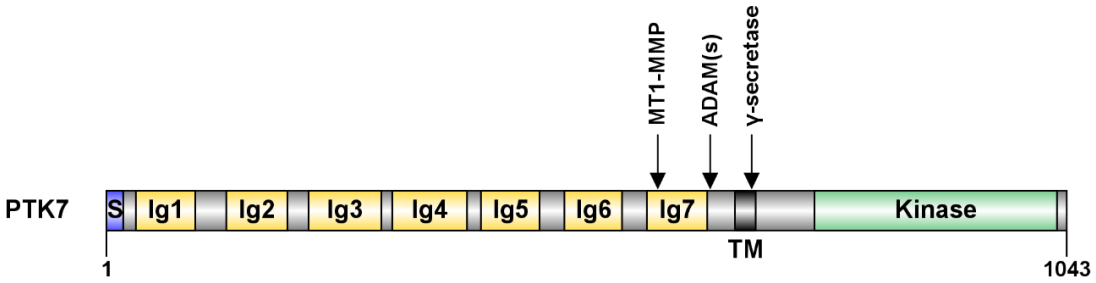

Fig. 9: Structure of PTK7 protein. PTK7 consists a signal peptide (S), seven immunoglobulin-like domains (Ig), a transmembrane (TM) and an inactive kinase domain. MT1-MMP, ADAM and γ-secretase approximate cleavage sites are indicated by arrows. Numbers at the ends display number of amino acids (own illustration).

and the transmembrane domain (fig. 9) (Golubkov and Strongin, 2012; Golubkov et al., 2010; Na et al., 2012). Proteolysis leads to a N-terminal soluble PTK7 fragment which can stimulate RhoA activity and interacts with full-length PTK7. The proteolysis by MT1-MMP and ADAM is followed by the intramembrane cleavage by γ-secretase resulting in a C-terminal PTK7 fragment (Golubkov and Strongin, 2012; Na et al., 2012). The C-terminal fragment can be degraded in the proteasome but interestingly it can also be translocated into the cell nucleus and increase gene transcription (Golubkov and Strongin, 2014; Na et al., 2012).

1.6.2 PTK7 in PCP signaling and NC cell migration

PTK7 loss of function leads to PCP phenotypes. PTK7 deficient mice shows disoriented stereociliar bundle orientation and fail to close their neural tube from the midbrain-hindbrain boundary to the base of the spin (craniorachischisis) (fig. 10 A) (Lu et al., 2004). Neural tube defects caused by PTK7 loss of function can also be found in zebrafish and *Xenopus* (fig. 10 B) (Hayes et al., 2013; Lu et al., 2004). In some human patients, which show neural tube defects or idiopathic scoliosis, missense variants in one of the Ig domains of PTK7 could be found (Hayes et al., 2014; Wang et al., 2015b; Wang et al., 2018). Also overexpression of a PTK7 construct which lacks the kinase domain (ΔkPTK7) can lead to neural tube defects in *Xenopus* (Lu et al., 2004). This implicates that the extracellular domain as well as the intracellular kinase homology domain are important for proper neural tube formation. Recent studies show that PTK7 function is not only involved in neural tube closure, it is also important for NC cell migration. In *Xenopus*, PTK7 is expressed in NC cells and knockdown of PTK7 leads to NC migration defects (fig. 10 C-E) (Shnitsar and Borchers, 2008). Furthermore, overexpression of ΔkPTK7 also leads to defects in NC cell migration (Shnitsar and Borchers, 2008). It is still not known how PTK7 acts downstream to affect NC cell migration. However, recent research shows that PTK7 activates PCP signaling by recruiting Dsh to the plasma membrane (Shnitsar and Borchers, 2008; Wehner et al., 2011). In *Xenopus* ectodermal explants PTK7 enables the Dsh membrane localization by interaction of its kinase homology domain with RACK1 (Receptor of Activated protein Kinase C 1). RACK1 in turn interacts with PKCδ1 (Protein Kinase C Delta 1) which leads to membrane recruitment of Dsh (Wehner et al., 2011).

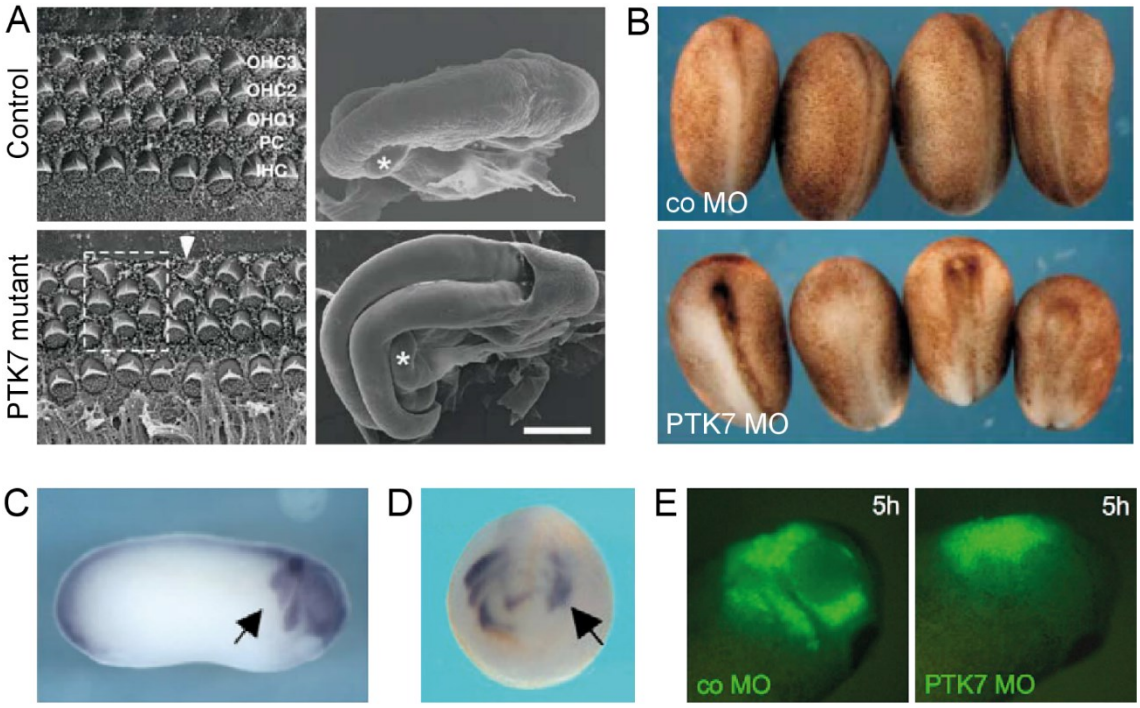

Fig. 10: PTK7 is involved in PCP signaling. A PTK7 knockout in mice leads to misoriented stereociliar bundles of outer hair cells (OHC) of the inner ear cells compared to control mouse and an open neural tube; pillar cells (PC), inner hair cells (IHC). **B** Also in *Xenopus* leads a PTK7 knockdown by morpholino (MO) injection to neural tube closure defects. While embryos injected with control (co) MO show closed neural tubes (Lu et al., 2004). **C** PTK7 is expressed in NC cells (arrow). **D** NC cell migration can be impaired by injection of PTK7 MO (arrow). **E** Also transplanted NC cells with PTK7 knockdown are not able to migrate properly (5 h indicate time span after transplantation) (Shnitsar and Borchers, 2008).

Recruitment of Dsh to the plasma membrane is a strong evidence for activation of PCP signaling and the PCP receptor Fz7 is also able to recruit Dsh to the plasma membrane (Axelrod et al., 1998; Medina and Steinbeisser, 2000). Interestingly, PTK7 interacts with the receptor Fz7 but the PTK7-mediated Dsh recruitment is independent of Fz, but recruitment of Dsh by Fz is PTK7-dependent (Peradziryi et al., 2011; Shnitsar and Borchers, 2008; Wehner et al., 2011). Further evidence of PTK7 as a PCP activator is the activation of JNK phosphorylation (Martinez et al., 2015; Shnitsar and Borchers, 2008). But further downstream PCP signaling mediated by PTK7 in NC cell migration has not been investigated yet. However, there is evidence that membrane recruitment of Dsh leads to the activation of RhoA/ROCK and thereby to the re-organization of the actin cytoskeleton (Amano et al., 2010; Habas et al., 2001). And indeed, in MDCK (Madin-Darby canine kidney) epithelial cells PTK7 is localized at cell-cell contacts and there mediates ROCK2 phosphorylation resulting in the re-organization of the actomyosin cytoskeleton (Andreeva et al., 2014; Golubkov et al., 2010). It has also been shown that the soluble form of PTK7 can increase RhoA activity in MDCK cells. However, a recent study shows that PTK7 promotes Rac1 and myosin II activity in the epithelium of the Wolffian duct (Xu et al., 2018). Moreover, in mouse sensory epithelium and neural plate

cells PTK7 promotes myosin II localization to align PCP (Lee et al., 2012; Williams et al., 2014). It has to be investigated if and how PTK7 mediates cytoskeleton organization by RhoA/Rac1 signaling in NC cells.

1.7 PTK7 and the canonical Wnt pathway

1.7.1 The canonical Wnt pathway

Recent studies show that PTK7 activates not only the PCP pathway, it also affects the canonical Wnt pathway (reviewed in (Berger et al., 2017a)).

The canonical Wnt pathway is evolutionary highly conserved and plays important roles e.g. in axis specification and tissue homeostasis (reviewed in (Steinhart and Angers, 2018)). In absence of Wnt ligands, a β-catenin destruction complex is formed with Axin, APC (adenomatous polyposis coli), GSK3 (glycogen synthase kinase 3) and CK1 (casein kinase 1) (fig. 11). The initial degradation of β-catenin starts by its binding to Axin, which is followed by serial phosphorylation by GSK3 and CK1, poly-ubiquitination and final proteosomal degradation (Ikeda et al., 1998; Liu et al., 2002; Winston et al., 1999). In the cell nucleus, the transcriptional repressor Groucho is associated with LEF/TCF (lymphoid-enhancing factor/T-cell factor), inhibiting Wnt target gene transcription (Cavallo et al., 1998; Roose et al., 1998). Wnt binding to Fz and the co-receptor LRP5/6 (low-density lipoprotein receptor-related protein) leads to inhibition of the β-catenin destruction complex and thereby to an accumulation of β-catenin in the cytoplasm (fig. 11). Cytoplasmic β-catenin can translocate to the nucleus where it displaces Groucho, binds to LEF/TCF and activates Wnt target gene transcription (Brunner et al., 1997; Huber et al., 1996; Molenaar et al., 1996). However, there are different opinions how the β-catenin destruction complex is inhibited (see review (Tortelote et al., 2017)). The “classical model” predicts the dissociation of the destruction complex (fig. 11). After heterodimerization of Fz and LRP, initiated by binding to Wnt proteins, many intracellular events are induced. The cytosolic protein Dsh gets phosphorylated, is translocated to the membrane and interacts with Fz (Tauriello et al., 2012; Yanagawa et al., 1995). Dsh DIX domain interacts with Axin, which leads to the recruitment of the Axin-GSK3 complex to the membrane (Fiedler et al., 2011; Kishida et al., 1999; Schwarz-Romond et al., 2007). The Axin-GSK3 complex in turn leads to phosphorylation of LRP, this in turn provides additional docking sites for Axin (Mao et al., 2001; Tamai et al., 2004; Zeng et al., 2005; Zeng et al., 2008). With the dissociation of the β-catenin destruction complex β-catenin is stabilized in the cytoplasm, gets translocated into the nucleus and acts as a co-transcription factor for e.g. *c-myc*, *engrailed-2* and *siamos* (Brannon et al., 1997; He et al., 1998; McGrew et al., 1999).

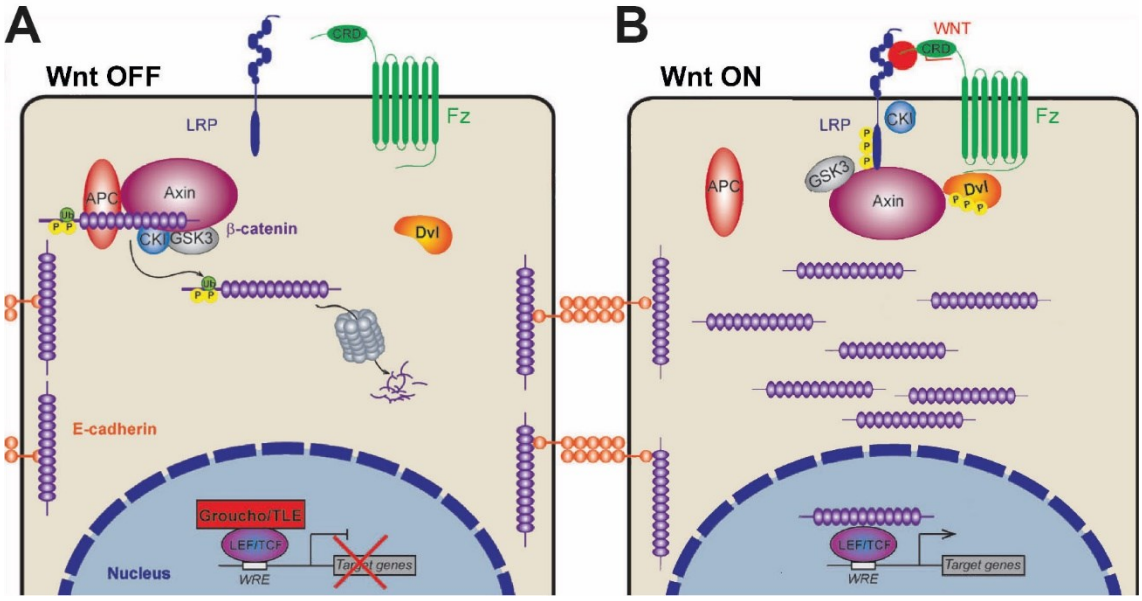

Fig. 11: Canonical Wnt signaling pathway. A In absence of Wnt ligands, the destruction complex phosphorylates β-catenin which leads to its ubiquitination and proteosomal degradation. Gene transcription is inactive due to the binding of Groucho/TLE (transducing-like enhancer) to the transcription factors LEF/TCF. **B** Binding of Wnt to Frizzled (Fz) and LRP leads to the dissociation of the destruction complex and accumulation of β-catenin in the cytoplasm. β-catenin can translocate to the nucleus and act as a co-transcription factor to initiate gene transcription (modified after (Grainger and Willert, 2018; Kim et al., 2013)).

1.7.2 PTK7 affects the canonical Wnt pathway

As mentioned before PTK7 can interact with Fz7. The interaction of Fz7 and PTK7 not only activate PCP signaling but also allows PTK7 to bind canonical Wnt but not non-canonical Wnt proteins (Peradziryi et al., 2011). Co-immunoprecipitations show that PTK7 interacts with the canonical Wnt3a and Wnt8. Previously it could be shown that PTK7 together with canonical Wnt proteins were endocytosed and so inhibit the canonical Wnt pathway (Berger et al., 2017b). Endocytosis of PTK7 could not be observed due to non-canonical Wnt treatment. Concluding that PTK7 binds canonical Wnt proteins to inhibit the canonical Wnt signaling pathway. However, other studies show conflicting findings of PTK7 in the canonical Wnt pathway. Puppo and colleagues show that PTK7 interacts with β-catenin and that it is important for β-catenin transcriptional activity upon Wnt3a stimulation (Puppo et al., 2011). PTK7 also regulates and interacts with the canonical co-receptor LRP6 and positively influences the canonical signaling pathway in neural convergent extension cell movements together (Bin-Nun et al., 2014). It is suggested that PTK7 is involved in the activation and not the inactivation of canonical Wnt signaling.

Current investigations show that the composition of the PTK7 co-receptor complex may modulate different Wnt signaling pathways in different kinds of tissues and organisms.

PTK7 downstream signaling can lead to the activation of c-jun, AKT, Ras/ERK, CREB/ATF1, SRC and inhibition of JNK signaling (Andreeva et al., 2014; Chen et al., 2014b; Golubkov and Strongin, 2014; Jin et al., 2014). Furthermore, PTK7 interaction with other receptors such as Plexin and VEGF receptors support this hypothesis and suggest that PTK7 is a versatile co-receptor (Peradziryi et al., 2012).

1.8 The PTK7 interaction partner Ror2 functions in PCP signaling

Recently it has been shown that PTK7 interacts with another Wnt receptor, Ror2, which can replace PTK7 function in *Xenopus* development (Martinez et al., 2015; Podleschny et al., 2015). Ror2 is a transmembrane protein with an extracellular Ig domain, a CRD (Frizzled-like cysteine-rich domain) and a Kringle domain. Intracellular Ror2 consists of a tyrosine kinase, proline-rich and serine-threonine-rich domains (fig. 12 A) (Masiakowski and Carroll, 1992). Ror2 binds multiple Wnt proteins via its CRD domain where the non-canonical Wnt protein Wnt5a seems to be the primary ligand (reviewed in (Stricker et al., 2017)). Wnt binding to Ror2 can lead to Ror2 dimerization, phosphorylation and its activation (Liu et al., 2007; Liu et al., 2008a; Yamamoto et al., 2007). Furthermore, active Ror2 can interact and phosphorylate Dsh leading to activation of the small GTPases RhoA and Rac1 resulting in cytoskeletal remodeling (Dai et al., 2017; Ho et al., 2012; Nishita et al., 2006; Nishita et al., 2010; Witte et al., 2010). However, the Wnt5a/Ror2 complex inactivates canonical Wnt signaling by competing for Wnt3a binding to Fz (Grumolato et al., 2010; Mikels and Nusse, 2006; Mikels et al., 2009; Witte et al., 2010). In addition, Wnt5a/Ror2/Fz leads to the recruitment of Dsh, Axin and GSK3 to the membrane (fig. 12 B) (Grumolato et al., 2010; Yamamoto et al., 2007). GSK3 phosphorylates and activates Ror2, which results in activation of PCP signaling. An overexpression of Ror2 in *Xenopus* results in a shortened anterior-posterior axis, indicating an important role of Ror2 in convergent extension movements during gastrulation and neurulation (Hikasa et al., 2002). Ror2 regulates convergent extension movements by transcriptional regulation of PAPC (paraxial protocadherin) by JNK activation and modulation of RhoA and Rac1 (Brinkmann et al., 2016; Feike et al., 2010; Nomachi et al., 2008; Oishi et al., 2003; Schambony and Wedlich, 2007; Schille et al., 2016; Unterseher et al., 2004).

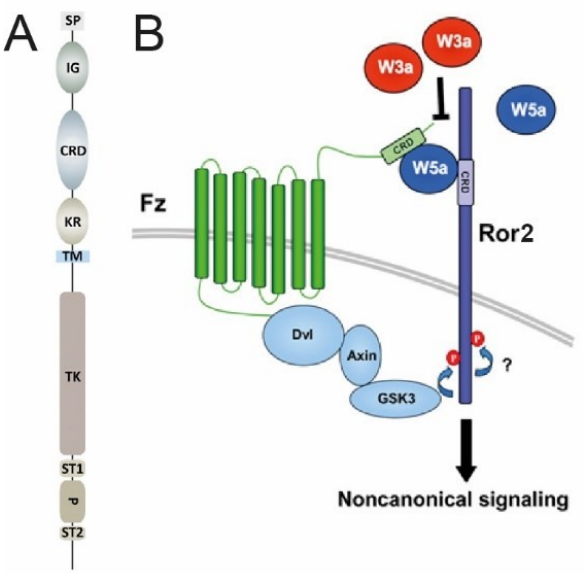

Fig.12: Ror2 functions in PCP signaling. A Ror2 domain structure, signal peptide (SP), immunoglobulin domain (IG), Frizzled-like cysteine-rich domain (CRD), Kringle domain (KR), tyrosine kinase (TK), serine-threonine-rich (ST) part and proline-rich domain (P), (Stricker et al., 2017). **B** Wnt5a/Ror2/Fz complexes recruits Dsh, Axin and GSK3 to the plasma membrane resulting in phosphorylation of Ror2 and activation of PCP signaling (Grumolato et al., 2010).

In *Xenopus*, Ror2 is expressed starting from gastrulation to tadpole stages where Ror2 is highly expressed at the neural plate border and in NC cells (Hikasa et al., 2002). Ror2 activates BMP signaling at the neural plate border, which leads to NC cell induction (Schille et al., 2016). A function of Ror2 in NC cell migration has not been further investigated but recently it could been shown that Ror2 can substitute PTK7 function in NC cell migration (Podleschny et al., 2015). This and the interaction of Ror2 and PTK7 can indicate a Ror2/PTK7 receptor complex in NC cell migration.

1.9 Aims of this study

PTK7 is expressed in NC cells and previous findings of our laboratory revealed that PTK7 is localized at NC cell-cell contact sites. During this study, the dynamic localization of PTK7 in migrating NC cells will be further investigated. Therefore, NC cells overexpressing different GFP-tagged PTK7 constructs will be observed using live cell imaging. In addition, due to its localization at cell-cell contacts, it will be examined if PTK7 is able to exhibit homophilic binding.

PTK7 activates the non-canonical Wnt pathway indicated, for example, by the recruitment of Dishevelled to the plasma membrane in *Xenopus* ectodermal explants. However, further downstream PCP signaling mediated by PTK7 in *Xenopus* is unknown. Thus, the aim of this study is to investigate further components of the PTK7 signaling especially during NC cell migration. Therefore, overexpression experiments with known PCP proteins will be performed in PTK7-morphant embryos and NC cell migration will be analyzed using *in situ* hybridization. In addition, co-immunoprecipitation will be performed to analyze potential PTK7 interaction partners.

PTK7 also regulates the canonical Wnt pathway. There are contradictory views whether PTK7 activates or inhibits canonical Wnt pathway. During this study, it will be analyzed if PTK7 affects canonical Wnt signaling during NC cell migration. For this propose, the activity of the canonical Wnt pathway will be investigated in explanted NC cells with a PTK7 knockdown. Furthermore, the canonical Wnt pathway will be inhibited in PTK7-morphant embryos and NC cell migration will be analyzed by *in situ* hybridization.

2. Materials and Methods

2.1 Model Organism

In this study the African clawed frog *Xenopus laevis* (*X. laevis*) was used as a model organism. Adult frogs were obtained from Nasco (Ft. Atkinson, USA).

2.2 Bacteria

The cloning experiments were performed with the *Escherichia coli* (*E. coli*) strain XL1-Blue (RecA1, endA1, gyrA96, thi-1, hsdR17, supE44, relA1, lac[F'proAB, ZΔM15, Tn10(Tetr)]^c (Stratagene)).

2.3 Cell lines

The following human cell lines were used in this study:

HEK293, human embryonic kidney cells, ATCC® No (CRL-1573)

2.4 Chemicals, Buffers and Media

All used chemicals were obtained from the following companies: AppliChem (Darmstadt), Merck (Darmstadt), Roth (Karlsruhe) and Sigma-Aldrich (Munich).

Agarose-Gel: 1% Agarose in TAE

Alkaline phosphatase buffer (APB): 100 mM Tris (pH 9.5), 50 mM $MgCl_2$, 100 mM NaCl, 0.1% Tween-20

Cell culture medium for HEK293 cells: VLE-DMEM (Very Low Endotoxin-Dulbecco's Modified Medium), 10% (v/v) FCS, 100 U/ml penicillin, 100 µg/ml streptomycin

Cell culture medium for MCF7 cells: RPMI 1640 Medium, 10% (v/v) FCS, 100 U/ml penicillin, 100 µg/ml streptomycin

Cell culture medium for stable transfected MCF7 cells: cell culture medium for MCF7 cells, 6 µg/ml Blasticidine, 1 µg/ml Hygromycin

Co-IP lysis buffer (NOP buffer): 150 mM Tris, 10 mM HEPES (pH 7.4), 2 mM EDTA, 1% (v/v) NP-40, 0.1% SDS Complete Protease inhibitor mix EDTA free (Roche)

Cysteine solution: 2% L-Cysteine, pH 8.0-8.3

Danilchik's buffer: 53 mM NaCl, 15 mM $NaHCO_3$, 13.5 mM Na_2CO_3, 4.5 mM K-Gluconate, 5 mM Bicine, adjusted with HEPES (1 M) to pH 8.3, 1 mM $MgSO_4$, 1 mM $CaCl_2$, sterile filtrate, storage at -20 °C

Danilchik's for Amy (DFA): 53 mM NaCl, 5 mM Na_2CO_3, 4.5 mM K-Gluconate, 32 mM Na-Gluconate, 1 mM $MgSO_4$, 1 mM $CaCl_2$, 0.1% BSA, adjusted with bicine (1 M) to pH 8.3 before adding BSA, sterile filtrate, storage at -20 °C

Denhardt's (100x): 2% BSA, 2% PCP (polyvinylpyrolidone), 2% Ficoll 400

Hybridization-Mix: 50% Formamide (v/v), 5x SSC, 1 mg/ml Torula RNA, 100 µg/ml Heparin, 1x Denhardt's, 0.1% Tween-20 (v/v), 0.1% CHAPS (w/v), 10 mM EDTA

Injection buffer: 2% Ficoll® PM 400, 1x MBS

Laemmli sample buffer (6x): 350 mM Tris-HCl (pH 6.8), 9.3% Dithiotreitol, 30% Glycerin, 10% SDS, 0.02% Bromphenolblue or OrangeG

Laemmli running buffer (10x): 250 mM Tris, 1.92 M Glycerin, 1% SDS

Luria-Bertani (LB)-Medium: 1% (w/v) Bacto-Trypton, 0.5% (w/v) yeast extract, 1% (w/v) NaCl, pH 7.5

LB-Agar: 1.5% Agar-Agar in liquid LB-Medium

LB-Amp plates: 100 µg/ml Ampicillin in LB-Agar

LB-Kan plates: 50 µg/ml Kanamycin in LB-Agar

MAB (Maleic acid buffer): 150 mM NaCl, 100 mM Maleic acid, pH 7.5

MBS (Modified Barth´s Solution) (5x): 440 mM NaCl, 12 mM $NaHCO_3$, 5 mM KCl, 50 mM HEPES (pH 7.4), 4.1 mM $MgSO_4$, 2.05 mM $CaCl_2$, 1.65 mM $Ca(NO_3)_2$, pH 7.4

MEM (10x): 1 M MOPS, 20 mM EGTA, 10 mM $MgSO_4$, pH 7.4-7.5

MEMFA: 1x MEM, 3.7% (v/v) Formaldehyde

Nile blue dye: 0.5 M Na_2HPO_4, 1 M NaH_2PO_4, 0.01% Nile blue, pH 7.8

PAK washing buffer: 50 mM Tris (pH 7.2), 150 mM NaCl, 5 mM $MgCl_2$, 1% Triton™ X-100, Complete Protease inhibitor mix EDTA free (Roche)

PBS (10x): 8% (w/v) NaCl, 2% (w/v) KCl, 100 mM Na_2HPO_4, 18 mM KH_2PO_4, pH 7.4

Penicillin/Streptomycin/PBS (Pen/Strep/PBS): 100 U/ml Penicillin, 100 µg/ml Streptomycin, 1x PBS

PTw: 0.1% Tween-20, 1x PBS

Rac-RIPA buffer: 50 mM Tris (pH 7.2), 150 mM NaCl, 5 mM $MgCl_2$, 1% Triton™ X-100, 0.1% SDS, Complete Protease inhibitor mix EDTA free (Roche)

SSC (20x): 3 M NaCl, 0.3 M Na-Citrate

TAE: 40 mM Tris-Acetate (pH 8.0), 1 mM EDTA

TBS: 50 mM Tris-HCl (pH 7.5), 150 mM NaCl

TBST: 0.5% Tween-20, TBS

Transfer buffer: 25 mM Tris, 192 mM Glycine, 20% Ethanol

Triethanolamine: 0.1 M Triethanolamine, pH 7.5

X-Gal staining solution: 1 mg/ml X-Gal, 5 mM $K_3Fe(CN)_6$, 5 mM $K_4Fe(CN)_6$, 2 mM $MgCl_2$, 1x PBS

2.5 Additional chemical, substances and reagents

Anti-Digoxygenin-Antibody (150 U), Roche
DAPI (1 mg/ml), Roth
Dexamethasone, Sigma-Aldrich
Digoxigenin-11-UTP, Roche
DNA Gel Loading Dye (6x), Thermo Scientific
DNA Ladder (FastRuler™, ready-to-use), Thermo Scientific
DTT (Dithiolthreitol), Thermo Scientific
Dynabeads™ Protein G, Invitrogen
Fibronectin (from bovine plasma), F1141-5MG, Sigma Aldrich
Fluorescein-Dextran, Life Technologies
Fluorescent mounting medium, Dako
GelRed® Nucleic Acid Gel Stain, Biotium
Glutathione Sepharose™ 4B, Fisher Scientific
GTPγS (10 mM), Merck
H_2O_2 (30%), Sigma-Aldrich
Human chorionic gonadotropin, Sigma-Aldrich
JetPEI®, Polyplus

NBT/BCIP stock solution, Sigma-Aldrich
PageRuler™ Plus Prestained Protein Ladder, Thermo Scientific
Propidium iodide, Sigma-Aldrich
Spectra™ Multicolor High Range Protein Ladder, Thermo Scientific

2.6 Enzymes

BamHI (FastDigest®), Thermo Scientific
ClaI (FastDigest®), Thermo Scientific
EcoRI (FastDigest®), Thermo Scientific
FastDigest® Buffer (10x), Thermo Scientific
HindIII (FastDigest®), Thermo Scientific
NotI (FastDigest®), Thermo Scientific
Phusion High-Fidelity DNA Polymerase (2 U/µl), Thermo Scientific
Proteinase K, Merck Millipore
RNase A/T1 Mix, Thermo Scientific
SacI (FastDigest®), Thermo Scientific
T4 DNA Ligase (5 U/ml), Thermo Scientific
T7 RNA Polymerase (20 U/µl), Thermo Scientific
DreamTaq™ DNA Polymerase (5 U/µl), Thermo Scientific
XbaI (FastDigest®), Thermo Scientific
XhoI (FastDigest®), Thermo Scientific

2.7 Kits

GenJet Gel Extraction Kit, Thermo Scientific
GenJet PCR Purification Kit, Thermo Scientific
GenJet Plasmid Miniprep Kit, Thermo Scientific
illustra™ RNAspin Mini RNA Isolation Kit, GE Healthcare
NucleoBond® Xtra Midi Kit, Macherey-Nagel
SP6 mMESSAGE mMACHINE®, Ambion
SuperSignal™ West Dura Extended Duration Substrate, Thermo Fisher Scientific
Zymoclean™ Gel DNA Recovery Kit, Zymo Research

2.8 Software & online tools

Adobe Photoshop and Illustrator CS6, Adobe Systems
Fiji (Schindelin et al., 2012)
IBS, The CUCKOO Workgroup (Liu et al., 2015)
ImageJ (Schneider et al., 2012)

Image Studio™ 5.2, LI-COR® Biotechnology
Leica LAS AF Lite, Leica Microsystems
MATLAB R2017b, MathWorks®
Microsoft Office 2013 and 2016, Microsoft Corporation
SMART, EMBL Heidelberg (Letunic and Bork, 2018)
ZEN Blue, Zeiss

2.9 Vectors and Constructs

2.9.1 Vectors

pCDNA3.1 is a mammalian expression vector with CMV promotor (Invitrogen).

pCS2+ is an expression vector, which can be used in the *Xenopus* model system. It contains a strong promotor/enhancer region (simian CMV IE94), polylinker and SV40 viral polyadenylation signal. The SP6 viral promotor allows *in vitro* transcription of sense polyadenylated mRNA for microinjections and the T7 viral promotor can be used for *in vitro* transcription of antisense RNA for *in situ* hybridization (Turner and Weintraub, 1994).

pCS2+eGFP was constructed by amplifying eGFP from the pEGFP-C1 vector and inserted into XhoI/XbaI sites of pCS2+ (Wehner et al., 2011).

pCS2+Myc was generated from pCS2+ and contains six copies of the Myc epitope tag (Rupp et al., 1994).

pCS2+HA was modified by insertion of hemagglutinin (HA) epitope into pCS2+ vector.

pBSK+ (Stratagene) and **pGEM-T** (Promega) are cloning vectors.

pMT.HAtag is an expression vector which encodes an initiator methionine codon followed by a HA epitope tag sequence immediately upstream of the cloning site (Serra-Pagès et al., 1995).

pPCR-Script Amp SK(+) is a derivative of pBluescript II SK(+) vector with an SrfI site for inserting blunt PCR products (Agilent Technologies).

pUAST is a P element-based expression vector, which is used in the *Drosophila* model system (Brand and Perrimon, 1993).

2.9.2 Expression constructs

Table 1 presents the expression constructs used during this study whereas table 2 and 3 includes information about enzymes for linearization of DNA constructs and RNA polymerases for *in vitro* transcription.

Tab. 1: Expression constructs.

Name	**Vector**	**Insert**	**Cloning strategy/Citation**
AP-2	pBSK+	*X. laevis* AP-2α	(Winning et al., 1991)
Myc-Dsh	pCS2+ Myc	*X. laevis* Dishevelled 2 with N-terminal Myc tag	(Sokol, 1996)
DshΔDEP	pCS2+	*X. laevis* Dishevelled 2 with deleted DEP domain	Gift from D. Gradl
DshΔDIX	pCS2+	*X. laevis* Dishevelled 2 with deleted DIX domain	Gift from D. Gradl
DshΔPDZ	pCS2+	*X. laevis* Dishevelled 2 with deleted PDZ domain	Gift from D. Gradl
Eos-β-Catenin	pCS2+	β-Catenin with N-terminal mEos FP tag	(Holzer et al., 2012)
mEos (cloning)	pCS2+	monomeric Eos FP with no start codon	Amplified from Eos-β-Catenin excluding its start codon with Eos_ClaI_f and Eos-XhoI_r primer and inserted into ClaI/XhoI restriction sites of the pCS2+ vector.
H2B-mcherry	pCS2+	Histone 2B with mcherry tag	(Kashef et al., 2009)
LacZ	pCS2+	Bacterial *β-galactosidase*	(Smith and Harland, 1991)
lifeact-RFP	pCDNA3.1	17 aa of actin-binding protein Abp140 with RFP tag	(Riedl et al., 2008)
mbGFP	pCS2+	GFP with GAP43 myristilation signal, membrane associated	(Moriyoshi et al., 1996)

mbRFP	pCS2+	monomeric RFP fused with 2x Lck membrane localization signal sequence	(Megason and Fraser, 2003)
PTK7-GFP	pCS2+ eGFP	Full-length *X. laevis* PTK7 with eGFP tag	(Wehner et al., 2011)
PTK7-HA	pCS2+	Full-length *X. laevis* PTK7 with HA tag	(Shnitsar and Borchers, 2008)
PTK7-Myc	pCS2+Myc	*X. laevis* PTK7 with Myc tag	(Shnitsar and Borchers, 2008)
ΔkPTK7-GFP	pCS2+ eGFP	*X. laevis* PTK7 without kinase homology domain, eGFP tag	(Wehner et al., 2011)
ΔE1-7PTK7-Myc	pCS2+Myc	*X. laevis* PTK7 lacks immunoglobulin domains 1 to 7 but keeps its signal peptide, with Myc tag	Amplified from PTK7-Myc by circle PCR using primers SP-PTK7_SacI_rw and TM-PTK7_SacI_fw. PCR product was cut with SacI, followed by T4 ligation.
ΔE1-7PTK7-GFP	pCS2+	*X. laevis* PTK7 lacks immunoglobulin domains 1 to 7 but keeps its signal peptide, with eGFP tag	Myc tag was cut out with ClaI/XbaI, eGFP from PTK7-GFP (cut with ClaI/XbaI) was ligated in.
ΔE3-7PTK7-Myc	pCS2+Myc	*X. laevis* PTK7 with deleted immunoglobulin domains 3 to 7, with Myc tag	Amplified from PTK7-Myc by circle PCR using primers IG2-PTK7_SacI_rw and IG7-PTK7_SacI_fw. PCR product was cut with SacI, followed by T4 ligation.
ΔE3-7PTK7-GFP	pCS2+	*X. laevis* PTK7 with deleted immunoglobulin	Myc tag was cut out with ClaI/XbaI and eGFP from

		domains 3 to 7, with eGFP tag	PTK7-GFP (cut with ClaI/XbaI) was ligated in.
cPTK7-HA	pCS2+ HA	PTK7 cytoplasmic domain, started with first Met after transmembrane domain, with HA tag	Constructed by I. Shnitsar, amplified with BamHI and ClaI restriction sites and inserted into pCS2+HA .
cPTK7-GFP	pCS2+ eGFP	PTK7 cytoplasmic domain with eGFP tag	cPTK7 was cut of cPTK7-HA with BamHI and XhoI and inserted into BamHI/XhoI sites of pCS2+ eGFP.
PTK7-CYFP	pCS2+	*X. laevis* PTK7 with c-terminal CYFP tag, linked with Myc tag	PTK7 was amplified using Primers BamHI-Start-PTK7_f and XhoI-PTK7_r and inserted into BamHI/XhoI restriction sites of Myc-CYFP/pCS2+.
PTK7-NYFP	pCS2+	Full-length PTK7 with NYFP tag, linked with HA tag	PTK7 was generated using BamHI-Start-PTK7_f and XhoI-PTk7_r primer and ligated into BamHI/XhoI restriction sites of HA-NYFP/pCS2+.
PTK7-mEos	pCS2+	Full-length *X. laevis* PTK7 with mEos FP tag	PTK7 was amplified using the primers BamHI-Start-PTK7_f and PTK_no-st_Cla_r and ligated into BamHI/ClaI restriction sites of mEos/pCS2+.
Ror2-HA	pCS2+ HA	Mouse Ror2 with HA tag	(Podleschny et al., 2015)
Tcf3ΔC-GR	pCS2+	*Xenopus* Tcf3A with depleted CtBP binding domain and a	(Maj et al., 2016)

		glucocorticoid receptor tag	
HA-hTrio	pMT. HAtag	Full-length human Trio with N-terminal HA tag	(Medley et al., 2003)
GFP-hTrio	pEGFP-N1	Full-length human Trio with N-terminal eGFP tag	(Moore et al., 2013)
Twist	pGEM-T	Full-length *X. laevis* Twist	(Hopwood et al., 1989)
Venus YFP	pUAST	Yellow fluorescent protein with venus substitution	Gift from S. Önel
CYFP-Myc (cloning)	pCS2+	C-terminal venus YFP fragment (aa 158-240) with Myc tag, no stop codon (for cloning)	Generated from venus YFP with following primers: BamHI-Sta-CYF_f and XhoI-CYFP-MT_r; ligated into BamHI/XhoI restriction sites of pCS2+.
Myc-CYFP (cloning)	pCS2+	Myc tag to C-terminal venus YFP fragment (aa 158-240), no start codon (for cloning)	Amplified from venus YFP using the primers XhoI-MT-CYFP_f and XbaI-Stop-CYFP_r and inserted into XhoI/XbaI restriction sites of pCS2+.
Myc-CYFP (control)	pCS2+	Myc tag to C-terminal venus YFP fragment (aa 158-240) with start and stop codon (for control)	Generated from venus YFP with BamHI-ATG-MT_f and XbaI-Stop-CYFP_r primer, ligated into BamHI/XbaI restriction sites of pCS2+.
NYFP-HA (cloning)	pCS2+	N-terminal venus YFP fragment (aa 1-157) with Myc tag, no stop codon (for cloning)	Amplified from venus YFP using BamHI-Sta-NYF_f and XhoI-NYFP-HA_r primer, ligated into

			BamHI/XhoI restriction sites of pCS2+.
HA-NYFP (cloning)	pCS2+	HA tag to N-terminal venus YFP fragment (aa 1-157), no start codon (for cloning)	Amplified from venus YFP using the primers XhoI-HA-NYFP_f and XbaI-Stop-NYFP_r and inserted into XhoI/XbaI restriction sites of pCS2+.
HA-NYFP (control)	pCS2+	HA tag to N-terminal venus YFP fragment (aa 1-157) with start and stop codon (for control)	Generated from venus YFP using the primer: BamHI-ATG-HA_f and XbaI-Stop-NYFP_r, inserted into BamHI/XbaI restriction sites of pCS2+.

Tab. 2: Linearization of DNA constructs and *in vitro* transcription for mRNA synthesis

Construct	Restriction enzyme	Polymerase
Myc-Dsh	NotI	SP6
DshΔDIX	NotI	SP6
DshΔPDZ	NotI	SP6
DshΔDEP	NotI	SP6
H2B-mcherry	NotI	SP6
LacZ	NotI	SP6
lifeact-RFP	DraIII	T7
mbGFP	NotI	SP6
mbRFP	NotI	SP6
PTK7-GFP	NotI	SP6
PTK7-HA	NotI	SP6
PTK7-Myc	NotI	SP6
ΔkPTK7-GFP	NotI	SP6
ΔE1-7PTK7-Myc	NotI	SP6
ΔE1-7PTK7-GFP	NotI	SP6
ΔE3-7PTK7-Myc	NotI	SP6
ΔE3-7PTK7-GFP	NotI	SP6
cPTK7-HA	NotI	SP6

cPTK7-GFP	NotI	SP6
PTK7-CYFP	NotI	SP6
PTK7-NYFP	NotI	SP6
PTK7-mEos	NotI	SP6
Ror2-HA	NotI	SP6
Tcf3ΔC-GR	NotI	SP6

Tab. 3: Linearization of plasmids and *in vitro* Transcription of *in situ* probes

Construct	**Restriction enzyme**	**Polymerase**
AP-2	HindIII	T7
Twist	EcoRI	T7

2.10 Oligonucleotides

2.10.1 Cloning Primer

Cloning oligonucleotides were purchased from Eurofins Genomics (Ebersberg). The primer sequence is given in 5'→3' direction. The enzyme restriction sites are indicated in underlined bold letters and the HA or Myc overhang are marked in blue letters.

BamHI-ATG-HA_f: tact**GGATCC**ATGTACCCTTACGATGTACCGGA

BamHI-ATG-MT_f: tact**GGATCC**ATGGAACAAAAACTCATCTCAGA

BamHI-Sta-CYF_f: agct**GGATCC**ATGCAGAAGAACGGCATCAAGGT

BamHI-Sta-NYF_f: tact**GGATCC**ATGGTGAGCAAGGGCGAGGA

BamHI-Start-PTK7_f: tt**GGATCC**ATGGGGCCGATTGTGCTC

Eos_ClaI_f: cact**ATCGAT**AGTGCGATTAAGCCAGACAT

Eos-XhoI_r: tacc**CTCGAG**TTATCGTCTGGCATTGTCAGGCA

IG2-PTK7_SacI_rw atct**GAGCTC**CAGGGTGAAGTTGCGATT

PTK7_no-st_Cla_r: ccat**ATCGAT**CCCTTGTGTCTTGCTGCC

SP-PTK7_SacI_rw ttgc**GAGCTC**AGTAAATAGGATAGCTGCTCT

TM-PTK7_SacI_fw taat**GAGCTC**GCCTGTGACATCAAGCAC

XbaI-Stop-CYFP_r: gaat**TCTAGA**TTACTTGTACAGCTCGTCCATGC

XbaI-Stop-NYFP_r: taat**TCTAGA**TTACTTGTCGGCGGTGATAT

XhoI-CYFP-MT_r: gaat**CTCGAG**CAGATCCTCTTCTGAGATGAGTTTTTGTTCC TTGTACAGCTCGTCCATGC

XhoI-HA-NYFP_f: tact**CTCGAG**TACCCTTACGATGTACCGGATTACGCAGTGA GCAAGGGCGAGGAGCT

XhoI-MT-CYFP_f: agct**CTCGAG**GAACAAAAACTCATCTCAGAAGAGGATCTGCAGAAGAACGGCATCAAGGT

XhoI-NYFP-HA_r: taat**CTCGAG**TGCGTAATCCGGTACATCGTAAGGGTACTTGTCGGCGGTGATATAGAC

XhoI-PTK7_r: ccat**CTCGAG**CCCTTGTGTCTTGCTGCC

2.10.2 Morpholino oligonucleotides

Antisense Morpholino oligonucleotides (Morpholinos, MO) were purchased from Gene Tools, LLC (Philomath, USA). MOs were dissolved in RNase-free water to a concentration of 80 mg/10 ml and stored at 4 °C. The MOs were heated up at 65 °C for 5 min prior to every use. The sequences of the MOs are presented in table 4. The used PTK7 MO is a combination of 2 MOs, which bind to different target sites at the 5' UTR of PTK7.

Tab. 4: Antisense Morpholino oligonucleotides

Morpholino name	**Target gene**	**Sequence 5'→3'**	**Citation**
PTK7 MO2	*X. laevis* PTK7	TGCATCGCGGCCTCTCCCCTCA	(Wehner et al., 2011)
PTK7 MO3	*X. laevis* PTK7	TTCCTGCCCCGGATCCTCTCACTGC	
Trio MO	*X. laevis* Trio	TTTTTTTCAGCTGTAGCTATGCGCA	(Moore et al., 2013)
Standard Control oligo-nucleotide	Negative control oligo-nucleotide	CCTCTTACCTCAGTTACAATTTATA	

2.11 Antibodies

Antibodies used for immunofluorescence (IF), western blot (WB) and immunoprecipitation (IP) are listed in table 5.

Tab. 5: Antibodies used during this study.

Name	Company	Antibody type	Dilution		
			IF	WB	IP
α-β-Catenin	Gift from R. Rupp	Primary rat antibody against β-Catenin	1:50		
α-GFP	Roche, 11814460001	Primary mouse monoclonal antibody against GFP	1:1000	1:1000	
α-GFP	Abcam, ab290	Primary rabbit polyclonal antibody against GFP	1:1000	1:2000	1:250
α-HA	Covance, MMS-101P	Primary mouse monoclonal antibody against HA	1:500	1:1000	1:150
α-HA	Abcam, ab9110	Primary rabbit polyclonal antibody against HA		1:1000	1:150
α-Myc	Abcam, ab19234	Primary goat polyclonal antibody against Myc	1:250	1:1000	1:250
α-Myc (9E10)	Sigma, M5546	Primary mouse monoclonal antibody against C-myc		1:2000	
α-Rac1	BD Biosciences, 610651	Primary mouse monoclonal antibody to human Rac1		1:1000	
α-RhoA	Santa Cruz, sc-418	Primary mouse monoclonal antibody against aa 120-150 of human RhoA		1:500	
α-goat Alexa Fluor® 488	Thermo Fisher Scientific,	Secondary donkey anti goat IgG coupled with Alexa Fluor® 488	1:400		

	A-11055				
α-rabbit Alexa Fluor® 488	Thermo Fisher Scientific, A-11008	Secondary donkey anti rabbit IgG coupled with Alexa Fluor® 488	1:400		
α-goat Alexa Fluor® 594	Thermo Fisher Scientific, A-11058	Secondary donkey anti goat IgG coupled with Alexa Fluor® 594	1:400		
α-rabbit Alexa Fluor® 594	Thermo Fisher Scientific, A-11012	Secondary goat anti rabbit IgG coupled with Alexa Fluor® 594	1:400		
α-rat Alexa Fluor® 594	Thermo Fisher Scientific, A-21209	Secondary donkey anti rat IgG coupled with Alexa Fluor® 594	1:400		
α-mouse Alexa Fluor® 488	Thermo Fisher Scientific, A-11005	Secondary goat anti mouse IgG coupled with Alexa Fluor® 488	1:400		
α-goat-IRDye®680	LI-COR, 926-68074	Secondary donkey anti goat IgG coupled with IRDye 680CW		1:7500	
α-goat-IRDye®800	LI-COR, 926-32214	Secondary donkey anti goat IgG coupled with IRDye 800CW		1:7500	
α-mouse-IRDye®680	LI-COR, 926-32212	Secondary donkey anti mouse IgG coupled with IRDye 680CW		1:7500	
α-mouse-IRDye®800	LI-COR, 926-68072	Secondary donkey anti mouse IgG coupled with IRDye 800CW		1:7500	

α-mouse-HRP	Santa Cruz, sc-516102	Secondary goat anti mouse IgG coupled with horseradish peroxidase		1:5000	
α-rabbit-IRDye®680	Li-COR, 956-68073	Secondary donkey anti rabbit IgG coupled with IRDye 680CW		1:7500	
α-rabbit-IRDye®800	Li-COR, 926-32213	Secondary donkey anti rabbit IgG coupled with IRDye 800CW		1:7500	

2.12 DNA methods

2.12.1 DNA restriction digestion

The restriction digestion of the DNA was performed with restriction endonuclease enzymes (Thermo Scientific) according to the manufacturer's protocol. The digested DNA were purified with the GenJet PCR Purification Kit or purified after agarose gel electrophoresis (3.12.2).

2.12.2 Agarose gel electrophoresis

To separate DNA or RNA fragments, standard agarose gel electrophoresis was used. A 1% agarose gel was made, which contained GelRed™ (1:20000) to visualize the DNA or RNA bands. 1x TAE buffer was used as running buffer. The samples were mixed with DNA Gel Loading Dye and were loaded on the gel. Additionally, a DNA Ladder (Thermo Scientific) was loaded on the gel. For purification of desired DNA fragments obtained by DNA restriction digestion or PCR, the DNA fragment was cut of the agarose gel and purified with the Zymoclean™ Gel DNA Recovery Kit or with the GenJet Gel Extraction Kit according to the manufacturer's protocol.

2.12.3 Polymerase chain reaction (PCR)

To amplify DNA fragments a standard PCR reaction was used (Mullis et al., 1986). For cloning procedure, the Phusion High-Fidelity DNA Polymerase was utilized and the DreamTaq™ DNA Polymerase for analytical DNA amplification. The standard PCR reaction were carried out according to manufacturer's instructions.

2.12.4 DNA ligation

For DNA ligation the T4 DNA Ligase was used according to the manufacturer's protocol. The total amount of vector DNA was 50-100 ng and the molar ratio of vector and insert DNA was 1:3. The ligation was performed overnight at 16 °C.

2.12.5 Chemical transformation of bacterial cells

200 µl chemical competent *E. coli* XL1blue cells were thawed on ice. 5 µl ligation mixture or 100 ng of plasmid DNA were added to the bacteria and incubated for 30 min on ice. Afterwards a heat-shock for 60 s at 42 °C was performed. Immediately after the heat-shock the bacteria were incubated on ice for 2-5 min. 800 µl of pre-warmed LB medium was added to the cells and then incubated at 37 °C for 40-60 min. 200 µl of the medium were plated on LB-Amp plates for the selection of transformed cells. The colonies were grown overnight at 37 °C.

2.12.6 Plasmid DNA preparation

For plasmid DNA preparation 5 ml or 50 ml LB medium with appropriate antibiotic (100 µg/ml Ampicillin or 50 µg/ml Kanamycin) was inoculated with one *E. coli* colony. Bacteria were grown over night at 37 °C and 220 rpm. Isolation of plasmid DNA from bacteria cultures was performed with the GenJet Plasmid Miniprep Kit or the NucleoBond® Xtra Midi Kit according to the manufacturer's instructions. The DNA was eluted in 50 µl H_2O and the concentration was measured using the NanoDrop™ 2000 Spectrophotometer (Thermo Fisher Scientific). Afterwards the DNA was sent for sequencing to Eurofins GATC (Cologne) according to the manufacturer's instructions.

2.13 RNA methods

2.13.1 *In vitro* transcription of sense capped mRNA

For microinjections of *Xenopus* embryos sense capped mRNA was synthesized using the SP6 mMESSAGE mMACHINE® System according to the manufacturer's protocol. The synthesized RNA was purified with the illustra™ RNAspin Mini RNA Isolation Kit after the manufacturer's instructions. The RNA was eluted in 30 µl H_2O (RNase-free) and stored at -80 °C. The RNA concentration was measured using the NanoDrop™ 2000 Spectrophotometer and RNA quality was controlled by loading 1 µl RNA on a 1% agarose gel (3.12.2).

2.13.2 *In vitro* transcription of labeled antisense RNA

The following reaction mixture was used for the synthesis of digoxigenin labeled antisense RNA for whole-mount *in situ* hybridization:

5 µl linearized DNA template
2 µl T7 RNA Polymerase
2 µl DTT (0.75 M)
2 µl RNaseOUT
8 µl Digoxigenin-11-UTP
8 µl 5x transcription buffer
13 µl H_2O (RNase-free)

The incubation took place at 37 °C for 2.5 h followed by 15 min treatment with 1 µl TURBO DNase I (Ambion). The synthesized RNA was purified using the illustra™ RNAspin Mini RNA Isolation Kit according to the manufacturer's protocol. The quality of the RNA probe was controlled by loading 1 µl of the RNA on a 1% agarose gel (3.12.2). The RNA probe was stored in hybridization mix at -20 °C.

2.14 *Xenopus* methods

2.14.1 Preparation of *Xenopus laevis* testis

The *Xenopus* male was placed into benzocaine (0.05%) for 15-20 min at room temperature. Afterwards the frog was decapitated and the testes were removed. The testes were washed with 1x MBS and stored in fresh 1x MBS at 4 °C.

2.14.2 *Xenopus* culture and microinjection

X. laevis female frogs were injected into the dorsal lymph sac with 500 units human chorionic gonadotropin (hCG, Sigma-Aldrich) hormone. Egg collection, *in vitro* fertilization, de-jellying and cultivation of embryos were performed as described in (Sive et al., 2000). Albino embryos were stained with Nile blue dye to distinguish between the animal and vegetal pole of the embryos and for classification of the developmental stages. The developmental stages were defined according to (Nieuwkoop and Faber, 1994). Before injection, the embryos were placed in injection buffer. The mRNA or DNA and MOs were injected animally into one blastomere of one or two-cell stage embryos or into the dorsal blastomere of eight-cell stage embryos. The injected volume was 10 nl for one or two-cell or 4 nl for eight-cell injections. After the injection procedure, the embryos were kept in injection buffer for at least 20 min before they were washed 3 times with 0.1x MBS and cultured in 0.1x MBS at 14-18 °C. Dexamethasone treatment took place at stage 13 according to (Maj et al., 2016).

2.14.3 X-Gal staining and Whole-mount *in situ* hybridization (WMISH)

To determine the injected side *LacZ* RNA were co-injected as a lineage tracer. When Embryos reach the desired developmental stage, the embryos were fixed for 30 min in MEMFA and washed 3 x 10 min with PTw afterwards. The LacZ staining were performed as described in (Sive et al., 2000). The LacZ staining was followed by MEMFA fixation overnight at room temperature and was replaced by EtOH afterwards. To visualize the NC cells *in vivo* a WMISH against *twist* or *AP-2* were performed. The WMISH is based on the Harland Lab protocol (Harland, 1991). For bleaching of pigmented embryos, embryos were washed 3 x 5 min with 2x SSC and bleached in 1% H_2O_2/5% Formamide/0.5x SSC until the embryos lost their natural pigment. Afterwards, the embryos were re-fixed for 30 min in MEMFA and washed 3 x 10 min with PTw. The embryos were documented using a Leica M165FC microscope and a Leica DFC450C camera. Analyzed embryos were stored in EtOH at 4 °C.

2.14.4 Cranial neural crest explants

Explantation of NC cells was carried out as described in (Borchers et al., 2000; Maj et al., 2016). The explants were incubated for at least 30 min at 14 °C to ensure adherence of the cells. Propidium iodide (10 µg/ml) staining was carried out 5 h after explantation. Time-lapse analysis of NC cell migration or protein localization in NC cells was performed with spinning disc microscopy (Podleschny et al., 2015).

2.14.5 Immunostaining of ectodermal explants

In addition to the explants used for live cell imaging, NC explants were prepared for immunostaining. Therefore, NC explants were cultured on fibronectin (10 µg/ml in PBS) coated chamber slides or cover glass (Maj et al., 2016). The explants were incubated for at least 3 h at room temperature, if not indicated otherwise, and then fixed. For fixation the explants were incubated in MEMFA (β-catenin staining) or 4% PFA/PBS for 11 min. Afterwards, the explants were washed 3 x 10 min with PTw and stained according to the following protocol:

- Blocking with 10% fetal bovine serum (FBS) in PTw for 1 h at room temperature or overnight at 4 °C
- Incubation with primary antibody diluted in blocking buffer overnight at 4 °C
- 3 x 10 min PTw
- Secondary antibody in blocking buffer for 2 h at room temperature
- 3 x 10 min PTw
- DAPI staining (1 µg/ml DAPI in PTw) for 10 min

The explants on the cover glass were embedded in fluorescent mounting medium (Dako) and the explants in chamber slides were stored in Pen/Strep/PBS at 4 °C. Protein localization was analyzed using fluorescence microscope (Axio Observer Z1 with Apotome, Zeiss), confocal laser scanning microscope (Leica TCS *SP5*) or spinning disk microscope (Zeiss AxioObserver.Z1).

2.14.6 Image analysis of NC cells

Image analysis of NC cells was performed using Zen blue, ImageJ, Fiji or Matlab software. The nuclear fluorescent intensity of β-catenin was measured using ImageJ. Therefore, the area of each nucleus was determined by DAPI staining and the Integrated Density of β-catenin fluorescent signal was measured. The Integrated Density of each cell of a particular condition were averaged and normalized to NC cells injected with control MO. The fluorescent intensity of membrane β-catenin were measured using plot profile in Fiji. Therefore, a line was drawn from a nucleus of one cell to the nucleus of a neighboring cell. The fluorescent intensity of β-catenin was measured and plotted from the membrane and up to 2 µm away from the membrane. The fluorescent intensity of membrane β-catenin was measured from 5 random cells per explant. Live cell images were analyzed by measuring the cell dispersion, single cell velocity, cell contact time during collision and changes in the direction of migration after collision. The dispersion of NC cells was measured using the Delaunay triangulation plugin in ImageJ and Matlab. Single cell velocity was calculated by ImageJ using Manual Tracker and Chemotaxis Tool plugin. Changes in the direction of migration after cell collision of single NC cells was analyzed using custom-made Matlab script (see appendix, kindly provided by S. Becker (Becker et al., 2013)). The change in the location of the cells after cell-cell contact was determined. The coordinates of the cells before (t-Δt), during (t) and after the cell-cell contact (t+Δt') (fig. 13) were determined by manual tracking with ImageJ. The time

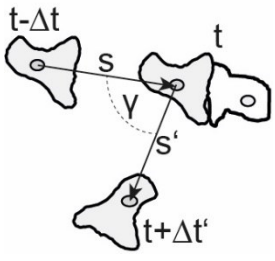

Fig. 13: Collision analysis. Schematic overview of analysis of velocity and the change of direction of single NC cells after cell-cell contact. With the coordinates before (t-Δt), during (t) and after the cell-cell contact (t+Δt') and the time interval the velocity and the changed angle after collision (γ) can be calculated.

interval (Δt and Δt') was determined with Zen blue software. The velocity (v=s'/Δt') and the changed angle (γ) after cell-cell contacts (fig. 13) were illustrated as vector diagrams

and show the change of the direction of migration of 9 different NC cells of 3 independent experiments.

2.15 Cell culture methods

2.15.1 Propagation of HEK293 and MCF7 cells

HEK293 and MCF7 cells were kept in 75 cm^2 cell culture flask with appropriate cell culture medium. The cells were cultured in a sterile incubator at 37 °C, 5% CO_2 and 95% humidity. The cells were split one to two times a week with a subcultivation ration of 1:10. At first, the cells were rinsed once with 1x PBS. Afterwards, trypsin-EDTA (0.025% Trypsin, 0.53 mM EDTA) was added to the cells for 5-10 min at 37 °C to detach cells from the flask. An addition of cell culture medium stops trypsin activation and an appropriate volume of the cell suspension was transferred into a new cell culture flask containing medium. For long term storage cells were frozen in FCS supplemented with 10% DMSO in cryotubes (Nunc™, Thermo Scientific) and kept in liquid nitrogen.

2.15.2 Cell transfection using jetPEI®

DNA transfection of cell culture cells were performed with jetPEI® DNA transfection reagent. Briefly, one day before transfection cells were plated into an appropriate culture vessel to reach a confluence of 50-70% at the time of transfection (see table 6). For protein extraction, cells were seeded in 25 cm^2 culture flask. For localization assays, cells were seeded on glass coverslips in 24-well plates. On the day of transfection, the medium was exchanged and transfection were performed using jetPEI® according to manufacturer's instructions.

Tab. 6: Volume of culture media, amount of DNA and jetPEI®

Culture vessel	Volume of medium	Amount of DNA (µg)	Volume of jetPEI® (µl)
24-well	500 µl	0.5-1	2
6 cm/25 cm^2	5 ml	0.7-4	6-10

2.16 Protein techniques

2.16.1 Preparation of protein extracts from mammalian cell lines

Cells were washed twice in cold 1x PBS and lysed in cold NOP buffer. Therefore, cells were scraped in 300 µl NOP buffer from the surface of the cell culture flask. The cells were transferred immediately into a 1.5 ml reaction tube and lysed by pushing the cells five times through a 27 G syringe and incubation for 30-45 min at 4 °C on an end-over-end rotator. After centrifugation for 15 min at 13000 rpm and 4 °C, the supernatant was transferred into a new reaction tube. Protein extracts were used for co-

immunoprecipitation or mixed with 6x Laemmli buffer, heated for 5 min at 95 °C and analyzed by western blotting or stored at -20 °C.

2.16.2 Co-immunoprecipitation (co-IP)

Co-IPs were performed using Dynabeads® Protein G beads (Thermo Scientific) according to manufacturer's protocol. For Trio IP a few changes were made. Briefly, protein lysates were incubated with indicated antibody for 2 h at 4 °C on an end-over-end rotator. Afterwards, the lysates were added to 40 µl Dynabeads® and incubated for 30 min at 4 °C on an end-over-end rotator. At last the beads were washed 3 x with 500 µl 0.02% Tween-20/PBS. The beads were mixed with 20 µl 6x Laemmli loading buffer, heated for 5 min at 95 °C and stored at -20 °C.

2.16.3 Rho GTPase pull down activation assay

Xenopus embryos were co-injected with DNA, RNA or MO together with 0.25 µg/µl Fluorescein-Dextran to distinguish injected from un-injected embryos. Control embryos were injected only with Fluorescein-Dextran. 25 embryos of stage 20-22 were collected for each condition and lysate in 250 µl Rac-RIPA buffer. As a positive control, lysates of wild type embryos were incubated with GTPγS (Sigma-Aldrich) according to manufactures' instruction. Rho or Rac pull down assay were performed as described in (Benard et al., 1999; Ren et al., 1999). GST-PAK and GST-RBD Protein were kindly provided by K. Giehl. Samples were heated for 5 min at 95 °C and stored at -20 °C.

2.16.4 Protein electrophoresis (SDS-PAGE)

To separate denatured proteins according to their size in an electric filed the SDS-polyacrylamide gel electrophoresis (SDS-PAGE) was performed (Laemmli, 1970). The protocol from (Russell and Sambrook, 2001) was used to prepare 7%, 8% or 12% polyacrylamide gels. Before loading on the SDS polyacrylamide gel, protein extracts were heated for 2 min at 95 °C. A maximum volume of 20 µl of protein extracts and 5 µl protein marker were loaded on SDS polyacrylamide gels. The BioRad Mini Protean Tetra Cell system was used for SDS-PAGE according to manufacturer's instructions. Initially, the electrophoresis started with 80 V. When the proteins reached the separation gel (visualized by the buffer front) the voltage were increased up to 120 V.

2.16.5 Western blotting

The separated proteins in polyacrylamide gels were transferred by electro-blotting onto a nitrocellulose blotting membrane (0.45 µm, Amersham Protran®) (Towbin et al., 1979). The wet blotting procedure was performed using the Mini Trans-Blot® Cell System (Bio-Rad) at 100 V for 1 h (proteins <50 kDa) or 1.5-2 h (proteins >50 kDa) according to manufacturer's protocol. Subsequently, the nitrocellulose membrane was blocked with TBST + 5% (w/v) milk powder for 1 h at room temperature on a shaker. Afterwards the nitrocellulose membrane was incubated with the appropriated antibody overnight at 4 °C. The antibodies were diluted in TBST + milk powder (or 3% BSA/TBST for GTPase antibody) as indicated in table 5. Unbound antibodies were washed off the membrane by washing 3 x 5-10 min with TBST. Secondary antibody coupled with horseradish peroxidase (HRP) were incubated on the membrane for 2 h at room temperature followed by 3 x 10 min washing steps with TBST. Finally, the membrane was incubated with the chemiluminescent substrate SuperSignal® West Dura Extended Duration (Thermo Scientific) according to manufacturer's protocol. The chemiluminescent signal was detected by LI-COR Odyssey Fc System. When infrared-coupled secondary antibodies were used, a few steps have been modified to reduce background signal of the nitrocellulose membrane. First, the nitrocellulose membrane was air dried after electro-blotting for 1 h at room temperature. Second, instead of TBST the TBS buffer were used and all steps were performed in the dark. The LI-COR Odyssey Fc System detected the infrared signal.

3. Results

3.1 PTK7 loss of function can be rescued by overexpression of Ror2

PTK7 functions in NC cell migration but its signaling mechanism in NC migration has not been investigated yet. Recent studies show that PTK7 and the Wnt receptor Ror2 can interact via their extracellular domains and co-localize in NC cells (Martinez et al., 2015; Podleschny et al., 2015). Because Ror2 has similar functions as PTK7 in canonical and non-canonical Wnt signaling (Berger et al., 2017a; Billiard et al., 2005; Oishi et al., 2003; Schambony and Wedlich, 2007), it has been investigated if Ror2 can substitute PTK7 in NC migration. Therefore, *Xenopus* embryos were injected with control MO or PTK7 MO alone and in combination with *Ror2* RNA together with membrane-targeted GFP (*mbGFP*) and mcherry-tagged H2B (*H2B-mcherry*) to visualize cell shape and polarity of NC cells. NC cells were explanted, cultured on a fibronectin coated chamber slide and NC cell migration were analyzed by spinning disc microscopy (fig. 14, movie 1). At the beginning of imaging (0 h), NC cell clusters are about the same size (fig. 14 A-D). After 4 and 8 h of imaging, NC cells with control MO and in combination with Ror2 dispersed rapidly (fig. 14 A, B). Tracking of individual cells over the time period of imaging shows that single NC cells detached from the cell cluster and dispersed (fig. 14 A and B middle panel). In addition, cell dispersion of the whole NC clusters was illustrated by Delaunay triangulation (fig. 14 A and B lower panel). By using the Delaunay triangulation all nearest neighbors are connected and their spatial proximity is quantified (Chen et al., 2014a). NC cells with PTK7 depletion could not migrate properly (fig. 14 C). The NC cluster stayed about the same size during the 8 h of imaging and only few cells detached from the cluster. Overexpression of Ror2 in PTK7 morphant NC cells rescued the NC migration defects as illustrated by time-lapse imaging, cell tracking and Delaunay triangulation (fig. 14 D). In addition, quantification of NC cell migration shows that overexpression of *Ror2* in PTK7 morphant NC cells significantly reduced NC migration defects (fig. 14 E).

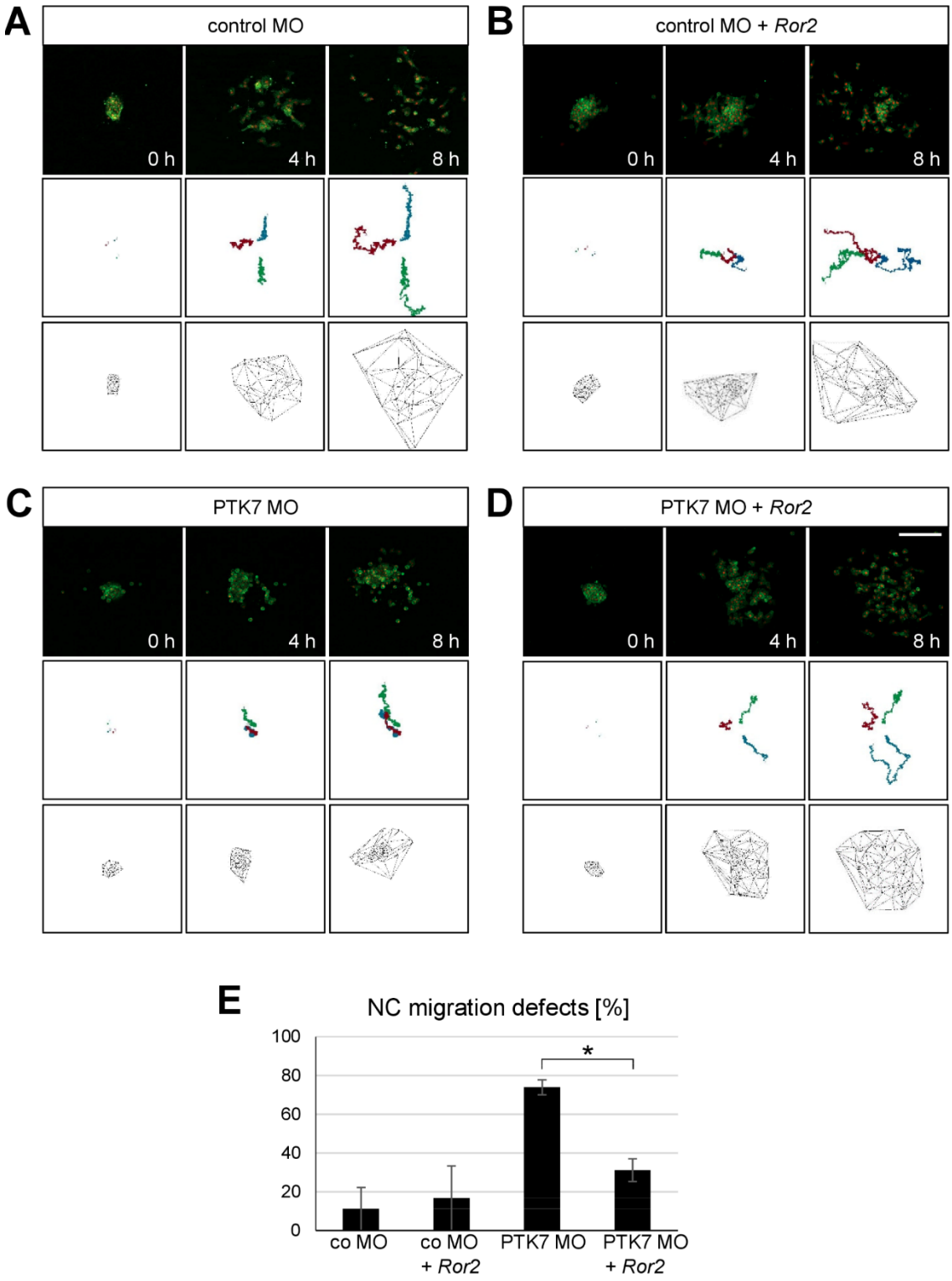

Fig. 14: The PCP receptor Ror2 rescues the NC cell migration defect caused by PTK7 loss of function *in vitro*. Embryos were co-injected with 7.5 ng MO, 50 pg *mbGFP*, 250 pg *H2B-mcherry* and 150 pg *Ror2* RNA in one blastomere at two-cell stage. NC cells were explanted at stage 16 and cultured for 2 h before imaging. **A-D** Time-lapse images (upper panel), cell tracking (middle panel) and Delaunay triangulation (lower panel) are shown for the various settings. Scale bar = 200 µm. **E** Graph summarizing percentage of migration defects of 3 independent experiments (total of 39 explants). Standard error of the means (s.e.m) are shown. Asterisk indicates a *p*-value in a Student's t-test < 0.05.

3.2 PTK7 does not appear to inhibit canonical Wnt signaling during NC cell migration

PTK7 and Ror2 are both able to inhibit the canonical and activate the non-canonical Wnt pathway (Berger et al., 2017a; Billiard et al., 2005; Oishi et al., 2003; Schambony and Wedlich, 2007). For NC cell migration it is crucial to inhibit canonical Wnt signaling as an over-activation of canonical Wnt signaling leads to NC cell migration defects (Maj et al., 2016; Rabadán et al., 2016). On the other hand, the non-canonical Wnt pathway is active during NC cell migration (see review (Mayor and Theveneau, 2014)). Since Ror2 is able to rescue NC migration defects caused by PTK7 knockdown (fig. 14) it has to be analyzed if PTK7 is important for inhibition of the canonical Wnt pathway or for the activation of PCP signaling during NC cell migration. To analyze if PTK7 affects canonical Wnt signaling in NC cell migration, *Xenopus* embryos were injected with different concentrations of PTK7 MO and glucocorticoid-receptor (GR)- inducible *Tcf3ΔC*. The Tcf3ΔC construct lacks the C-terminal domain of Tcf3 required for CtBP binding and activation of canonical Wnt-mediated gene transcription (Pukrop et al., 2001). Meaning that an activation of Tcf3ΔC-GR by Dexamethasone treatment leads to an inhibition of canonical Wnt signaling (Maj et al., 2016). NC migration was analyzed by whole-mount *in situ* hybridization using the NC marker *twist* (fig. 15). Injection of 7.5 ng of control MO did not lead to NC migration defects (6.6% ± 2.7%) (fig. 15 A, G). Whereas 7.5 ng PTK7 MO led to an inhibition of NC cell migration in 54.0% (± 7.4%) embryos (fig. 15 B, G). Co-injection of 7.5 ng PTK7 MO and 50 pg *Tcf3ΔC-GR* led to a significant increase of NC migration defects up to 78.1% (± 3.7%) (fig. 15 C, G). As co-injection of 7.5 ng PTK7 MO and 50 pg *Tcf3ΔC-GR* led to an increase of NC migration defects lower MO and RNA concentration were injected. Injection of 5 ng control MO did only lead to NC migration defects of 0.6% (± 0.6%) (fig. 15 D, G). Whereas an injection of 5 ng PTK7 MO led to 50.3% (± 12.5%) NC migration defects (fig. 15 E, G). The inhibition of the canonical Wnt pathway by co-injection of 10 pg *Tcf3ΔC-GR* did not significantly decrease the NC migration defects (42.4% ± 3.7%) (fig. 15 F, G).

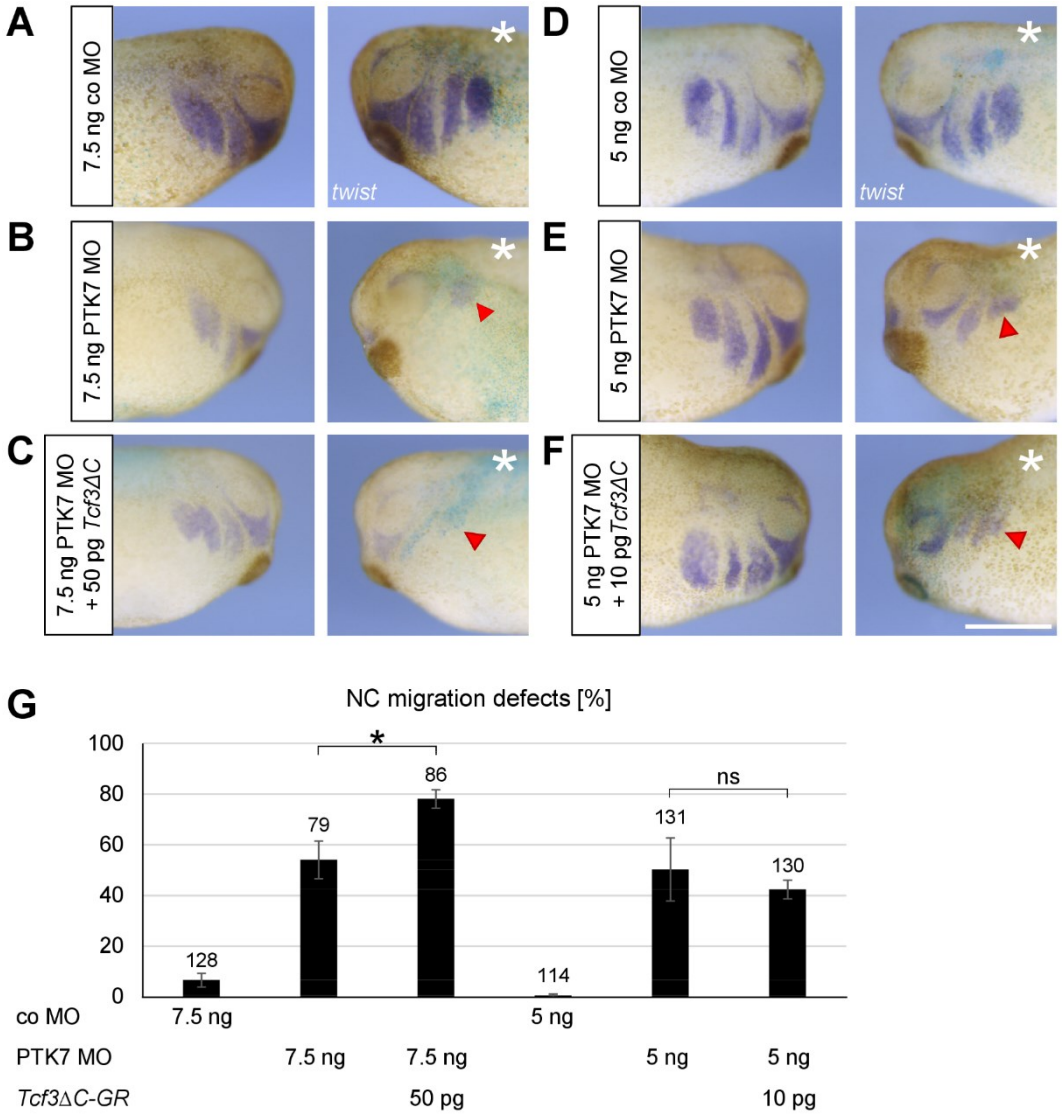

Fig. 15: Inhibition of canonical Wnt signaling does not rescue NC migration defects caused by PTK7 loss of function. *Xenopus* embryos were injected with different MO and RNA concentrations together with 75 pg *LacZ* RNA into one blastomere of two-cell staged embryos and NC cells were analyzed by *twist in situ* hybridization. **A, D** 7.5 and 5 ng control (co) MO does not impact NC migration. **B, E** PTK7 LOF induced by 7.5 ng or 5 ng PTK7 MO leads to NC migration defects. **C, F** Inhibition of the canonical Wnt pathway by 50 or 10 pg *Tcf3ΔC-GR* in PTK7 morphants does not rescue the NC migration defects. Asterisks indicate injected side, red arrowheads indicate inhibited NC migration, scale bar = 500 µm. **G** Graph summarizes percentage of NC migration defects, number of embryos and s.e.m. are indicated for each column, *p<0.05, ns = not significant (Student's t-test).

The NC migration defects caused by PTK7 loss of function do not appear to be improved by inhibition of the canonical Wnt pathway in the tested concentrations (fig. 15). To analyze whether PTK7 activates the canonical Wnt pathway in NC cells in general, β-catenin staining was performed (fig. 16). The nuclear localization of β-catenin is a readout for active canonical Wnt signaling (Barker and van den Born, 2008). In pre-migratory NC cells β-catenin is located in the nucleus and its nuclear localization is reduced during NC cell migration (Maj et al., 2016). To analyze if PTK7 possibly affect

canonical Wnt activity, PTK7-morphant NC cells were explanted and stained for β-catenin. NC cells were explanted at stage 16-18 and cultured for 3-4 h before fixation. β-catenin is predominantly localized at the cell membrane in NC cells with control or PTK7 MO (fig. 16 A, B).

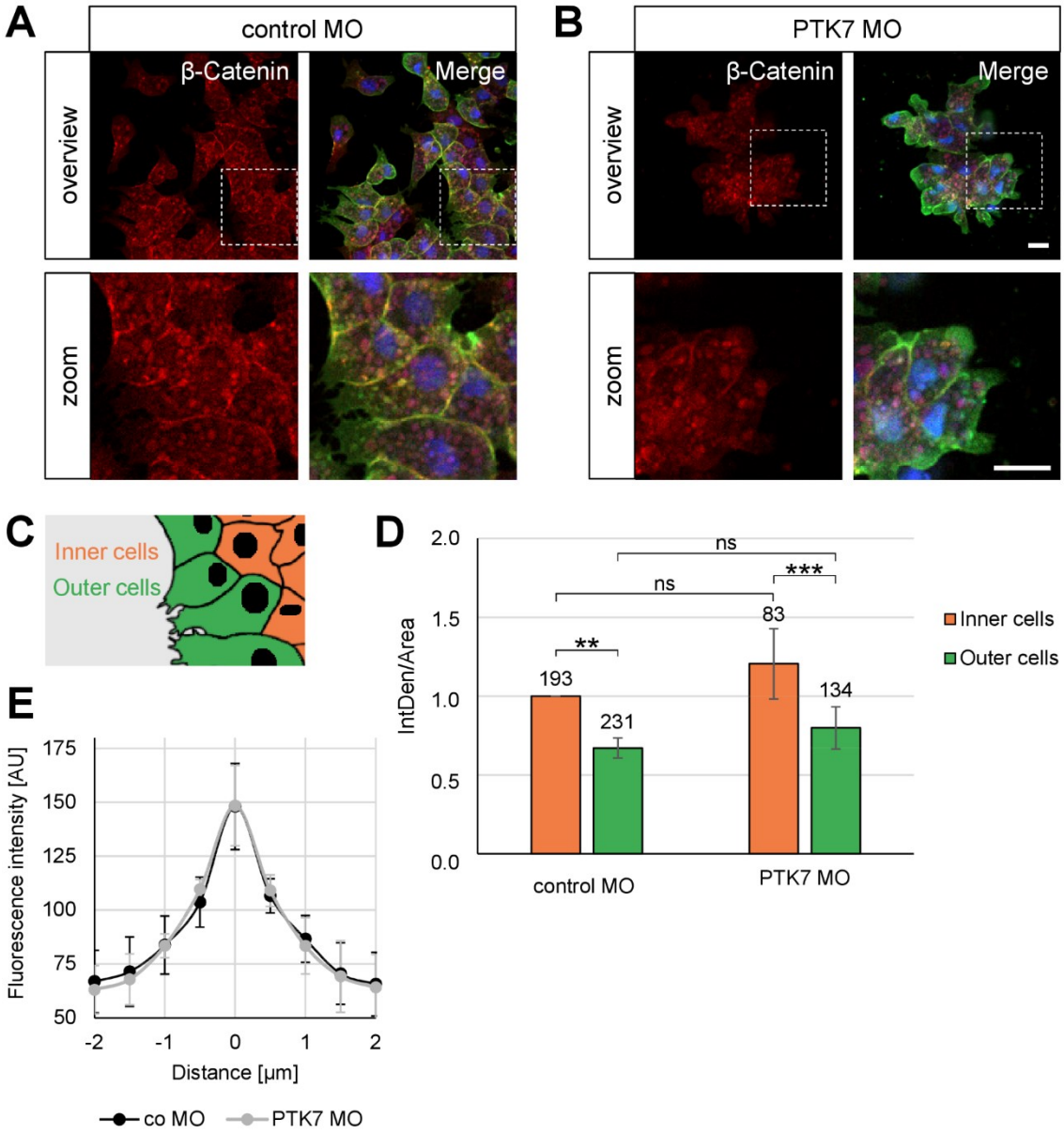

Fig. 16: PTK7 LOF does not lead to β-catenin translocation to the nucleus. Injection of 7.5 ng MO with 50 pg *mbGFP* RNA into one blastomere of two-cell staged embryos. NC cells were dissected at stage 16-18, cultured for 3-4 h and stained with anti-β-Catenin, anti-GFP and DAPI. NC explants with (**A**) control (co) MO and (**B**) PTK7 MO show β-catenin localization at the cell membrane but not in the cell nucleus, scale bars = 20 µm. **C** Schematic figure indicates the classification in outer and inner cells. **D** Graph summarizes averaged Integrated Density (IntDen) of nuclear β-catenin staining of outer and inner cells of three independent experiment. IntDen were normalized to inner cells with co MO. Number of cells and s.e.m. are indicated for each column, $^{**}p<0.01$, $^{***}p<0.001$, ns = not significant (One-Way ANOVA test). **E** β-catenin fluorescence intensity at cell-cell contact (0 µm) for NC cells with co or PTK7 MO. Graphic shows three independent experiments were at least five cells in at least two explants per experiment were analyzed, s.e.m. are shown.

To analyze if membrane localized β-catenin had changed in PTK7 loss of function cells, the fluorescent intensity of β-catenin was measured and plotted from the membrane and up to 2 µm from the membrane. Measurement of the fluorescence intensity of membrane β-catenin shows that β-catenin is not de- or increased at the cell membrane in PTK7-deficient NC cells (fig. 16 E). In the quantification of nuclear β-catenin, a distinction was made between inner and outer NC cells. Inner cells are characterized by being completely surrounded by other NC cells whereas outer cells are at the edge of the cell cluster (fig. 16 C). The graphic shows that the inner NC cells have a significant higher Integrated Density of nuclear β-catenin than outer cells (fig. 16 D). This can be observed in NC cells injected with control MO or PTK7 MO. However, the Integrated Density of nuclear β-catenin in PTK7 morphant NC cells is not significantly higher as in NC cells with control MO. This applies for the inner as well as the outer NC cells (fig. 16 D).

3.3 PTK7 loss of function can be rescued by Dsh

Dsh is a core protein of the canonical as well as the non-canonical Wnt pathway (reviewed in (Mlodzik, 2015)) and interacts with Fz and Ror2 (Medina and Steinbeisser, 2000; Tauriello et al., 2012; Witte et al., 2010; Wong et al., 2003). Dsh also interacts with PTK7 via RACK and PKCδ1 (Shnitsar and Borchers, 2008; Wehner et al., 2011). In addition, PTK7 recruits Dsh to the plasma membrane in ectodermal explants, which indicates activation of non-canonical Wnt signaling (Axelrod et al., 1998; Medina and Steinbeisser, 2000; Rothbächer et al., 2000). To investigate if Dsh acts downstream of PTK7 in NC cell migration rescue experiments were performed and NC migration was analyzed using *twist* and *AP-2 in situ* hybridization (fig. 17). As already shown in previous experiments, injection of control MO had no effect on NC migration (fig. 17 A and B upper panel, C, D) and injection of PTK7 MO led to NC migration defects, which can be seen by an impaired or inhibited NC cell migration (fig. 17 A and B middle panel, C, D). However, co-injection of *Dsh* RNA together with PTK7 MO could partially rescue the NC cell migration phenotype (fig. 17 A and B lower panel). The migration defects decreased to 48.1% (± 4.8%) (*twist*) or to 35.3% (± 5.8%) (*AP-2*) (fig. 17 C, D). Further experiments showed that overexpression of Dsh could also rescue the cell dispersion of PTK7-morphant NC cells *ex vivo* (fig. 17 E, movie 2).

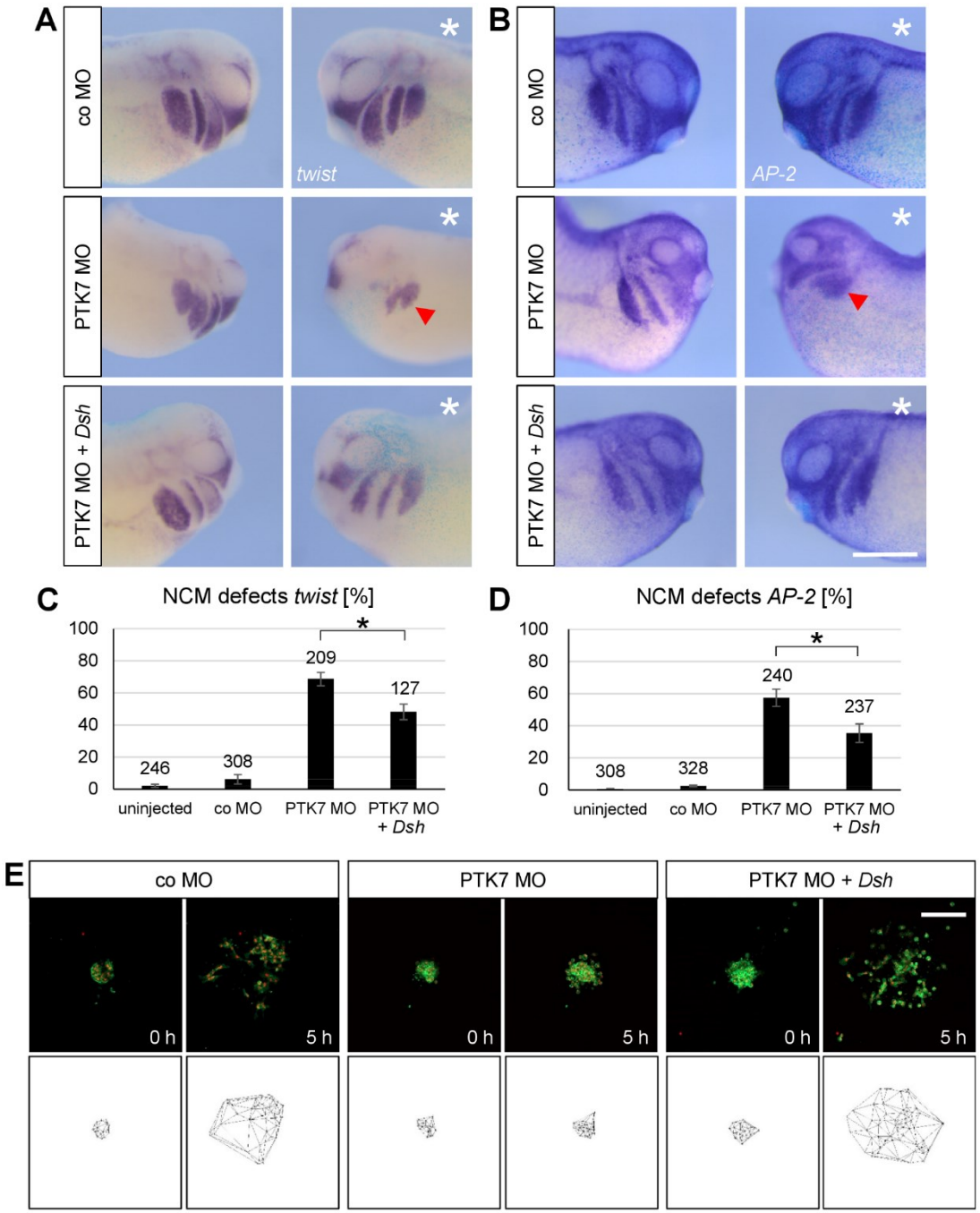

Fig. 17: Co-injection of *Dsh* with PTK7 MO can partial rescue NC cell migration defects. **A-D** Injection of 7.5 ng MO, 150 pg *Myc-Dsh* and 75 pg *LacZ* RNA in one blastomere of two-cell staged embryos. NC cells were marked by (A) *twist* and (B) *AP-2 in situ* hybridization. White asterisks indicate injected side, red arrowheads indicate inhibited NC cell migration, scale bar = 500 µm. **C, D** Graph summarizing percentage of NC migration (NCM) defects of three (*twist*) or five (*AP-2*) independent experiments. Number of embryos and s.e.m. are indicated for each column. Black asterisks indicate *p*-value in a Student's t-test < 0.05. **E** Injection of 2 ng MO, 40 pg *Myc-Dsh*, 15 pg *mbGFP* and 60 pg *H2B-mcherry* RNA in one dorsal blastomere of eight-cell stage embryos. NC cells were dissected at stage 15-17 and cultured for 2.5 h before imaging. Time-lapse images (upper panel) and Delaunay triangulation (lower panel) are shown for the different conditions, scale bar = 200 µm.

3.4 Dsh DIX domain is not involved in PTK7 signaling during NC migration

Dsh is an essential scaffold protein that activates the canonical or non-canonical Wnt pathway by its different domains. Via its DIX domain it can regulate canonical Wnt signaling whereas its DEP domain regulates the non-canonical/PCP pathway (Mlodzik, 2015; Sharma et al., 2018). The PDZ domain is important for both the canonical and PCP pathway. As Dsh can improve NC cell migration of PTK7 knockdown embryos (fig. 17) it is interesting to investigate which domain is necessary for PTK7/Dsh signaling. Therefore, Dsh deletion constructs (fig. 18 A) were co-injected with PTK7 MO and NC cell migration was analyzed by *twist in situ* hybridization (fig. 18). As mentioned earlier, control MO did not influence NC migration whereas PTK7 MO led to NC migration defects (fig. 18 B, C). NC migration defects caused by PTK7 MO could be significantly reduced by co-injection of Dsh, which lacks its DIX domain (46.7% ± 11.8%) (fig. 18 B, C). On the other hand, Dsh constructs lacking the PDZ or DEP domain could not improve NC migration defects in PTK7-morphant embryos (73.4% ± 1.6% or 66.5% ± 7.5%) (fig. 18 B, C).

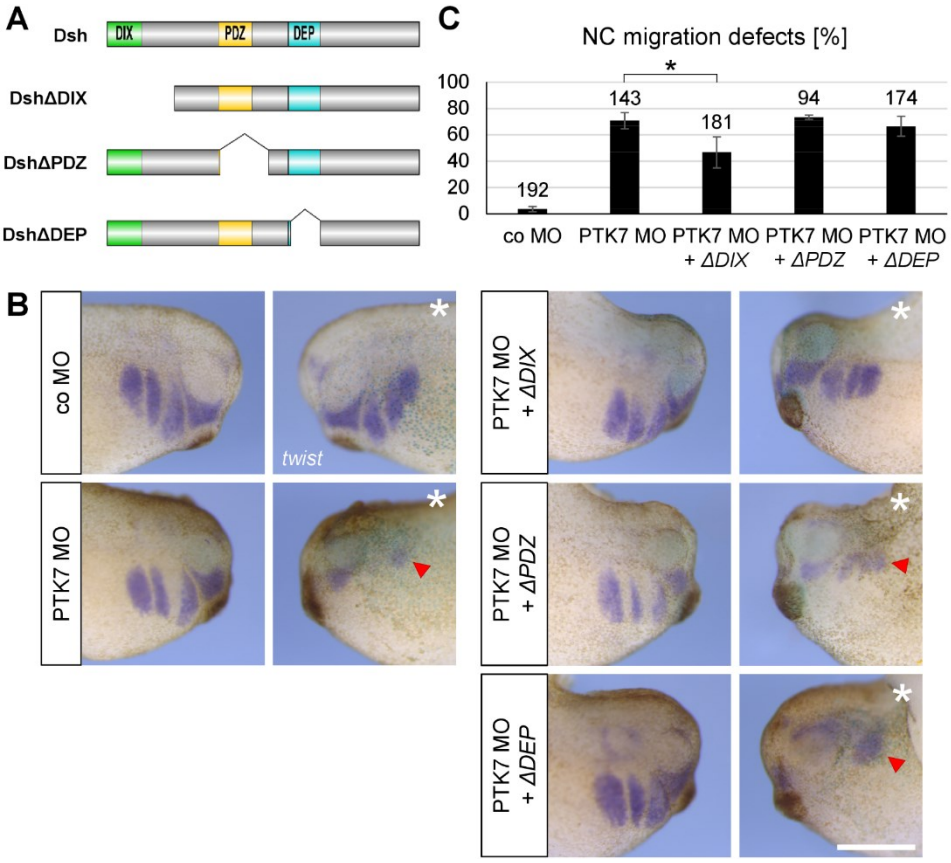

Fig. 18: Dsh with deleted DIX domain can partially rescue NC cell migration defects caused by PTK7 MO. A Schematic overview of Dishevelled (Dsh) deletion constructs. **B** Injection of 7.5 ng MO, 150 pg *DshΔDIX, DshΔPDZ or DshΔDEP* and 75 pg *LacZ* RNA in one blastomere of two-cell staged embryos. NC cells were marked by *twist in situ* hybridization. White asterisks indicate injected side, red arrowheads indicate inhibited NC migration, scale bar = 500 µm. **C** Graph summarizing percentage of NC migration defects of four independent experiments. Number of embryos and s.e.m. are indicated for each column. Black asterisk indicates *p*-value in a Student's t-test < 0.05.

3.5 PTK7 is localized at NC cell-cell contact sites

As PTK7 is enriched at NC cell-cell contact sites (P. Wehner, PhD Thesis 2012), further live cell imaging was performed to investigate the dynamic localization of PTK7. Therefore, NC cells expressing PTK7-GFP and H2B-mcherry were analyzed by spinning disc microscopy. NC cells show highly localized PTK7 at cell-cell contact sites (fig. 19). If a migrating NC cell (fig. 19 A) collided with another NC cell PTK7 accumulated at the cell-cell contact site (fig. 19 B, movie 3). The NC cell formed protrusion to the opposite side of the contact site (fig. 19 C). After cell-cell contact was broken, PTK7 was no longer accumulated at the membrane and the NC cell migrated away (fig. 19 D, movie 3).

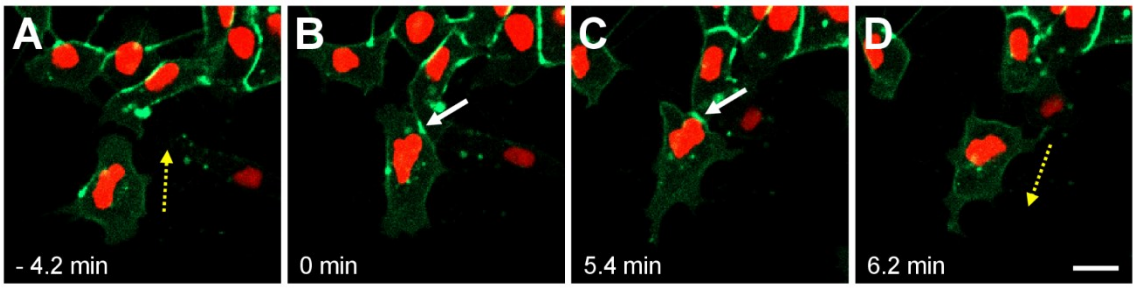

Fig. 19: PTK7-GFP accumulates at cell-cell contact sites. 250 pg *PTK7-GFP* and 250 pg *H2B-mcherry* RNA were injected into one blastomere of two-cell stage embryos. NC cells were explanted at stage 17. **A** A single NC cell before collision with another NC cell. Yellow dotted arrow indicates direction of migration. **B** PTK7-GFP accumulates at cell-cell contact sites of colliding NC cells (white arrow). **C** PTK7-GFP is located at the membrane during the entire time of cell-cell contact (white arrow). **D** After collision the NC cell migrate away (yellow dotted arrow). NC explants were observed using spinning disc microscopy. Time series starts 4.2 min before cell-cell contact (0 min), scale bar = 20 µm.

3.6 The extracellular domain of PTK7 affects its localization

To investigate which domain is necessary for the dynamic localization of PTK7, several GFP-tagged deletion constructs were cloned (fig. 20 A). The different PTK7 constructs were co-injected with *H2B-mcherry* RNA and the localization of the different constructs were analyzed in NC cells using time-lapse microscopy. A PTK7 construct which lacks its kinase homology domain (ΔkPTK7) was localized at cell-cell contacts like full-length PTK7 (fig. 20 B). If a migrating NC cell gets in contact with another NC cell, ΔkPTK7 accumulated at the cell-cell contact site (fig 20 C white arrow, movie 4). However, the cell contact time is increased in ΔkPTK7 expressing NC cells in comparison to full-length PTK7 (fig. 21 A). Furthermore, even after cell-cell contact was broken ΔkPTK7 stayed at the membrane (fig. 20 C red arrow) unlike to full-length PTK7. In addition, ΔkPTK7 vesicles at the membrane translocate into the cytoplasm (movie 4). A PTK7 construct lacking its immunoglobulin-like domains 3 to 7 (ΔE3-7PTK7) (fig. 20 A) localized at the membrane (fig. 20 D, movie 5). But unlike to full-length and ΔkPTK7, ΔE3-7PTK7 did not accumulate at cell-cell contact sites (fig. 20 E 0 min, movie 5) and did not affect cell

contact time during cell collision in comparison to full-length PTK7 (fig. 21 A). A deletion of all seven immunoglobulin-like domains (ΔE1-7PTK7) (fig. 20 A) led to a localization in intracellular compartments, despite its signal peptide and transmembrane domain (fig. 20 F, movie 6). ΔE1-7PTK7 also did not accumulate at the cell membrane when a NC

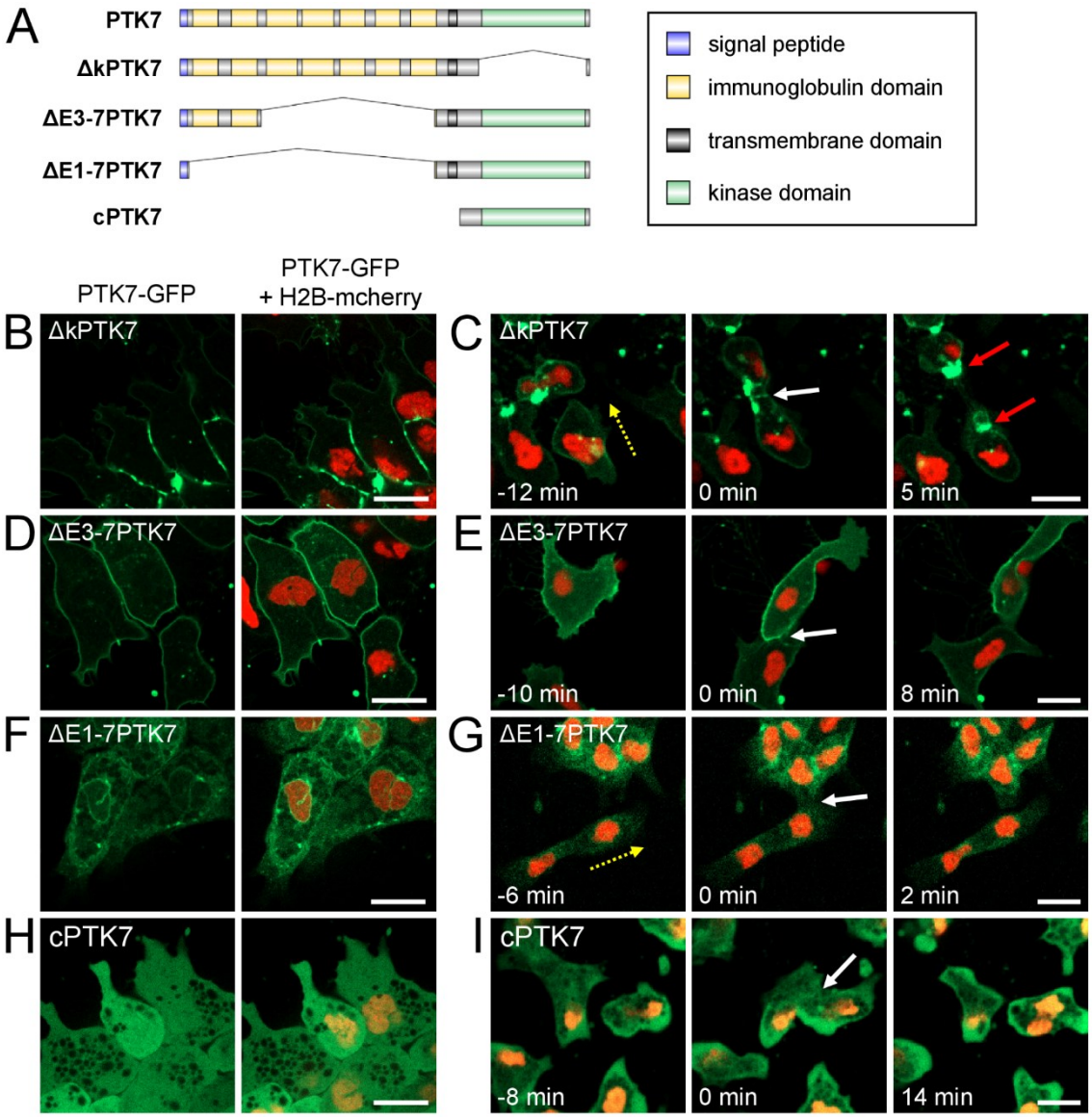

Fig. 20: Extracellular domain of PTK7 is important for its accumulation at cell-cell contact sites. *Xenopus* embryos were injected with 200 pg *ΔkPTK7-GFP*, 200 pg *ΔE3-7PTK7-GFP* or *ΔE1-7PTK7-GFP* or 100 pg *cPTK7-GFP* and 200 pg *H2B-mcherry* RNA in one blastomere of two-cell stage. NC cells were explanted at stage 16-18. **A** Schematic overview of PTK7 and different deletion constructs. **B** ΔkPTK7-GFP is localized at cell-cell contacts. **C** ΔkPTK7-GFP accumulates at cell-cell contact site of migrating NC cells (white arrow). After cell separation, ΔkPTK7-GFP is still highly enriched at former contact site (red arrow). **D** ΔE3-7PTK7-GFP is localized at the membrane of NC cells. **E** ΔE3-7PTK7-GFP did not accumulate at cell-cell contact site (white arrow). **F, G** ΔE1-7PTK7-GFP is not localized at the cell membrane nor at cell-cell contacts (white arrow). **H** cPTK7 is localized in the cytoplasm and nucleus of NC cells. **I** Cell-cell contact does not lead to an accumulation of cPTK7 at the membrane (white arrow). Direction of migration of NC cell is indicated by yellow dotted lines. 0 min indicates time point of NC cell-cell contact. Scale bars = 20 µm.

cell got in contact with another NC cell (fig. 20 G 0 min). Overexpression of the intracellular part of PTK7 (cPTK7) (fig. 20 A) showed a highly localization in the cytoplasm especially in the lamellipodia but it did not accumulate at cell-cell contact sites and did not affect cell contact time (fig. 20 H, I, fig. 21 A, movie 7). In addition, cPTK7 localized in the cell nucleus (fig. 20 H). Taken together, these results indicate that the extracellular domain of PTK7 is important for its localization at cell-cell contacts in migrating NC cells.

After cell-cell contact, NC cells change the direction of migration, a phenomenon called contact inhibition of locomotion (CIL). To analyze, if overexpression of the PTK7 constructs effected CIL behavior, the relative velocity vector of single cell collision was calculated (fig. 21 C, D). Therefore, the velocity before and after cell-cell contact as well as the changed angle after collision were determined. NC cells which overexpressed the different PTK7 constructs showed no change in CIL behavior (fig. 21 D), the analyzed NC cells changed their direction of migration after contact with another NC cell. In addition, also the velocity of single NC cells showed no alteration in NC cells overexpressing the deletion PTK7 constructs in comparison to full-length PTK7 besides NC cells expressing cPTK7, which showed a significant decrease in cell velocity (fig. 21 B). Because the ΔE1-7PTK7 construct seems not processed properly, no further analysis has been done.

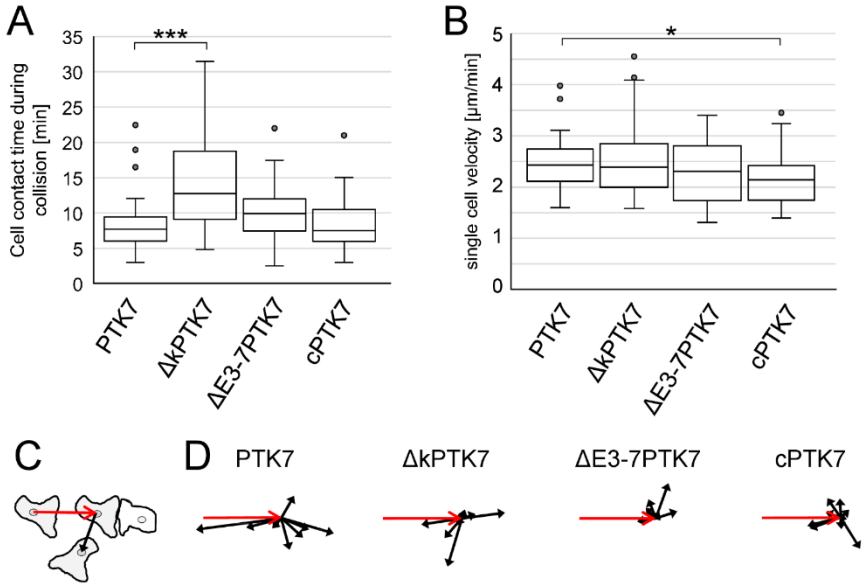

Fig. 21: Overexpression of ΔkPTK7 leads to longer cell-cell contact time during cell collision. A Graph blotting cell-cell contact time during collision of NC cells expressing various PTK7 constructs; n_{PTK7}=22, $n_{\Delta kPTK7}$=28, $n_{\Delta E3\text{-}7PTK7}$=21, n_{cPTK7}=17 of three independent experiments. **B** Graph blotting single cell velocity of NC cells expressing indicated PTK7 constructs; n_{PTK7}=34, $n_{\Delta kPTK7}$=27, $n_{\Delta E3\text{-}7PTK7}$=26, n_{cPTK7}=40 of three independent experiments. **C** Schematic overview of the analysis the migration direction of colliding NC cells, red arrow shows velocity vector before collision, black arrow shows velocity vector after collision. **D** Relative velocity vectors of NC cells with different PTK7 constructs shows change in the direction of migration after cell collision, n = 9 of three independent experiments. Box and whiskers plot: the box extends from the 25th to the 75th percentile, the median is plotted as a line inside the box. *p < 0.05, *** p < 0.005 in One-Way ANOVA test.

3.7 PTK7 intracellular domain can improve NC cell migration in PTK7-morphant embryos

An overexpression of ΔkPTK7 leads to NC cell migration defects *in vivo* (Shnitsar and Borchers, 2008). This could indicate that the kinase homology domain is important for NC migration. To prove this further, rescue experiments with cPTK7 were performed. Therefore, control or PTK7 MO were injected alone or in combination with *cPTK7* RNA and NC migration was analyzed by *AP-2 in situ* hybridization (fig. 22). Injection of control MO alone (3.1% ± 0.8) or together with *cPTK7* (4.1% ± 2.4%) did not influence NC migration (fig. 22 A, B). Whereas PTK7 loss of function led to inhibited NC migration (53.7% ± 3.1%) (fig. 22 A, B). Co-injection of *cPTK7* RNA with PTK7 MO led to an improved but not complete NC cell migration in comparison to the uninjected side (fig. 22 A). Quantification of the experiments shows that overexpression of the intracellular domain of PTK7 in PTK7-morphant embryos did not significantly rescued NC cell migration (fig. 22 B).

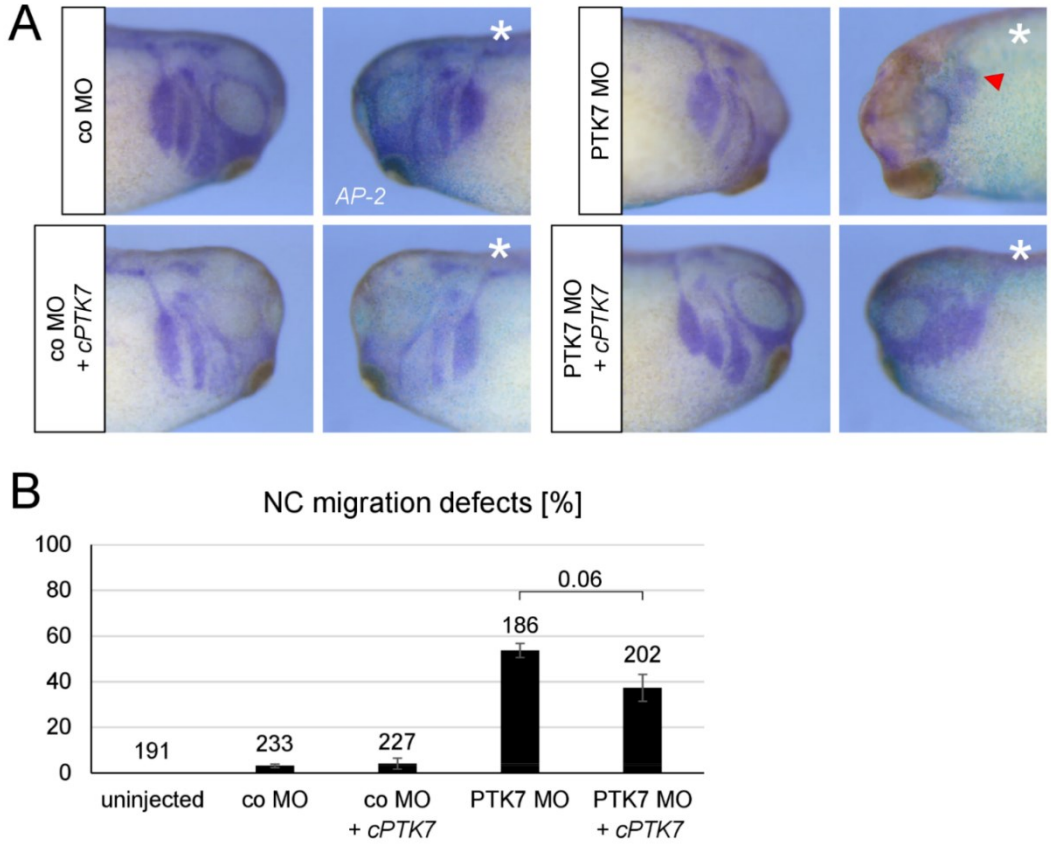

Fig. 22: C-terminus of PTK7 reduce NC cell migration defects caused by PTK7 loss of function. Injection of 7.5 ng control (co) or PTK7 MO, 200 pg *cPTK7-HA* and 75 pg *LacZ* RNA in one blastomere of two-cell stage embryos. Migration of NC cells were analyzed by whole mount *in situ* hybridization using *AP-2* antisense RNA probe. **A** Representative Embryos injected with MO with or without cPTK7. Asterisks indicate injected sides, red arrowhead indicates inhibited NC cell migration. **B** Graphic shows average of three independent experiments. Number of embryos and s.e.m. are indicated for each column. *p*-value = 0.06 in One-Way ANOVA test.

3.8 PTK7 mediates homophilic binding by its extracellular domain

PTK7 accumulation at cell-cell contact sites indicates homophilic binding of PTK7. To investigate if this is the case, co-IPs using tagged PTK7 constructs have been performed (fig. 23, 24). First of all, PTK7-Myc could co-precipitate PTK7-GFP and *vice versa* showing a homophilic interaction of PTK7 (fig. 23 B, C). To further investigate the domains necessary for this interaction, different PTK7 deletion constructs were used (fig. 23 A, fig. 24 A). Co-IPs using GFP-tagged ΔkPTK7 and cPTK7 in combination with full-length PTK7-Myc revealed that PTK7 interacts with its extracellular but not with its intracellular part (fig. 23). Co-IPs using only the extracellular part (exPTK7-Myc) confirm that PTK7 mediates homophilic binding with its extracellular domain (fig. 24).

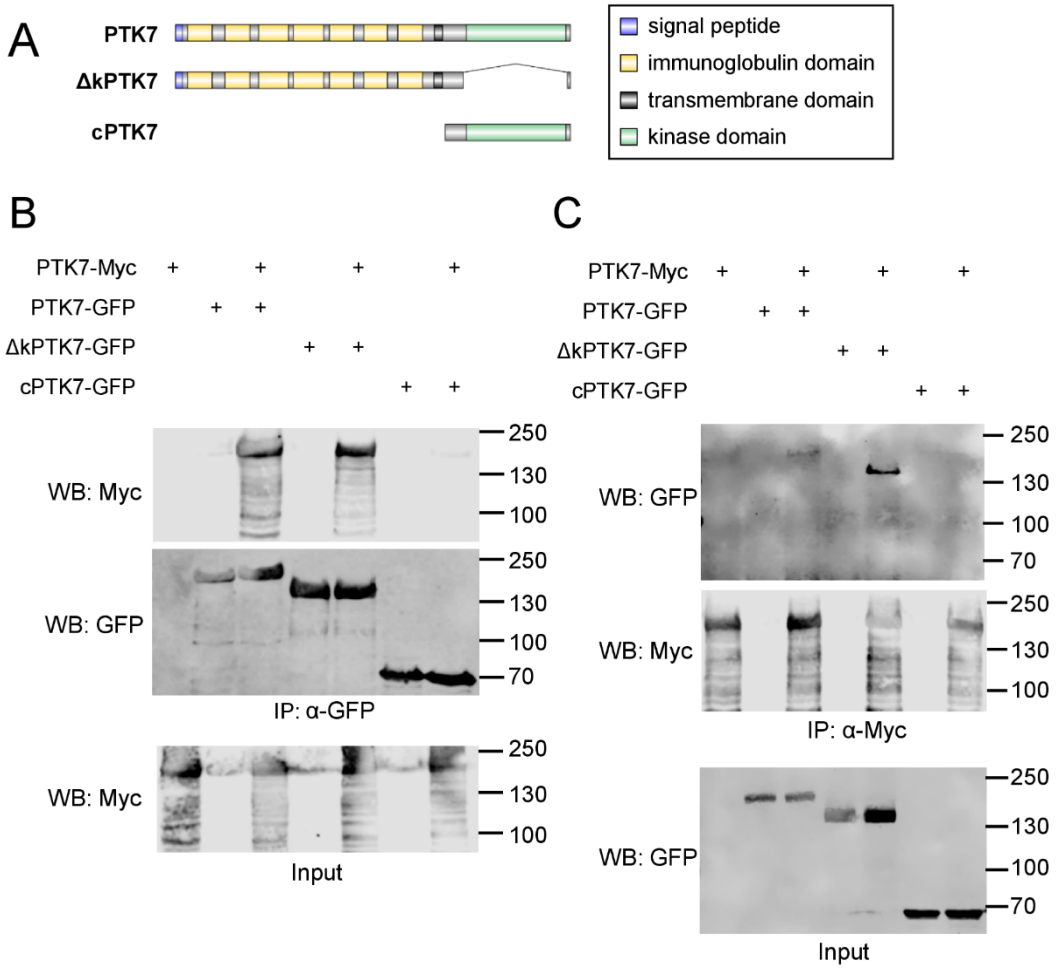

Fig. 23: PTK7 possess homophilic binding via its extracellular part. A Schematic overview of PTK7 constructs. **B, C** PTK7-Myc, PTK7-GFP, ΔkPTK7-GFP and cPTK7-GFP were transfected in HEK293 cells. The cell transfection scheme is indicated at the top. Co-IP was carried out using (B) α-GFP or (C) α-Myc antibodies. The cell lysates (input control) are shown in the bottom panels. Antibodies used in Western blotting (WB) are shown on the left, molecular weights are shown on the right indicated in kDa. Representative co-IPs were shown of two independent experiments.

Interestingly, deletion of the Ig domains 3 to 7 (ΔE3-7PTK7-Myc) could also slightly precipitate with full-length PTK7. And also the complete deletion of the Ig domains (ΔE1-7PTK7-Myc) shows a minor precipitation with full-length PTK7 but this was only observed in co-IPs were PTK7-HA were precipitated (fig. 24 B, C).

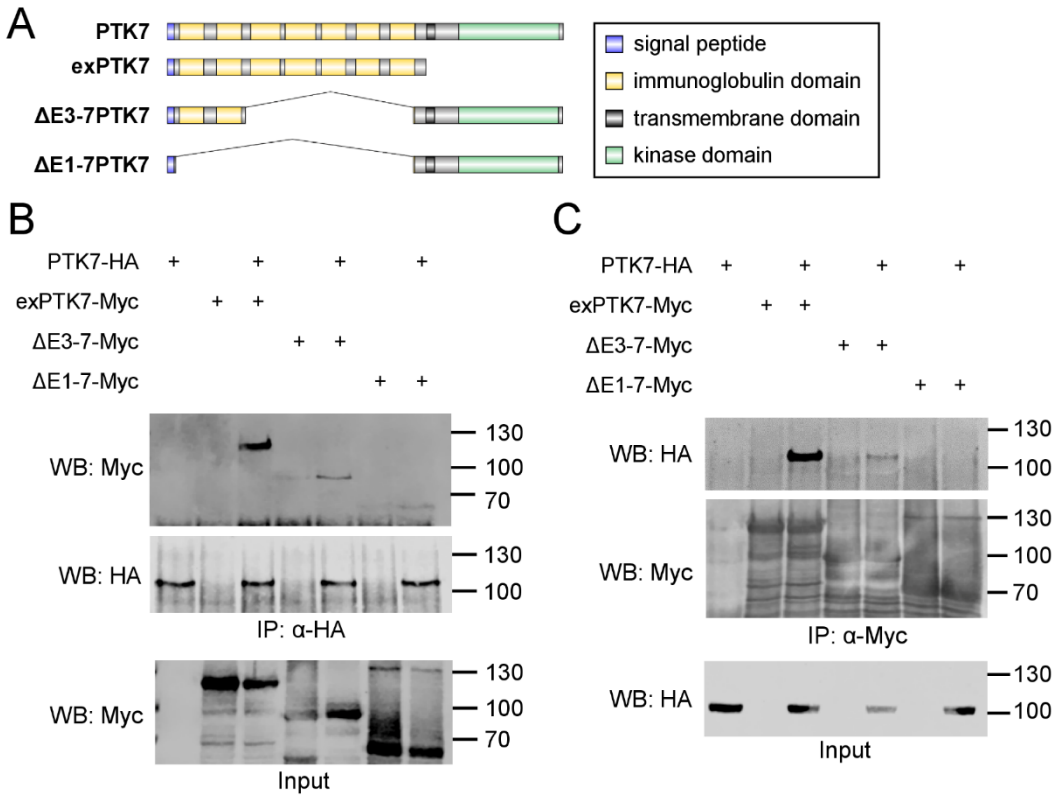

Fig. 24: PTK7 interact via its extracellular domain. A Schematic overview of PTK7 constructs. **B, C** PTK7-HA, extracellular PTK7 (exPTK7)-Myc, ΔE3-7PTK7-Myc, ΔE1-7PTK7-Myc were transfected in HEK293 cells. The cell transfection schemes are indicated at the top. Co-IP was carried out using (B) α-HA or (C) α-Myc antibodies. The cell lysates (input control) are shown in the bottom panel. Antibodies used in Western blotting (WB) are shown on the left, molecular weights are shown on the right indicated in kDa. Representative co-IPs were shown of at least three independent experiments.

3.9 PTK7 knockdown affects NC cell shape

Since PTK7 is expressed in NC cells and fluorescence-tagged PTK7 accumulates at cell-cell contact sites the question arises of how a PTK7 knockdown would affect NC cell morphology. To investigate this PTK7 MO were injected together with *mbGFP* and *H2B-mcherry* RNA to visualize NC cell shape and polarity. NC cells were explanted at stage 16/17 and analyzed by spinning disc microscopy. At the start of the experiment (0 min) control NC cells already showed lamellipodia and filopodia formation which could also be observed after 30 and 60 min (fig. 25 A, movie 8). Whereas NC cells injected with PTK7 MO showed no filopodia formation but blebbing formation instead over the time period of up to 60 min (fig. 25 A, movie 8). The cell shape of the NC cells can be analyzed by measurement of the cell circularity. The cell circularity depends on the perimeter and area of the cell and a circularity of 1 indicates a perfect circle. NC cells with PTK7 knockdown showed a higher cell circularity in comparison to NC cells with control MO (fig. 25 B).

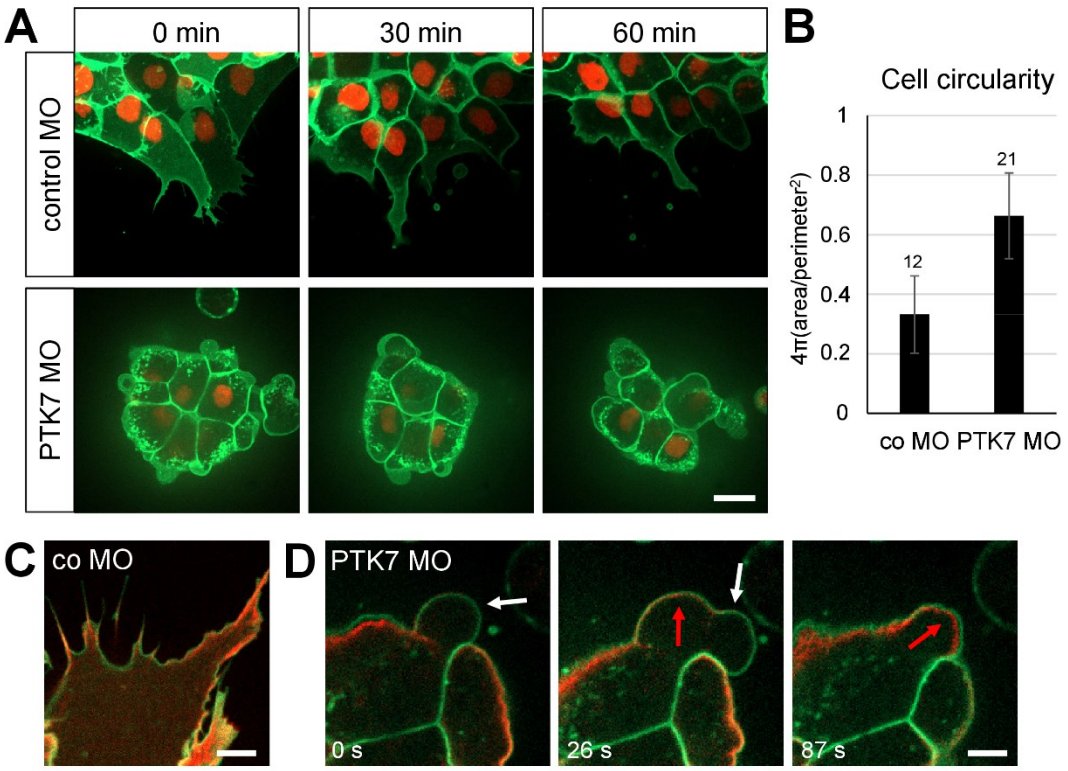

Fig. 25: PTK7 knockdown affects NC cell shape. A *Xenopus* embryos were injected with 7.5 ng control MO (upper panel) or PTK7 MO (lower panel), 50 pg *mbGFP* and 250 pg *H2B-mcherry* RNA into one blastomere at two-cell stage. NC cells were explanted at stage 17, cultured for 1.5 h and imaged with spinning disc microscopy. Time series starts at the beginning of imaging (0 min), pictures show maximum intensity projections, scale bar = 20 µm. **B** Averaged cell circularity of control (co) and PTK7 MO-injected NC cells of three independent experiments, number of cells and s.e.m. are shown for each column. A circularity of a circle is 1. **C, D** Co-injection of 7.5 ng co or PTK7 MO with 50 pg *mbGFP* and 300 pg *lifeact-RFP* RNA, scale bars = 5 µm. (C) NC cell with control (co) MO exhibits filopodia with actin strands. (D) Time series of NC cells with PTK7 MO showing membrane expansion (white arrow) followed by reformation of actin filaments under bleb membrane (red arrow).

The formation of lamellipodia and filopodia is mediated by the actin cytoskeleton (Mattila and Lappalainen, 2008). Lifeact is an excellent marker to visualize F-actin in living cells (Riedl et al., 2008). In NC cells injected with control MO, F-actin cable was visible in forming lamellipodia and filopodia (fig. 25 C, movie 9). PTK7-depleted NC cells showed membrane blebbing where at first the membrane expands and inflowing cytoplasm enlarges the bleb (fig. 25 D white arrow, movie 10). F-actin was reformed under the bleb membrane and the cell bleb retracted (fig 25 D red arrow). Cell blebbing is usually associated with apoptosis (reviewed in (Charras and Paluch, 2008; Ikenouchi and Aoki, 2017)). To analyze if this cell blebbing of the PTK7-morphant NC cells is because of starting apoptosis a Propidium iodide (PI) staining was performed. PI can stain DNA and cytoplasmic dsRNA but is not able to penetrate the cell membrane of living cells, which make it useful to detect apoptotic cells (Martin et al., 2005; Suzuki et al., 1997). For PI staining NC cells with control or PTK7 MO and mbGFP were cultured in DFA containing PI. The cells were observed from the start of the treatment (0 h) to 6 h (fig. 26). NC cells injected with control MO exhibited filopodia and single cells detach from the cell cluster (fig. 26 A). No PI staining in NC cells was detectable for up to 3 h. After 6 h the first cells died, indicated by their roundish cell shape and PI staining (fig. 26 A red arrow and box). Some NC cells with PTK7 MO showed a roundish cell shape already at the beginning of the experiment. Two of these blebbing NC cells were tracked throughout the 6 h and they showed no PI staining (fig. 26 B white arrow and box). On the other hand, PI stained NC cells which showed a roundish cell shape after 3 h of imaging (fig. 26 B red arrow and box). In conclusion, the PI staining showed that the NC cells with a roundish cell shape caused by PTK7 loss of function are not necessarily dead but cells died earlier than control MO injected NC cells.

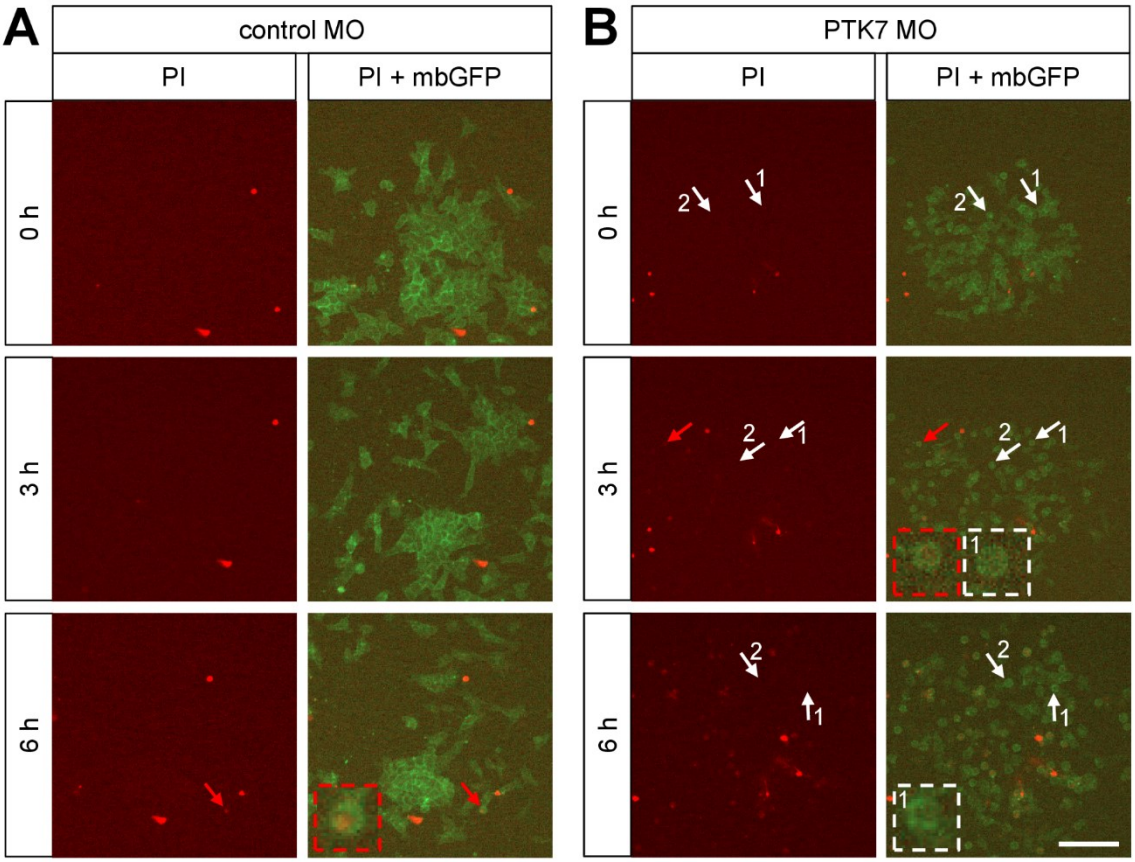

Fig. 26: PI staining shows that blebbing NC cells caused by PTK7 knockdown are not apoptotic. NC cells co-injected with (**A**) 7.5 ng control or (**B**) PTK7 MO together with 50 pg *mbGFP* RNA were explanted at stage 17/18 and cultured with Propidium iodide (PI, 10 µg/ml in DFA). PI is not membrane permeable but in apoptotic cells PI can stain nucleic acid (red). Red arrows indicate roundish cells with PI staining. White arrows point to cells with round cell shape and no PI staining (numbers indicate specific cells during time lapse imaging). Dashed squares show higher magnification of marked cells. Scale bar = 50 µm.

3.10 PTK7 affects the activity of the small GTPase Rac1 and RhoA

The small GTPases are essential for the formation of cell protrusion. However, since PTK7 loss of function interferes with the formation of filopodia, PTK7 may affect the activity of GTPases. To investigate this possibility, Rac and Rho pull down assays with whole embryo lysates have been performed. Overexpression of PTK7 did not impact Rac1 or RhoA activity (fig. 27). PTK7 knockdown using PTK7 MO significantly decreased Rac1-GTP whereas RhoA-GTP was slightly (but not significantly) increased (fig. 27).

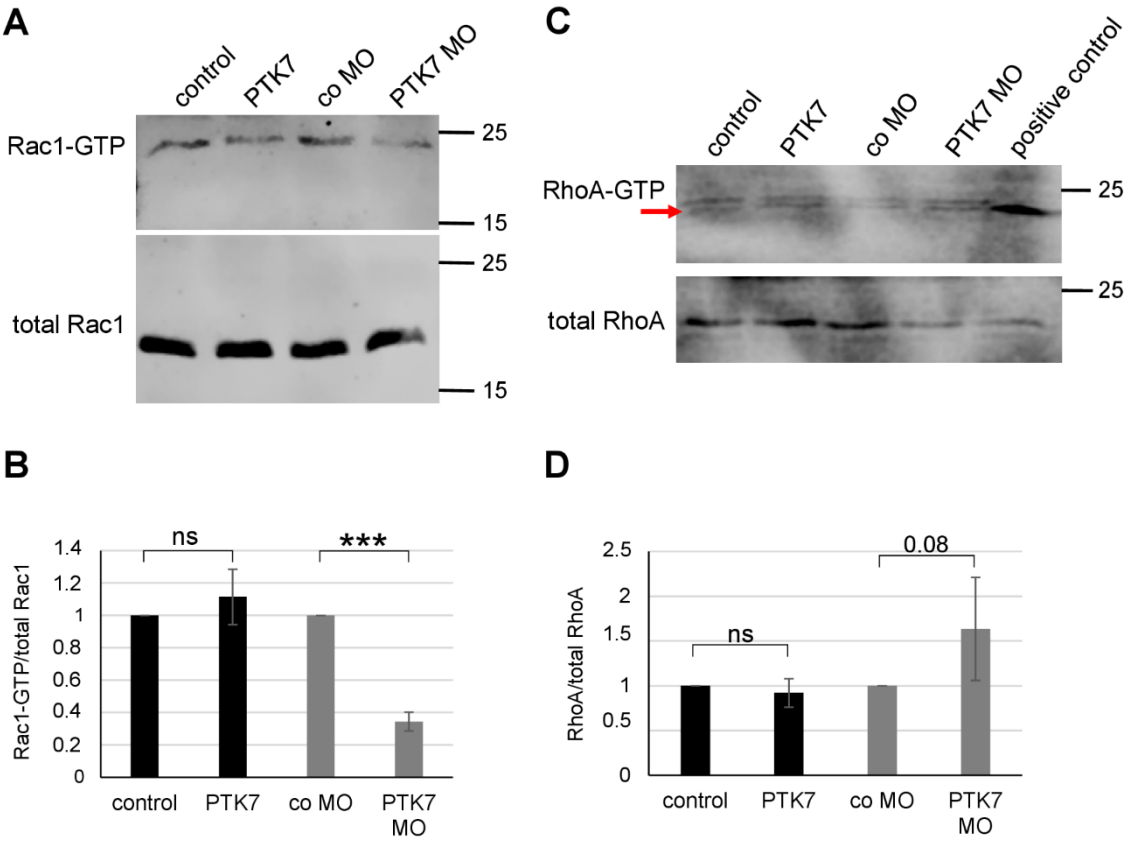

Fig. 27: PTK7 knockdown affects Rac1 and RhoA activity in *Xenopus* embryos. Embryos were injected with 0.25 µg/µl Fluorescein-Dextran (control) together with 800 pg *PTK7-HA*, 7.5 ng control (co) MO or PTK7 MO in 1-cell stage. GTPase pull down assays were performed with embryos at stage 20-22. **A** Western blot analysis of Rac1-GTP (upper panel) and total Rac1 (lower panel). Molecular weights are shown on the right indicated in kDa. **B** Graphic shows median of Rac1-GTP/total Rac1 of 3 independent experiments with standard error. **C** Western blot analysis of RhoA-GTP (upper panel) and total RhoA (lower panel). Molecular weights are shown on the right indicated in kDa. Red arrow indicates the height of RhoA-GTP bands. **D** Graphic shows median of RhoA-GTP/total RhoA of 3 independent experiments with standard error. *p*-value in One-Way ANOVA test ***<0.005, ns = not significant.

3.11 PTK7 and GEF-Trio

3.11.1 Rho-GEF Trio acts downstream of PTK7 in NC cell migration

In the PCP signaling pathway the downstream effects of Dsh is the activation of the small Rho GTPases RhoA or Rac1 (see review (Habas and He, 2006)). The activation of the GTPases results by the exchange of the bound GDP with GTP by guanine nucleotide exchange factors (GEF). Trio is a Rho-GEF which can activate RhoA as well as Rac1, is expressed in NC cells and important for their migration (Kashef et al., 2009; Kratzer et al., 2019; Schmidt and Debant, 2014). This makes Trio an interesting candidate for a downstream effector of PTK7 signaling. And indeed, overexpression of Trio in PTK7-morphant embryos could rescue NC cell migration defects (fig. 28). The improvement of NC migration by overexpression of Trio is concentration-dependent. Already a co-injection of 100 pg Trio DNA improved NC cell migration defects from 61.1% (± 1.0%) to 41.0% (± 7.0%), but an injection of 150 pg Trio DNA led to a significant rescue (29.0% ± 8.5%) (fig. 28 B).

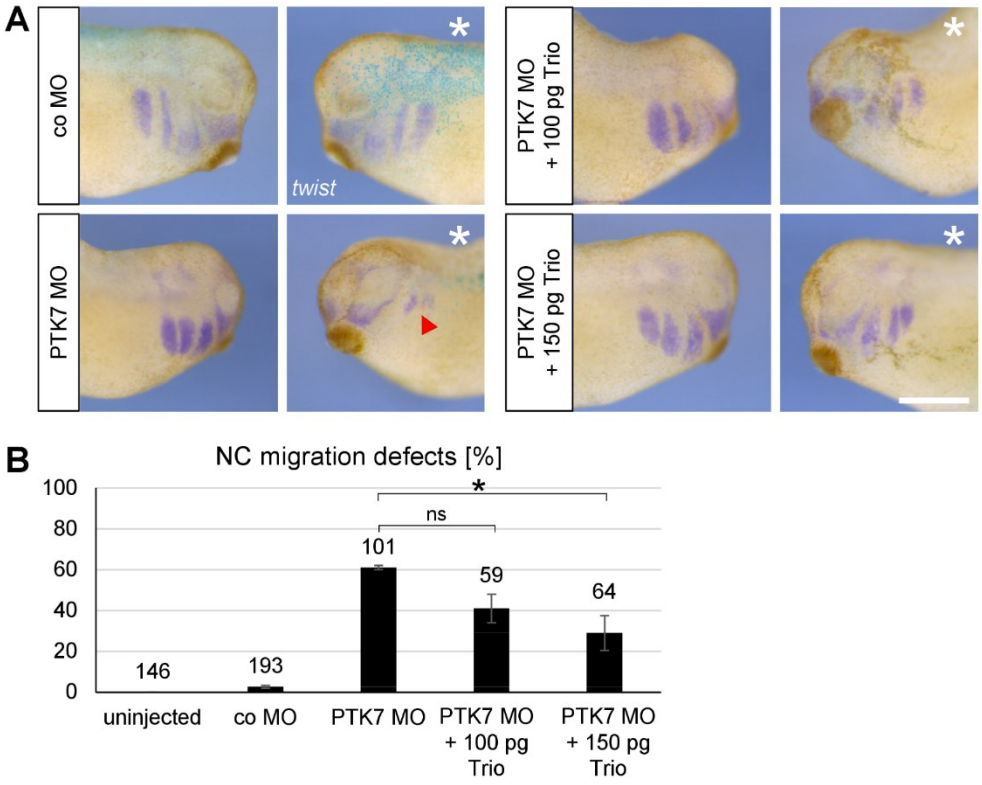

Fig. 28: NC cell migration defects caused by PTK7 knockdown can be rescued by Rho-GEF Trio. Embryos were co-injected with 7.5 ng co or PTK7 MO, 100 pg or 150 pg hTrio DNA and 75 pg *LacZ* RNA into one dorsal blastomere of eight-cell stages. **A** Representative embryos are shown for different conditions. NC cells are marked by *twist in situ* hybridization, white asterisks indicate injected side, red arrowhead indicates inhibited NC cell migration, scale bar = 500 µm. **B** Graph summarizes percentage of NC migration defects of three independent experiments, ns = not significant (p = 0.06), * < 0.05 in Student's *t*-test.

3.11.2 PTK7 and Trio co-localize in NC cells

Since Trio can compensate PTK7 loss of function in NC migration, it raises the question whether PTK7 and Trio interact. To analysis this, localization of PTK7 and Trio were analyzed in NC cells. Therefore, embryos were injected with *PTK7-RFP* RNA and GFP-Trio DNA alone or in combination (fig. 29 A-C). PTK7 was localized at cell-cell contacts and Trio was mainly localized in the cytoplasm but also at the membrane (fig. 29 A, B). Co-expression of PTK7 and Trio showed a co-localization of both at cell-cell contact sites but overexpression of PTK7 did not lead to an altered localization of Trio (fig. 29 C). To prove an interaction of PTK7 and Trio, co-IPs using HEK cells were carried out. And indeed, co-IP analysis revealed an interaction of HA-Trio and PTK7-Myc (fig. 29 D).

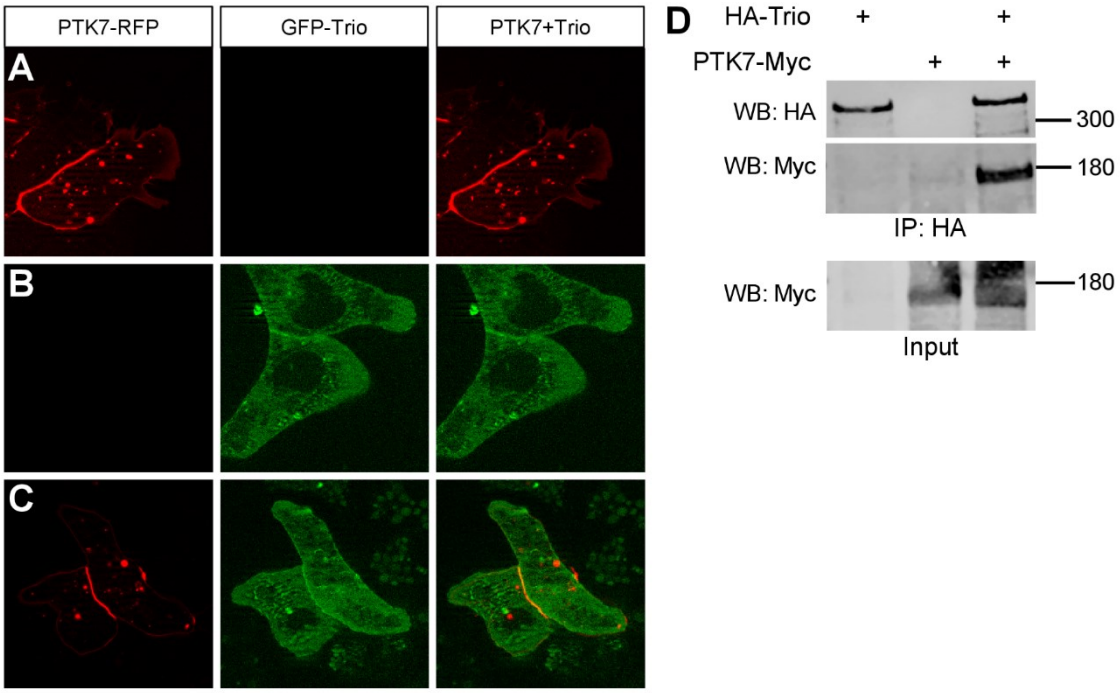

Fig. 29: PTK7 and Trio co-localize in NC cells and interact in HEK cells. A-C Embryos were injected with 400 pg *PTK7-RFP* RNA and 300 pg GFP-hTrio DNA in one blastomere of two-cell stage. NC cells were explanted at stage 17-19. **D** HA-hTrio and PTK7-Myc constructs were expressed in HEK293 cells. Representative co-IP of Trio and PTK7 is shown of at least three independent experiments. The cell transfection scheme is indicated at the top. Co-IPs were carried out using anti-HA. The cell lysates (input control) are shown in the bottom panel. Used antibodies in Western blot (WB) are shown on the left, molecular weights are shown on the right indicated in kDa.

3.11.3 Trio affects Rac1 and RhoA activity

Trio is a Rho-GEF for the small GTPases Rac1 and RhoA (Schmidt and Debant, 2014). Furthermore, Trio activates Rac1 at the leading edge of NC cells (Moore et al., 2013). To investigate the ability of Trio to activate Rac1 as well as RhoA in *Xenopus* embryos, pull down assays of whole embryos lysates were performed. Therefore, embryos were injected with full-length Trio DNA, *Trio-GEF1* (*GEF1*) or *Trio-GEF2* (*GEF2*) RNA and Trio MO (fig. 30). Injection of embryos were also performed by Marie-Claire Kratzer.
Overexpression of Trio and GEF1 significantly increased Rac1-GTP (fig. 30 A, B). Also GEF2 slightly increased Rac1-GTP in comparison to control embryos. Trio and its GEF domains alone were also able to activate RhoA (fig. 30 C, D). Knockdown of Trio by MO injection significantly decreased Rac1 as well as RhoA activity (fig. 30).

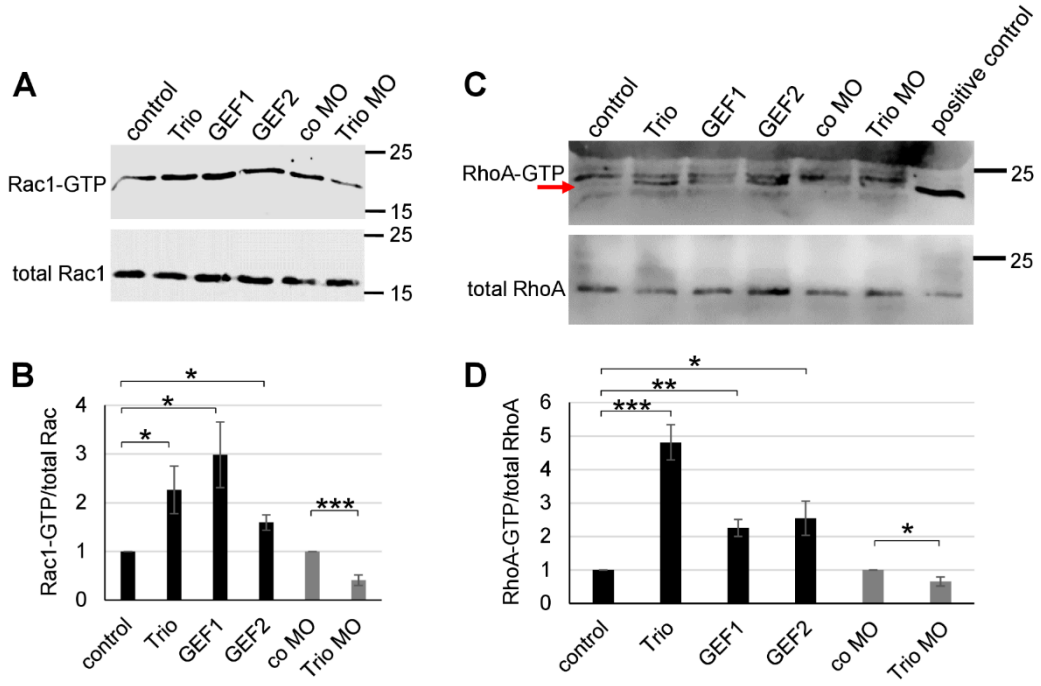

Fig. 30: Trio affects Rac1-GTP and RhoA-GTP in *Xenopus* embryos. Embryos were injected with 0.25 µg/µl Fluorescein-Dextran (control) in combination with 100 pg HA-Trio DNA, 250 pg *Trio-GEF1* or *Trio-GEF2* RNA, 5 ng control (co) or Trio MO in one-cell stage. (A, B) Rac or (C, D) Rho pull down assay were performed with embryos at stage 20-22. **A** Western blot analysis of Rac1-GTP (upper panel) and total Rac1 (lower panel). **B** Graphic shows median of Rac1-GTP/total Rac1 of 3 independent experiments. **C** Western blot analysis of RhoA-GTP (upper panel) and total RhoA (lower panel). Red arrow indicates the height of RhoA-GTP bands. **D** Graphic shows median of RhoA-GTP/total RhoA of 3 independent experiments. *<0.05, **<0.01, ***<0.005 in One-Way ANOVA-test, s.e.m are shown.

4. Discussion

PTK7 is a versatile receptor involved in canonical and non-canonical/PCP Wnt signaling (Berger et al., 2017a). PTK7 activates canonical Wnt signaling during *Xenopus* gastrulation (Martinez et al., 2015; Puppo et al., 2011) but is also able to inhibit canonical Wnt signaling in other tissues (Hayes et al., 2013; Peradziryi et al., 2011). Activation of non-canonical Wnt signaling by PTK7 is indicated by its ability to recruit Dsh to the cell membrane and activation of JNK in *Xenopus* ectodermal explants (Shnitsar and Borchers, 2008). However, little is known about PTK7 signaling in NC cell migration.

4.1 PTK7 is important for CIL

During NC cell migration, NC cells perform CIL when they get in contact with another NC cell, leading the NC cells to migrate in another direction (Carmona-Fontaine et al., 2008b). During CIL, PCP components are located at the cell-cell contact. So far, it has not yet been clearly demonstrated how these components get localized at the contact sites of NC cells. This study shows that PTK7 is possibly responsible for PCP activation at cell-cell contact sites. PTK7 accumulates at cell-cell contacts but is rapidly removed from the membrane if cell-cell contacts are broken. The dynamic localization of PTK7 is mediated by its extracellular domain. Deletion of parts of the extracellular domain prevented PTK7 accumulation. In addition, co-IPs using different PTK7 constructs revealed that PTK7 makes homophilic binding via its extracellular domain. These data indicate that the PTK7 extracellular domain of one NC cell binds to the PTK7 extracellular domain of another NC cell. This leads to an PTK7 accumulation and possibly localization of further PCP components at the cell-cell contact. An accumulation of PTK7 within a cell could also lead to an interaction of PTK7 proteins via their transmembrane domains. Interaction studies in *Drosophila* with the PTK7 orthologue Off-track reveals a homodimerization via its transmembrane domain (Linnemannstöns et al., 2014).

Overexpression of ΔkPTK7 causes NC cell migration defects, which indicates that the kinase domain, which is important for membrane recruitment of Dsh, is important for NC migration (Shnitsar and Borchers, 2008). But an overexpression of cPTK7 (which includes the kinase domain) in PTK7-morphant embryos only improve but not significantly rescue NC migration. Analysis of cPTK7 in NC cells *ex vivo* shows that it is localized in the cytoplasm and NC cells are slower than NC cells overexpressing full-length PTK7. But embryos overexpressing cPTK7 show no NC migration defects *in vivo*. In conclusion, the localization of cPTK7 and its inability to rescue NC migration defects caused by PTK7 knockdown could indicate that the kinase domain has to be membrane tethered for proper PTK7 downstream signaling in NC cell migration. To prove this, overexpression of a ΔEPTK7 construct in PTK7-morphant embryos should rescue NC

migration. But since the extracellular part of PTK7 is important for its localization and maybe also for proper localization of PCP components at cell-cell contact, a ΔEPTK7 construct may also only improve NC cell migration like cPTK7. The NC migration defects caused by overexpression of ΔkPTK7 can also be caused by strong cell-cell adhesion. In comparison to full-length PTK7, overexpression of ΔkPTK7 leads to an increased contact time during cell-cell collision. That the ΔkPTK7 expressing NC cells still exhibit normal migration behavior is probably because during this study lower concentration of ΔkPTK7 were used to avoid protein accumulation caused by overexpression.

In human cell lines, PTK7 is a target for proteolytic cleavage and a C-terminal fragment can also translocate into the cell nucleus and increase gene transcription (Golubkov and Strongin, 2012; Na et al., 2012). A recent study shows that also in *Xenopus* embryos a C-terminal PTK7 fragment is able to increase gene transcription and is important for early nervous system development (Lichtig et al., 2019). However, during this study a localization in the nucleus was only observed in NC cells injected with cPTK7, which cannot substitute full-length PTK7 in NC cell migration. In addition, cPTK7 enhances migration in colon cancer cell (Na et al., 2012) but in NC cells cPTK7 decreases cell velocity in comparison to full-length PTK7.

Taken together, for proper NC cell migration PTK7s extracellular as well as intracellular domains are important but further experiments are necessary to prove this in detail.

4.2 PTK7 signaling in NC cell migration

4.2.1 Ror2 can restore NC cell migration in PTK7-morphants

At cell-cell contacts, PTK7 could activate non-canonical Wnt signaling alone or in interaction with other PCP receptors. Ror2 share similar functions in Wnt signaling as PTK7 and is also expressed in migrating NC cells (reviewed in (Stricker et al., 2017)), which makes Ror2 an interesting candidate to investigate a possible Ror2/PTK7 interaction in NC migration. Indeed, Ror2 is able to interact with PTK7 and fluorescently-tagged Ror2 and PTK7 co-localize in NC cells (Martinez et al., 2015; Podleschny et al., 2015). Moreover, overexpression of *Ror2* mRNA in PTK7-morphant embryos can rescue NC migration defects *ex vivo* (this study) and *in vivo* (Podleschny et al., 2015). However, a PTK7/Ror2 signaling function has still to be investigated. PTK7 and Ror2 both inhibit canonical Wnt signaling but the PTK7-mediated inhibition of canonical Wnt signaling seems to be independent of Ror2 (Berger et al., 2017b). Like PTK7, Ror2 is a Fz co-receptor and actives PCP signaling (reviewed in (Stricker et al., 2017)). Ror2-Dsh interaction activates RhoA, Rac1 and JNK (Bai et al., 2014; Nishita et al., 2006; Nishita et al., 2010; Nomachi et al., 2008; Oishi et al., 2003; Wu et al., 2019). PTK7 is also able to activate JNK (Shnitsar and Borchers, 2008). Since the kinase domain of Ror2, which

is important for JNK activation (Mikels et al., 2009), is required to rescue PTK7 knockdown (Podleschny et al., 2015), possibly PTK7 and Ror2 interaction leads to Dsh signaling and JNK activation. It is also possible that PTK7, Ror2 and Fz7 form a triple complex to activate PCP signaling. A detailed function of PTK7 and Ror2 interaction in NC cell migration needs to be further investigated to rule out that Ror2 not only compensate the PTK7 knockdown in NC cell migration. However, analyzing Ror2 function in migrating NC cells is difficult because Ror2 is important for NC induction and Ror2 overexpression does not lead to NC cell migration defects (Podleschny et al., 2015; Schille et al., 2016). To investigate, if Ror2 loss of function shows the same phenotype as PTK7 loss of function in NC cell migration photoactivatable MOs can be used. Photoactivatable MOs are caged MOs and get activated by UV light, which makes it a useful tool to spatiotemporal block specific mRNA translation (Figueiredo et al., 2017; Shestopalov et al., 2007).

4.2.2 Dsh acts downstream of PTK7 during NC cell migration

Not much is known about the PTK7 downstream effectors in NC migration. Previously, Dsh was identified to interact with PTK7 via RACK in ectodermal explants (Shnitsar and Borchers, 2008; Wehner et al., 2011) and Dsh is also important for NC cell migration (De Calisto et al., 2005). To investigate, if Dsh can restore NC cell migration in PTK7-morphant embryos rescue experiments were performed. Overexpression of Dsh could partial rescue NC migration defects caused by PTK7 knockdown and NC cells showed normal migration behavior. Co-injection of Dsh deletion constructs with PTK7 MO revealed that the PDZ and DEP domains and not the DIX domain of Dsh are both important to rescue NC cell migration. The PDZ domain has been shown to be crucial for PTK7 interaction (Shnitsar and Borchers, 2008) and the DEP domain is important for NC cell migration whereas the DIX domain is important for NC cell induction (De Calisto et al., 2005). First experiments could show that PTK7 and Dsh co-localize at cell-cell contacts (Shnitsar, 2009, phD Thesis). So an accumulation of PTK7 at cell-cell contact sites could lead to a recruitment of Dsh via its PDZ domain and the DEP domain activates PCP downstream signaling for proper CIL response. The PDZ and DEP domains activate Rac1 and RhoA in *Xenopus* ectodermal explants (Habas et al., 2001; Habas et al., 2003). The activation of RhoA by Dsh is mediated by binding to Daam1 (Habas et al., 2003). Daam1 is a formin homologue, affects cell polarity and movement (Ang et al., 2010) and is expressed during NC cell development (Nakaya et al., 2004). A Dsh and Daam1 function has been investigated during gastrulation (Habas et al., 2001; Liu et al., 2008b; Sato et al., 2006) but if Dsh, in particular PTK7/Dsh, also activates Daam1 during NC cell migration is currently unknown.

4.2.3 The GEF-Trio is a new PTK7 interaction partner

Analysis of PTK7-depleted NC cells *ex vivo* shows that NC cells do not form lamellipodia or filopodia instead the cells are blebbing. Cell blebbing is usually caused by over-activation of RhoA/ROCK signaling (reviewed in (Charras and Paluch, 2008; Fackler and Grosse, 2008; Ikenouchi and Aoki, 2017)). But alteration of Rac1 activity can also stimulate membrane blebbing indirectly, since Rac and Rho activity is tightly balanced (reviewed in (Guilluy et al., 2011; Nguyen et al., 2016)). PTK7 affects both Rac1 and RhoA activity but further analysis must show which GTPase is directly affected by PTK7. In migrating NC cells, Rac1 is active at the leading edge leading to protrusion formation (Carmona-Fontaine et al., 2008b). If a NC cell gets in contact with another NC cell, RhoA is activated at the cell-cell contact site, leading to filopodia collapse by actomyosin assembly and inhibition of Rac1 (Carmona-Fontaine et al., 2008b; Scarpa et al., 2015). As PTK7 accumulates at cell-cell contact sites, PTK7 could lead to RhoA activation and inhibition of Rac1 (directly or indirectly via RhoA) at the cell-cell contact, which leads to protrusion collapse and CIL.

Activation of Rac1 and RhoA is mediated by GEF proteins. Trio is a GEF for both GTPases in cell culture cells (Bellanger et al., 1998; Blangy et al., 2000; Debant et al., 1996) as well as in whole *Xenopus* embryo lysates (this study). Trio GEF1 domain is known to activate Rac1 and the GEF2 domain activates RhoA. Pull down assays with *Xenopus* embryos shows that GEF1 can also increase RhoA and the GEF2 domain slightly increases Rac1 activity. These effects may be attributed from the fact that the activation of one GTPase can lead to an activation of the other GTPase (reviewed in (Guilluy et al., 2011)). To exclude that GEF1 is able to activate RhoA and GEF2 to activate Rac1, the injected embryos should be treated with Rac1 or RhoA inhibitors to prevent mutual activation.

Recent findings shows that Trio is expressed in migrating NC cells (Kratzer et al., 2019) and is also able to interact with Dsh (M.-C. Kratzer, PhD Thesis). During this study it could be proved that Trio also interacts with PTK7 in HEK cells and co-localizes with PTK7 at cell-cell contacts of NC cells. Furthermore, overexpression of Trio could decrease NC cell migration defects caused by PTK7 loss of function. These data indicate that a PTK7/Trio or possibly PTK7/Dsh/Trio complex functions in NC cell migration. A PTK7/Dsh/Trio complex at cell-cell contacts could activate RhoA, leading to actomyosin stress fibers, and indirectly inhibiting Rac1 activity, which leads to cell protrusion collapse. It is also possible that PTK7 directly inhibits Rac1 activity by binding to Trio. The Trio GEF1 domain is autoinhibited by binding to the spectrin-like repeats (Chen et al., 2011). If a protein binds to the spectrin-like repeats, the GEF1 domain is released and able to activate Rac1 (Chen et al., 2011). Possible PTK7 binds Trio which inhibits

the ability of Trio to activate Rac1, leading to protrusion collapse. This idea is supported by current findings that the polarity protein Par3 interacts with Trio, which leads to a decreased Rac1 activity in NC cells (Moore et al., 2013). Moore and colleagues suggest that Trio-Rac1 is active in lamellipodia and promoting microtubule stability. Upon cell-cell contact, Par3 is localized at cell-cell contact sites and inhibits Trio-Rac1 activity, leading to microtubule catastrophe and protrusion collapse (Moore et al., 2013). It has to be investigated if PTK7 may also be involved in microtubule dynamics via Par3-Trio-Rac1 signaling.

4.3 PTK7 and canonical Wnt signaling in NC cell migration

Directional NC cell migration is regulated by non-canonical Wnt pathway whereas the canonical Wnt pathway induce NC cells and is inactive during NC migration (Carmona-Fontaine et al., 2008a; Maj et al., 2016; Stuhlmiller and García-Castro, 2012). PTK7 affects the canonical Wnt pathway (reviewed in (Berger et al., 2017a)). However, PTK7 function in canonical Wnt signaling is contradictorily. PTK7 activates canonical Wnt signaling during Spemann's organizer formation by interacting with β-catenin (Puppo et al., 2011) and in specification of posterior neural tissue by LRP6 modulation (Bin-Nun et al., 2014). Using whole *Xenopus* embryo lysates and cancer cells PTK7 inhibits canonical Wnt signaling (Berger et al., 2017b; Peradziryi et al., 2011). During this study it was investigated if PTK7 affects canonical Wnt signaling during NC cell migration. Over-activation of the canonical Wnt pathway during NC cell migration in *Xenopus* leads to defects in NC cell migration (Maj et al., 2016). If PTK7 inhibits canonical Wnt signaling in NC cell migration, a PTK7 knockdown should lead to an over-activation of canonical Wnt signaling in NC cells. To investigate this, a β-catenin staining in NC cells were performed. β-catenin has an important role in cell adhesion and in gene transcription in canonical Wnt signaling (reviewed in (Brembeck et al., 2006)). A nuclear localization of β-catenin is a good readout for active canonical Wnt signaling (Barker and van den Born, 2008). However, PTK7 loss of function does not increase canonical Wnt signaling in NC cells *ex vivo* or affects β-catenin expression at the cell membrane. In addition, an inhibition of the canonical Wnt pathway by overexpressing Tcf3ΔC in PTK7-morphant embryos does not improve NC cell migration. In conclusion, PTK7 does not inhibit canonical Wnt signaling in NC cell migration. Since the canonical Wnt signaling during NC cell migration must be tightly controlled (Maj et al., 2016) and PTK7 is also able to activate canonical Wnt signaling (Bin-Nun et al., 2014; Puppo et al., 2011), PTK7 could also lead to an activation of canonical Wnt signaling in NC cells. But also activation of the canonical Wnt signaling in PTK7-morphant embryos does not rescue NC cell migration *in vivo* (sup. fig. S1).

PTK7 binds to canonical Wnt ligands in presence of Fz7, leading to caveolin-dependent endocytosis and inhibition of canonical Wnt signaling (Berger et al., 2017b; Peradziryi et al., 2011). The inhibitory properties of PTK7 on the canonical Wnt pathway could apply during embryonic patterning (Hayes et al., 2013). In zebrafish, PTK7 inhibits canonical Wnt-dependent gene expression in early gastrula and inhibits the effects of Wnt8 overexpression (Hayes et al., 2013). For this activity the PTK7 extracellular domain but not the kinase domain is necessary. Interestingly, a human scoliosis patient exhibits a PTK7 mutation with a missense variant in the sixth extracellular immunoglobulin domain, and the mutation disrupts PTK7 function in inhibiting canonical Wnt signaling (Hayes et al., 2014). Taken together, PTK7 does not affect canonical Wnt signaling during NC cell migration and its effects on canonical Wnt signaling may depend on the tissue and interaction partner.

5. Conclusion

The Wnt co-receptor PTK7 is important for proper NC cell migration. The aim of this study was to investigate further PTK7 signaling events during NC cell migration. The data provide that PTK7 dynamically localizes during NC migration. If a NC cell migrates towards another NC cell (fig. 31 A) and they get in contact (fig. 31 B), NC cells interact via PTK7 extracellular domains and PTK7 accumulates at the cell-cell contact. With current findings it can be modeled that PTK7 leads to the membrane recruitment of Dsh and a PTK7/Dsh/Trio complex affects the activity of the small GTPases RhoA and Rac1. Active RhoA leads to the formation of actomyosin stress fibers, resulting in cell contraction, and inhibited Rac1 activity leads to protrusion collapse. At the other side of the NC cell, Rac1 is activated, leading to lamellipodia formation. As a result, the NC cell moves away from the other NC cell (fig. 31 C). If PTK7 affects the downstream signaling components alone or together with other PCP receptors like Fz7 or Ror2 has to be further investigated. PTK7 also affects the canonical Wnt pathway but a function of PTK7 in canonical Wnt signaling during NC cell migration could not be observed. However, this study demonstrates an important role of PTK7 in CIL and demonstrates further downstream components in PTK7 signaling during NC cell migration.

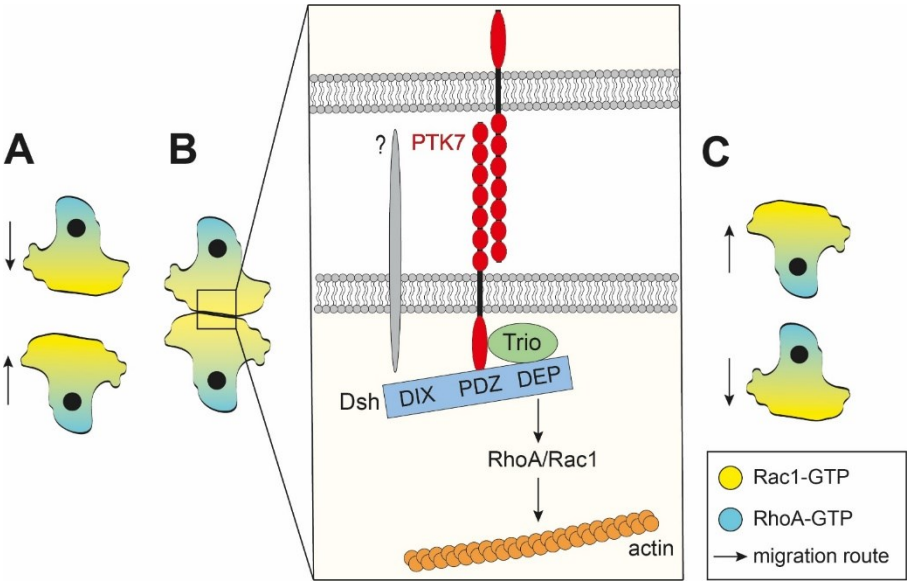

Fig. 31: Schematic overview of possible PTK7 signaling in NC cell migration. A Active Rac1 is localized at the front of migrating NC cells and RhoA is active at the back. **B** Upon cell-cell contact, PTK7 accumulates at contact sites and interacts via its extracellular domain with other PTK7 proteins. PTK7 recruits Dsh to the membrane and a possible PTK7/Dsh/Trio interaction affects RhoA/Rac1 activity. RhoA/Rac1 signaling leads to re-organization of the actin cytoskeleton. In the process of CIL, PTK7 could interact with the PCP receptors Ror2 or Fz7. **C** After cell contact, NC cells migrate away from each other.

6. Supplements

6.1 Activation of canonical Wnt signaling does not rescue NC cell migration defects caused by PTK7 loss of function

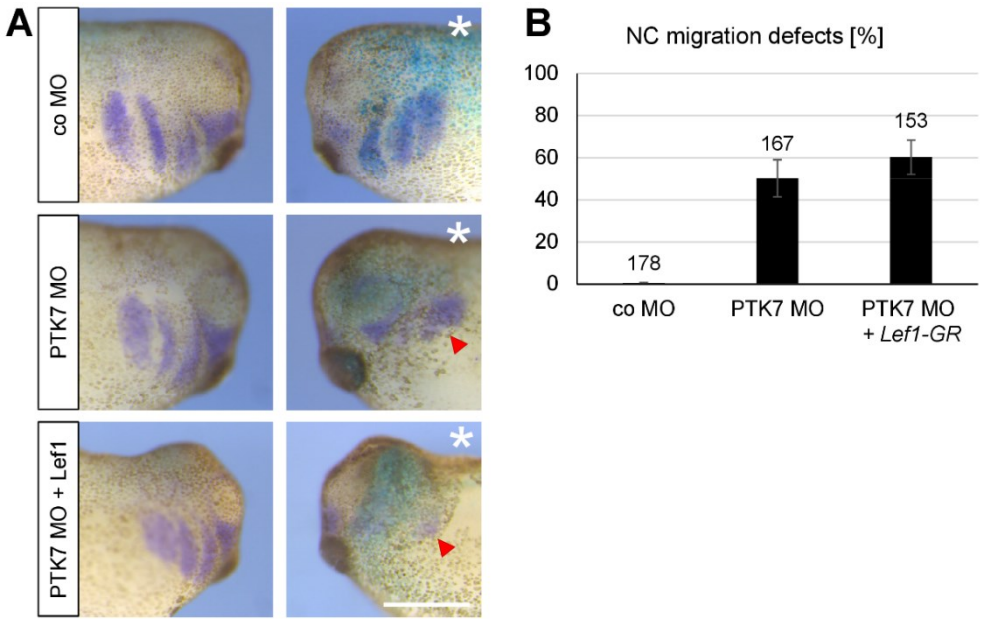

Fig. S1.: Activation of canonical Wnt signaling does not rescue NC migration defects caused by PTK7 LOF. *Xenopus* embryos were injected with 5/6 ng PTK7 MO and 10 pg *Lef1-GR* together with 75 pg *LacZ* into one blastomere of two-cell staged embryos. (A) NC cell migration were analyzed using *Twist in situ* hybridization. Asterisks indicate injected side, red arrow head indicate inhibited NC migration, scale bar = 500 µm. (B) Graph summarizes percentage of NC migration defects of four independent experiments, numbers of embryos and s.e.m. are indicated for each condition.

6.2 Time-lapse movies

Movie 1: Time-lapse movie showing that Ror2 expression rescues the PTK7-morphant phenotype. Explants injected with control MO (upper panel, left), control MO and Ror2 (upper panel, right), PTK7 MO (lower panel, left) or PTK7 MO and Ror2 (lower panel, right) together with mbGFP and H2B-mcherry are shown over a time interval of 8 hours and 20 minutes.

Movie 2: Time-lapse movie showing that Dsh expression rescues NC cell migration defects caused by PTK7 loss of function. Explants injected with control MO (left), PTK7 MO (middle) or PTK7 MO and Dsh (right) together with mbGFP and H2B-mcherry are shown over a time interval of 5 hours.

Movie 3: PTK7 accumulates at cell-cell contact sites. NC cells expressing PTK7-GFP and H2B-mcherry.

Movie 4: ΔkPTK7 accumulates at cell-cell contacts. NC cells expressing ΔkPTK7-GFP and H2B-mcherry, arrow indicates cell-cell contact shown in figure 20

Movie 5: ΔE3-7PTK7 localizes at the cell membrane. NC cells expressing ΔE3-7PTK7-GFP and H2B-mcherry, arrow indicates NC cell shown in figure 20.

Movie 6: ΔE1-7PTK7 is localized in intracellular compartments. NC cells expressing ΔE1-7PTK7-GFP and H2B-mcherry, arrow indicates cell-cell contact shown in figure 20.

Movie 7: cPTK7 Is localized in the cytoplasm and nucleus. NC cells expressing cPTK7-GFP and H2B-mcherry, arrow indicates NC cell shown in figure 20.

Movie 8: Time-lapse movie showing higher magnification of NC protrusion formation. NC cells injected with control MO (left) and PTK7 MO (right) together with mbGFP and H2B-mcherry.

Movie 9: F-actin dynamics in protrusion formation of NC cells injected with control MO. NC cells injected with control MO together with mbGFP and lifeact-RFP.

Movie 10: F-actin filaments are reformed under bleb membrane of PTK7 MO injected NC cells. NC cells injected with PTK7 MO together with mbGFP and lifeact-RFP, white arrow indicate bleb expansion and red arrows indicate reformation of F-actin shown in figure 25.

6.3 Matlab code for collision assay

```
% load the data; be aware of, and.; filename: wt.txt;
% structure first row: 1 dt1 dt2 x1 y1 x2 y2 x3 y3
datna = 'wt';
datname = [datna,'.txt']
daten = load(datname,'-ascii');
dt1 = daten(:,2);dt2 = daten(:,3);
x1 = daten(:,4);y1 = -daten(:,5);
x2 = daten(:,6);y2 = -daten(:,7);
x3 = daten(:,8);y3 = -daten(:,9);
% move point of origin to x2/y2
px1 = x1 - x2;py1 = y1 - y2;px3 = x3 - x2;py3 = y3 - y2;
% Cartesian to polar coordinate system with theta = angle in radiant and rho = distance in pixel
[thetaA,rhoA] = cart2pol(px1,py1);[thetaB,rhoB] = cart2pol(px3,py3); % in Radiant
% conversion from pixel to myem with 78px = 50mym
rhoA = rhoA./78.*50;rhoB = rhoB./78.*50;
% get the angle between vector A & B and the velocity after collision in mym/sec vwinkel = pi-
thetaA+thetaB;
velocity = rhoB./dt2;
% polar to cartesian system
[cx,cy] = pol2cart(vwinkel,velocity);
% insert the normalized vector (initial velocity vector) for velocity = 0.1 myem/sec ivvwinkel =
pi;ivvvelo = 0.1;
[vx,vy] = pol2cart(ivvwinkel,ivvvelo);
cx = [cx;vx];cy = [cy;vy];
% make the real compass
velofig = figure;
picvelo = compass(cx,cy,'-k');
hold on;
% Modify the velocity compass
radius2 = findall(gcf,'linestyle',':');
delete(radius2);
radtext=findall(gcf,'type','text');
delete(radtext);
set(picvelo,'LineWidth',1.1);
hold on;
filename = [datna,'velo.tif'];
saveas(velofig, filename);
```

7. Literature

Abercrombie, M. (1979). Contact inhibition and malignancy. *Nature* **281**, 259–262.

Alfandari, D., Cousin, H. and Marsden, M. (2010). Mechanism of Xenopus cranial neural crest cell migration. *Cell Adh. Migr.* **4**, 553–560.

Amano, M., Nakayama, M. and Kaibuchi, K. (2010). Rho-kinase/ROCK: A key regulator of the cytoskeleton and cell polarity. *Cytoskeleton* **67**, 545–554.

Andreeva, A., Lee, J., Lohia, M., Wu, X., Macara, I. G. and Lu, X. (2014). PTK7-Src Signaling at Epithelial Cell Contacts Mediates Spatial Organization of Actomyosin and Planar Cell Polarity. *Dev. Cell* **29**, 20–33.

Ang, S. F., Zhao, Z. S., Lim, L. and Manser, E. (2010). DAAM1 is a formin required for centrosome re-orientation during cell migration. *PLoS One* **5**,.

Arnold, T. R., Stephenson, R. E. and Miller, A. L. (2017). Rho GTPases and actomyosin: Partners in regulating epithelial cell-cell junction structure and function. *Exp. Cell Res.* **358**, 20–30.

Axelrod, J. D. (2001). Unipolar membrane association of Dishevelled mediates Frizzled planar cell polarity signaling. *Genes Dev.* **15**, 1182–1187.

Axelrod, J. D., Miller, J. R., Shulman, J. M., Moon, R. T. and Perrimon, N. (1998). Differential recruitment of dishevelled provides signaling specificity in the planar cell polarity and Wingless signaling pathways. *Genes Dev.* **12**, 2610–2622.

Aybar, M. J. and Mayor, R. (2002). Early induction of neural crest cells: Lessons learned from frog, fish and chick. *Curr. Opin. Genet. Dev.* **12**, 452–458.

Backer, S., Lokmane, L., Landragin, C., Deck, M., Garel, S. and Bloch-Gallego, E. (2018). Trio GEF mediates RhoA activation downstream of Slit2 and coordinates telencephalic wiring. *Development* **145**, dev153692.

Bai, Y., Tan, X., Zhang, H., Liu, C., Zhao, B., Li, Y., Lu, L., Liu, Y. and Zhou, J. (2014). Ror2 receptor mediates Wnt11 ligand signaling and affects convergence and extension movements in zebrafish. *J. Biol. Chem.* **289**, 20664–76.

Bajanca, F., Gouignard, N., Colle, C., Parsons, M., Mayor, R., Theveneau, E. and Mayor, R. (2019). In vivo topology converts competition for cell-matrix adhesion into directional migration. *Nat. Commun.* **10**, 1518.

Barker, N. and van den Born, M. (2008). Detection of beta-catenin localization by immunohistochemistry. *Methods Mol. Biol.* **468**, 91–98.

Barriga, E. H., Franze, K., Charras, G. and Mayor, R. (2018). Tissue stiffening coordinates morphogenesis by triggering collective cell migration in vivo. *Nature* **554**, 523–527.

Becker, S. F. S., Mayor, R. and Kashef, J. (2013). Cadherin-11 mediates contact inhibition of locomotion during Xenopus neural crest cell migration. *PLoS One* **8**,

e85717.

Bellanger, J. M., Lazaro, J. B., Diriong, S., Fernandez, A., Lamb, N. and Debant, A. (1998). The two guanine nucleotide exchange factor domains of Trio link the Rac1 and the RhoA pathways in vivo. *Oncogene* **16**, 147–152.

Bellanger, J. M., Astier, C., Sardet, C., Ohta, Y., Stossel, T. P. and Debant, A. (2000). The Rac1- and RhoG-specific GEF domain of trio targets filamin to remodel cytoskeletal actin. *Nat. Cell Biol.* **2**, 888–892.

Bellanger, J. M., Estrach, S., Schmidt, S., Briaŋcon-Marjollet, A., Zugasti, O., Fromont, S. and Debant, A. (2003). Different regulation of the Trio Dbl-Homology domains by their associated PH domains. *Biol. Cell* **95**, 625–634.

Benard, V., Bohl, B. P. and Bokoch, G. M. (1999). Characterization of Rac and Cdc42 activation in chemoattractant- stimulated human neutrophils using a novel assay for active GTPases. *J. Biol. Chem.* **274**, 13198–13204.

Berger, H., Wodarz, A. and Borchers, A. (2017a). PTK7 Faces the Wnt in Development and Disease. *Front. Cell Dev. Biol.* **5**, 1–7.

Berger, H., Breuer, M., Peradziryi, H., Podleschny, M., Jacob, R. and Borchers, A. (2017b). PTK7 localization and protein stability is affected by canonical Wnt ligands. *J. Cell Sci.* **130**, 1890–1903.

Billiard, J., Way, D. S., Seestaller-Wehr, L. M., Moran, R. A., Mangine, A. and Bodine, P. V. N. (2005). The Orphan Receptor Tyrosine Kinase Ror2 Modulates Canonical Wnt Signaling in Osteoblastic Cells. *Mol. Endocrinol.* **19**, 90–101.

Bin-Nun, N., Lichtig, H., Malyarova, A., Levy, M., Elias, S. and Frank, D. (2014). PTK7 modulates Wnt signaling activity via LRP6. *Development* **141**, 410–421.

Bishop, A. L. and Hall, A. (2000). Rho GTPases and their effector proteins. *Biochem. J.* **348**, 241–255.

Blanchoin, L., Amann, K. J., Higgs, H. N., Marchand, J.-B., Kaiser, D. A. and Pollard, T. D. (2000). Direct observation of dendritic actin filament networks nucleated by Arp2/3 complex and WASP/Scar proteins. *Nature* **404**, 1007–1011.

Blangy, A., Vignal, E., Schmidt, S., Debant, A., Gauthier-Rouvière, C. and Fort, P. (2000). TrioGEF1 controls Rac- and Cdc42-dependent cell structures through the direct activation of RhoG. *J. Cell Sci.* **113**, 729–39.

Borchers, A., Epperlein, H. H. and Wedlich, D. (2000). An assay system to study migratory behavior of cranial neural crest cells in Xenopus. *Dev. Genes Evol.* **210**, 217–222.

Bornschlögl, T. (2013). How filopodia pull: What we know about the mechanics and dynamics of filopodia. *Cytoskeleton* **70**, 590–603.

Boutros, M., Paricio, N., Strutt, D. I. and Mlodzik, M. (1998). Dishevelled activates

JNK and Discriminates between JNK pathways in Planar Polarity and wingless Signaling. *Cell* **94**, 109–118.

Braga, V. M. M. (2002). Cell – cell adhesion and signalling. *Curr. Opin. Cell Biol.* **14**, 546–556.

Brand, A. H. and Perrimon, N. (1993). Targeted gene expression as a means of altering cell fates and generating dominant phenotypes. *Development* **118**, 401–15.

Brannon, M., Gomperts, M., Sumoy, L., Moon, R. T. and Kimelman, D. (1997). A β-catenin/XTcf-3 complex binds to the siamois promoter to regulate dorsal axis specification in Xenopus. *Genes Dev.* **11**, 2359–2370.

Brembeck, F. H., Rosario, M. and Birchmeier, W. (2006). Balancing cell adhesion and Wnt signaling, the key role of beta-catenin. *Curr. Opin. Genet. Dev.* **16**, 51–59.

Bresnick, A. R. (1999). Molecular mechanisms of nonmuscle myosin-II regulation. *Curr. Opin. Cell Biol.* **11**, 26–33.

Brinkmann, E. M., Mattes, B., Kumar, R., Hagemann, A. I. H., Gradl, D., Scholpp, S., Steinbeisser, H., Kaufmann, L. T. and Özbek, S. (2016). Secreted Frizzled-related Protein 2 (sFRP2) redirects non-canonical Wnt signaling from Fz7 to Ror2 during vertebrate gastrulation. *J. Biol. Chem.* **291**, 13730–13742.

Brunner, E., Peter, O., Schweizer, L. and Basler, K. (1997). Pangolin encodes a Lef-1 homologue that acts downstream of Armadillo to transduce the Wingless signal in Drosophila. *Nature* **385**, 829–833.

Bryne, K., Monsefi, N., Dawson, J., Degasperi, A., Bukowski-Wills, J., Volinsky, N., Dobrzyński, M., Birtwistle, M., Tsyganov, M., Kiyatkin, A., et al. (2016). Bistability in the Rac1, PAK, and RhoA Signaling Network Drives Actin Cytoskeleton Dynamics and Cell Motility Switches. *Cell Syst.* **2**, 38–48.

Čajánek, L., Ganji, R. S., Henriques-Oliveira, C., Theofilopoulos, S., Koník, P., Bryja, V. and Arenas, E. (2013). Tiam1 Regulates the Wnt/Dvl/Rac1 Signaling Pathway and the Differentiation of Midbrain Dopaminergic Neurons. *Mol. Cell. Biol.* **33**, 59–70.

Carmona-Fontaine, C., Matthews, H. and Mayor, R. (2008a). Directional cell migration in vivo: Wnt at the crest. *Cell Adh. Migr.* **2**, 240–242.

Carmona-Fontaine, C., Matthews, H. K., Kuriyama, S., Moreno, M., Dunn, G. A., Parsons, M., Stern, C. D. and Mayor, R. (2008b). Contact inhibition of locomotion in vivo controls neural crest directional migration. *Nature* **456**, 957–961.

Carmona-Fontaine, C., Theveneau, E., Tzekou, A., Tada, M., Woods, M., Page, K. M., Parsons, M., Lambris, J. D. and Mayor, R. (2011). Complement fragment C3a controls mutual cell attraction during collective cell migration. *Dev. Cell* **21**, 1026–1037.

Cavallo, R. A., Cox, R. T., Moline, M. M., Roose, J., Polevoy, G. A., Clevers, H., Peifer, M. and Bejsovec, A. (1998). Drosophila Tcf and Groucho interact to repress wingless signalling activity. *Nature* **395**, 604–608.

Charras, G. and Paluch, E. (2008). Blebs lead the way: How to migrate without lamellipodia. *Nat. Rev. Mol. Cell Biol.* **9**, 730–736.

Charras, G. T., Hu, C. K., Coughlin, M. and Mitchison, T. J. (2006). Reassembly of contractile actin cortex in cell blebs. *J. Cell Biol.* **175**, 477–490.

Chen, W. S., Antic, D., Matis, M., Logan, C. Y., Povelones, M., Anderson, G. A., Nusse, R. and Axelrod, J. D. (2008). Asymmetric homotypic interactions of the atypical cadherin flamingo mediate intercellular polarity signaling. *Cell* **133**, 1093–1105.

Chen, S.-Y., Huang, P.-H. and Cheng, H.-J. (2011). Disrupted-in-Schizophrenia 1-mediated axon guidance involves TRIO-RAC-PAK small GTPase pathway signaling. *Proc. Natl. Acad. Sci.* **108**, 5861–5866.

Chen, K., Anthony, S. M. and Granick, S. (2014a). Extending particle tracking capability with Delaunay triangulation. *Langmuir* **30**, 4760–6.

Chen, R., Khatri, P., Mazur, P. K., Polin, M., Zheng, Y., Vaka, D., Hoang, C. D., Shrager, J., Xu, Y., Vicent, S., et al. (2014b). A Meta-analysis of Lung Cancer Gene Expression Identifies PTK7 as a Survival Gene in Lung Adenocarcinoma. *Cancer Res.* **74**, 2892–2902.

Chou, Y. H. and Hayman, M. J. (1991). Characterization of a member of the immunoglobulin gene superfamily that possibly represents an additional class of growth factor receptor. *Proc. Natl. Acad. Sci. U. S. A.* **88**, 4897–4901.

Coumans, J. V. F., Davey, R. J. and Moens, P. D. J. (2018). Cofilin and profilin: partners in cancer aggressiveness. *Biophys. Rev.* **10**, 1323–1335.

Dai, B., Yan, T. and Zhang, A. (2017). ROR2 receptor promotes the migration of osteosarcoma cells in response to Wnt5a. *Cancer Cell Int.* **17**, 1–9.

Dang, I., Gorelik, R., Sousa-Blin, C., Derivery, E., Guérin, C., Linkner, J., Nemethova, M., Dumortier, J. G., Giger, F. A., Chipysheva, T. A., et al. (2013). Inhibitory signalling to the Arp2/3 complex steers cell migration. *Nature* **503**, 281–284.

Das, G., Jenny, A., Klein, T., Eaton, S. and Mlodzik, M. (2004). Diego interacts with Prickle and Strabismus/Van Gogh to localize planar cell polarity complexes. *Development* **131**, 4467–4476.

De Calisto, J., Araya, C., Marchant, L., Riaz, C. F. and Mayor, R. (2005). Essential role of non-canonical Wnt signalling in neural crest migration. *Development* **132**, 2587–2597.

Debant, A., Serra-Pagès, C., Seipel, K., O'Brien, S., Tang, M., Park, S. H. and Streuli, M. (1996). The multidomain protein Trio binds the LAR transmembrane tyrosine phosphatase, contains a protein kinase domain, and has separate rac-specific and rho-specific guanine nucleotide exchange factor domains. *Proc. Natl. Acad. Sci. U. S. A.* **93**, 5466–5471.

Delorme, V., Machacek, M., DerMardirossian, C., Anderson, K. L., Wittmann, T., Hanein, D., Waterman-Storer, C., Danuser, G. and Bokoch, G. M. (2007). Cofilin Activity Downstream of Pak1 Regulates Cell Protrusion Efficiency by Organizing Lamellipodium and Lamella Actin Networks. *Dev. Cell* **13**, 646–662.

DerMardirossian, C. and Bokoch, G. M. (2005). GDIs: Central regulatory molecules in Rho GTPase activation. *Trends Cell Biol.* **15**, 356–363.

Desai, R. A., Gopal, S. B., Chen, S. and Chen, C. S. (2013). Contact inhibition of locomotion probabilities drive solitary versus collective cell migration. *J. R. Soc. Interface* **10**, 20130717.

Dupin, E., Creuzet, S. and Le Douarin, N. M. (2006). The contribution of the neural crest to the vertebrate body. In *Advances in Experimental Medicine and Biology*, pp. 96–119.

Etchevers, H. C., Dupin, E. and Le Douarin, N. M. (2019). The diverse neural crest: from embryology to human pathology. *Development* **146**, dev169821.

Fackler, O. T. and Grosse, R. (2008). Cell motility through plasma membrane blebbing. *J. Cell Biol.* **181**, 879–884.

Feike, A. C., Rachor, K., Gentzel, M. and Schambony, A. (2010). Wnt5a/Ror2-induced upregulation of xPAPC requires xShcA. *Biochem. Biophys. Res. Commun.* **400**, 500–6.

Fiedler, M., Mendoza-Topaz, C., Rutherford, T. J., Bienz, M. and Mieszczanek, J. (2011). Dishevelled interacts with the DIX domain polymerization interface of Axin to interfere with its function in down-regulating β-catenin. *Proc. Natl. Acad. Sci.* **108**, 1937–1942.

Figueiredo, A. L., Maczkowiak, F., Borday, C., Pla, P., Sittewelle, M., Pegoraro, C. and Monsoro-Burq, A. H. (2017). PFKFB4 control of AKT signaling is essential for premigratory and migratory neural crest formation. *Development* **144**, 4183–4194.

Friedl, P. and Gilmour, D. (2009). Collective cell migration in morphogenesis, regeneration and cancer. *Nat. Rev. Mol. Cell Biol.* **10**, 445–457.

Gammill, L. S., Gonzalez, C. and Bronner-Fraser, M. (2007). Neuropilin 2/semaphorin 3F signaling is essential for cranial neural crest migration and trigeminal ganglion condensation. *Dev. Neurobiol.* **67**, 47–56.

Golubkov, V. S. and Strongin, A. Y. (2012). Insights into Ectodomain Shedding and

Processing of Protein-tyrosine Pseudokinase 7 (PTK7). *J. Biol. Chem.* **287**, 42009–42018.

Golubkov, V. S. and Strongin, A. Y. (2014). Downstream signaling and genome-wide regulatory effects of PTK7 pseudokinase and its proteolytic fragments in cancer cells. *Cell Commun. Signal.* **12**, 15.

Golubkov, V. S., Chekanov, A. V., Cieplak, P., Aleshin, A. E., Chernov, A. V., Zhu, W., Radichev, I. A., Zhang, D., Dong, P. D. and Strongin, A. Y. (2010). The Wnt/Planar Cell Polarity Protein-tyrosine Kinase-7 (PTK7) Is a Highly Efficient Proteolytic Target of Membrane Type-1 Matrix Metalloproteinase Implications in cancer and embryogenesis. *J. Biol. Chem.* **285**, 35740–35749.

Grainger, S. and Willert, K. (2018). Mechanisms of Wnt signaling and control. *Wiley Interdiscip. Rev. Syst. Biol. Med.* e1422.

Groves, A. K. and LaBonne, C. (2014). Setting appropriate boundaries: Fate, patterning and competence at the neural plate border. *Dev. Biol.* **389**, 2–12.

Grumolato, L., Liu, G., Mong, P., Mudbhary, R., Biswas, R., Arroyave, R., Vijayakumar, S., Economides, A. N. and Aaronson, S. A. (2010). Canonical and noncanonical Wnts use a common mechanism to activate completely unrelated coreceptors. *Genes Dev.* **24**, 2517–2530.

Guilluy, C., Garcia-Mata, R. and Burridge, K. (2011). Rho protein crosstalk: Another social network? *Trends Cell Biol.* **21**, 718–726.

Guo, N., Hawkins, C. and Nathans, J. (2004). Frizzled6 controls hair patterning in mice. *Proc. Natl. Acad. Sci. U. S. A.* **101**, 9277–9281.

Habas, R. and He, X. (2006). Activation of Rho and Rac by Wnt/Frizzled signaling. *Methods Enzymol.* **406**, 500–511.

Habas, R., Kato, Y. and He, X. (2001). Wnt/Frizzled activation of Rho regulates vertebrate gastrulation and requires a novel formin homology protein Daam1. *Cell* **107**, 843–854.

Habas, R., Dawid, I. B. and He, X. (2003). Coactivation of Rac and Rho by Wnt/Frizzled signaling is required for vertebrate gastrulation. *Genes Dev.* **17**, 295–309.

Hall, B. K. (2000). The neural crest as a fourth germ layer and vertebrates as quadroblastic not triploblastic. *Evol. Dev.* **2**, 3–5.

Harland, R. M. (1991). In Situ Hybridization: an improved whole-mount method for Xenopus embryos. In *Methods in cell biology*, pp. 685–695.

Hayes, M., Naito, M., Daulat, A., Angers, S. and Ciruna, B. (2013). Ptk7 promotes non-canonical Wnt/PCP-mediated morphogenesis and inhibits Wnt/β-catenin-dependent cell fate decisions during vertebrate development. *Development* **140**, 1807–1818.

Hayes, M., Gao, X., Yu, L. X., Paria, N., Henkelman, R. M., Wise, C. A. and Ciruna, B. (2014). ptk7 mutant zebrafish models of congenital and idiopathic scoliosis implicate dysregulated Wnt signalling in disease. *Nat. Commun.* **5**, 4777.

He, T. C., Sparks, A. B., Rago, C., Hermeking, H., Zawel, L., Da Costa, L. T., Morin, P. J., Vogelstein, B. and Kinzler, K. W. (1998). Identification of c-MYC as a target of the APC pathway. *Science (80-.).* **281**, 1509–1512.

Heisenberg, C. P., Tada, M., Rauch, G. J., Saúde, L., Concha, M. L., Geisler, R., Stemple, D. L., Smith, J. C. and Wilson, S. W. (2000). Silberblick/Wnt11 mediates convergent extension movements during zebrafish gastrulation. *Nature* **405**, 76–81.

Hikasa, H., Shibata, M., Hiratani, I. and Taira, M. (2002). The Xenopus receptor tyrosine kinase Xror2 modulates morphogenetic movements of the axial mesoderm and neuroectoderm via Wnt signaling. *Development* **129**, 5227–5239.

Ho, H.-Y. H., Susman, M. W., Bikoff, J. B., Ryu, Y. K., Jonas, A. M., Hu, L., Kuruvilla, R. and Greenberg, M. E. (2012). Wnt5a-Ror-Dishevelled signaling constitutes a core developmental pathway that controls tissue morphogenesis. *Proc. Natl. Acad. Sci.* **109**, 4044–51.

Holzer, T., Liffers, K., Rahm, K., Trageser, B., Ozbek, S. and Gradl, D. (2012). Live imaging of active fluorophore labelled Wnt proteins. *FEBS Lett.* **586**, 1638–44.

Hopwood, N. D., Pluck, A. and Gurdon, J. B. (1989). A Xenopus mRNA related to Drosophila twist is expressed in response to induction in the mesoderm and the neural crest. *Cell* **59**, 893–903.

Huang, C., Kratzer, M.-C., Wedlich, D. and Kashef, J. (2016). E-cadherin is required for cranial neural crest migration in Xenopus laevis. *Dev. Biol.* **411**, 159–171.

Huber, O., Korn, R., McLaughlin, J., Ohsugi, M., Herrmann, B. G. and Kemler, R. (1996). Nuclear localization of β-catenin by interaction with transcription factor LEF-1. *Mech. Dev.* **59**, 3–10.

Ikeda, S., Kishida, S., Yamamoto, H., Murai, H., Koyama, S. and Kikuchi, A. (1998). Axin, a negative regulator of the Wnt signaling pathway, forms a complex with GSK-3beta and beta-catenin and promotes GSK-3beta-dependent phosphorylation of beta-catenin. *EMBO J.* **17**, 1371–1384.

Ikenouchi, J. and Aoki, K. (2017). Membrane bleb: A seesaw game of two small GTPases. *Small GTPases* **8**, 85–89.

Isenberg, G., Aebi, U. and Pollard, T. D. (1980). An actin-binding protein from acanthamoeba regulates actin filament polymerization and interactions. *Nature* **288**, 455–459.

Jenny, A., Darken, R. S., Wilson, P. A. and Mlodzik, M. (2003). Prickle and Strabismus form a functional complex to generate a correct axis during planar cell polarity

signaling. *EMBO J.* **22**, 4409–4420.

Jenny, A., Reynolds-Kenneally, J., Das, G., Burnett, M. and Mlodzik, M. (2005). Diego and Prickle regulate Frizzled planar cell polarity signalling by competing for Dishevelled binding. *Nat. Cell Biol.* **7**, 691–697.

Jessen, J. R., Topczewski, J., Bingham, S., Sepich, D. S., Marlow, F., Chandrasekhar, A. and Solnica-Krezel, L. (2002). Zebrafish trilobite identifies new roles for Strabismus in gastrulation and neuronal movements. *Nat. Cell Biol.* **4**, 610–615.

Jin, J., Ryu, H. S., Lee, K. B. and Jang, J.-J. (2014). High Expression of Protein Tyrosine Kinase 7 Significantly Associates with Invasiveness and Poor Prognosis in Intrahepatic Cholangiocarcinoma. *PLoS One* **9**, e90247.

Johnson, H. E., King, S. J., Asokan, S. B., Rotty, J. D., Bear, J. E. and Haugh, J. M. (2015). F-actin bundles direct the initiation and orientation of lamellipodia through adhesion-based signaling. *J. Cell Biol.* **208**, 443–455.

Jung, J. W., Shin, W. S., Song, J. and Lee, S. T. (2004). Cloning and characterization of the full-length mouse Ptk7 cDNA encoding a defective receptor protein tyrosine kinase. *Gene* **328**, 75–84.

Kadir, S., Astin, J. W., Tahtamouni, L., Martin, P. and Nobes, C. D. (2011). Microtubule remodelling is required for the front-rear polarity switch during contact inhibition of locomotion. *J Cell Sci* **124**, 2642–2653.

Kashef, J., Köhler, A., Kuriyama, S., Alfandari, D., Mayor, R. and Wedlich, D. (2009). Cadherin-11 regulates protrusive activity in Xenopus cranial neural crest cells and upstream of Trio and the small GTPases. *Genes Dev.* **23**, 1393–1398.

Keren, K., Pincus, Z., Allen, G. M., Barnhart, E. L., Marriott, G., Mogilner, A. and Theriot, J. A. (2008). Mechanism of shape determination in motile cells. *Nature* **453**, 475–480.

Kim, W., Kim, M. and Jho, E. (2013). Wnt/β-catenin signalling: from plasma membrane to nucleus. *Biochem. J.* **450**, 9–21.

Kim, J.-H., Kwon, J., Lee, H., Kang, M., Yoon, H., Lee, S.-T. and Park, J. (2014). Protein tyrosine kinase 7 plays a tumor suppressor role by inhibiting ERK and AKT phosphorylation in lung cancer. *Oncol. Rep.* **31**, 2708–2712.

Kishida, S., Yamamoto, H., Hino, S., Ikeda, S., Kishida, M. and Kikuchi, A. (1999). DIX domains of Dvl and axin are necessary for protein interactions and their ability to regulate beta-catenin stability. *Mol. Cell. Biol.* **19**, 4414–4422.

Kjøller, L. and Hall, A. (1999). Signaling to Rho GTPases. *Exp. Cell Res.* **253**, 166–179.

Klein, T. J. and Mlodzik, M. (2005). Planar cell polarization: an emerging model points

in the right direction. *Annu. Rev. Cell Dev. Biol.* **21**, 155–176.

Koestner, U., Shnitsar, I., Linnemannstöns, K., Hufton, A. L. and Borchers, A. (2008). Semaphorin and neuropilin expression during early morphogenesis of Xenopus laevis. *Dev. Dyn.* **237**, 3853–3863.

Kratzer, M.-C., England, L., Apel, D., Hassel, M. and Borchers, A. (2019). Evolution of the Rho guanine nucleotide exchange factors Kalirin and Trio and their gene expression in Xenopus development. *Gene Expr. Patterns* **32**, 18–27.

Kraynov, V. S., Chamberlain, C., Bokoch, G. M., Schwartz, M. A., Slabaugh, S. and Hahn, K. M. (2000). Localized Rac activation dynamics visualized in living cells. *Science (80-.).* **290**, 333–337.

Kuriyama, S. and Mayor, R. (2008). Molecular analysis of neural crest migration. *Philos. Trans. R. Soc. Lond. B. Biol. Sci.* **363**, 1349–1362.

Laemmli, U. K. (1970). Cleavage of structural proteins during the assembly of the head of bacteriophage T4. *Nature* **227**, 680–685.

Landin Malt, A., Dailey, Z., Holbrook-Rasmussen, J., Zheng, Y., Hogan, A., Du, Q. and Lu, X. (2019). Par3 is essential for the establishment of planar cell polarity of inner ear hair cells. *Proc. Natl. Acad. Sci.* **116**, 4999–5008.

Lee, S. T., Strunk, K. M. and Spritz, R. a (1993). A survey of protein tyrosine kinase mRNAs expressed in normal human melanocytes. *Oncogene* **8**, 3403–3410.

Lee, J., Andreeva, A., Sipe, C. W., Liu, L., Cheng, A. and Lu, X. (2012). PTK7 regulates myosin II activity to orient planar polarity in the mammalian auditory epithelium. *Curr. Biol.* **22**, 956–966.

Letort, G., Ennomani, H., Gressin, L., Théry, M. and Blanchoin, L. (2015). Dynamic reorganization of the actin cytoskeleton. *F1000Research* **4**, 940.

Letunic, I. and Bork, P. (2018). 20 years of the SMART protein domain annotation resource. *Nucleic Acids Res.* **46**, D493–D496.

Li, Y., Guo, Z., Chen, H., Dong, Z., Pan, Z. K., Ding, H., Su, S. B. and Huang, S. (2011). HOXC8-Dependent Cadherin 11 Expression Facilitates Breast Cancer Cell Migration through Trio and Rac. *Genes and Cancer* **2**, 880–888.

Lichtig, H., Cohen, Y., Bin-Nun, N., Golubkov, V. and Frank, D. (2019). PTK7 proteolytic fragment proteins function during early Xenopus development. *Dev. Biol.*

Lin, Y., Zhang, L.-H., Wang, X.-H., Xing, X.-F., Cheng, X.-J., Dong, B., Hu, Y., Du, H., Li, Y.-A., Zhu, Y.-B., et al. (2012). PTK7 as a novel marker for favorable gastric cancer patient survival. *J. Surg. Oncol.* **106**, 880–886.

Linnemannstöns, K., Ripp, C., Honemann-Capito, M., Brechtel-Curth, K., Hedderich, M. and Wodarz, A. (2014). The PTK7-related transmembrane proteins off-track and off-track 2 are co-receptors for Drosophila Wnt2 required for male

fertility. *PLoS Genet.* **10**, e1004443.

Liu, C., Li, Y., Semenov, M., Han, C., Baeg, G. H., Tan, Y., Zhang, Z., Lin, X. and He, X. (2002). Control of β-catenin phosphorylation/degradation by a dual-kinase mechanism. *Cell* **108**, 837–847.

Liu, Y., Ross, J. F., Bodine, P. V. N. and Billiard, J. (2007). Homodimerization of Ror2 Tyrosine Kinase Receptor Induces 14-3-3β Phosphorylation and Promotes Osteoblast Differentiation and Bone Formation. *Mol. Endocrinol.* **21**, 3050–3061.

Liu, Y., Rubin, B., Bodine, P. V. N. and Billiard, J. (2008a). Wnt5a induces homodimerization and activation of Ror2 receptor tyrosine kinase. *J. Cell. Biochem.* **105**, 497–502.

Liu, W., Sato, A., Khadka, D., Bharti, R., Diaz, H., Runnels, L. W. and Habas, R. (2008b). Mechanism of activation of the Formin protein Daam1. *Proc. Natl. Acad. Sci.* **105**, 210–215.

Liu, W., Xie, Y., Ma, J., Luo, X., Nie, P., Zuo, Z., Lahrmann, U., Zhao, Q., Zheng, Y., Zhao, Y., et al. (2015). IBS: An illustrator for the presentation and visualization of biological sequences. *Bioinformatics* **31**, 3359–3361.

Lu, X., Borchers, A., Jolicoeur, C., Rayburn, H., Baker, J. C. and Tessier-lavigne, M. (2004). PTK7/CCK-4 is a novel regulator of planar cell polarity in vertebrates. *Nature* **430**, 93–98.

Maekawa, M., Ishizaki, T., Boku, S., Watanabe, N., Fujita, A., Iwamatsu, A., Obinata, T., Ohashi, K., Mizuno, K. and Narumiya, S. (1999). Signaling from Rho to the actin cytoskeleton through protein kinases ROCK and LIM-kinase. *Science (80-.).* **285**, 895–898.

Maier, M., Baldwin, C., Aoudjit, L. and Takano, T. (2018). The Role of Trio, a Rho Guanine Nucleotide Exchange Factor, in Glomerular Podocytes. *Int. J. Mol. Sci.* **19**, 479.

Maj, E., Künneke, L., Loresch, E., Grund, A., Melchert, J., Pieler, T., Aspelmeier, T. and Borchers, A. (2016). Controlled levels of canonical Wnt signaling are required for neural crest migration. *Dev. Biol.* **417**, 77–90.

Mao, J., Wang, J., Liu, B., Pan, W., Farr, G. H., Flynn, C., Yuan, H., Takada, S., Kimelman, D., Li, L., et al. (2001). Low-density lipoprotein receptor-related protein-5 binds to Axin and regulates the canonical Wnt signaling pathway. *Mol. Cell* **7**, 801–809.

Martin, R. M., Leonhardt, H. and Cardoso, M. C. (2005). DNA labeling in living cells. *Cytom. Part A* **67**, 45–52.

Martinez, S., Scerbo, P., Giordano, M., Daulat, A. M., Lhoumeau, A.-C., Thome, V., Kodjabachian, L. and Borg, J.-P. (2015). The PTK7 and ROR2 receptors interact

in the vertebrate WNT/PCP pathway. *J. Biol. Chem.* **290**, 30562–30572.

Masiakowski, P. and Carroll, R. D. (1992). A novel family of cell surface receptors with tyrosine kinase-like domain. *J. Biol. Chem.* **267**, 26181–26190.

Mattila, P. K. and Lappalainen, P. (2008). Filopodia: Molecular architecture and cellular functions. *Nat. Rev. Mol. Cell Biol.* **9**, 446–454.

Mayor, R. and Theveneau, E. (2013). The neural crest. *Development* **140**, 2247–2251.

Mayor, R. and Theveneau, E. (2014). The role of the non-canonical Wnt-planar cell polarity pathway in neural crest migration. *Biochem. J.* **457**, 19–26.

McGrew, L. L., Takemaru, K. I., Bates, R. and Moon, R. T. (1999). Direct regulation of the Xenopus engrailed-2 promoter by the Wnt signaling pathway, and a molecular screen for Wnt-responsive genes, confirm a role for Wnt signaling during neural patterning in Xenopus. *Mech. Dev.* **87**, 21–32.

Medina, A. and Steinbeisser, H. (2000). Interaction of Frizzled 7 and Dishevelled in Xenopus. *Dev. Dyn.* **218**, 671–680.

Medley, Q. G., Serra-Pages, C., Iannotti, E., Seipel, K., Tang, M., O'Brien, S. P. and Streuli, M. (2000). The Trio guanine nucleotide exchange factor is a RhoA target: Binding of RhoA to the Trio immunoglobulin-like domain. *J. Biol. Chem.* **275**, 36116–36123.

Medley, Q. G., Buchbinder, E. G., Tachibana, K., Ngo, H., Serra-Pagès, C. and Streuli, M. (2003). Signaling between focal adhesion kinase and Trio. *J. Biol. Chem.* **278**, 13265–13270.

Megason, S. G. and Fraser, S. E. (2003). Digitizing life at the level of the cell: High-performance laser-scanning microscopy and image analysis for in toto imaging of development. *Mech. Dev.* **120**, 1407–1420.

Mikels, A. J. and Nusse, R. (2006). Purified Wnt5a protein activates or inhibits β-catenin-TCF signaling depending on receptor context. *PLoS Biol.* **4**, 570–582.

Mikels, A., Minami, Y. and Nusse, R. (2009). Ror2 receptor requires tyrosine kinase activity to mediate Wnt5A signaling. *J. Biol. Chem.* **284**, 30167–30176.

Miki, H., Sasaki, T., Takai, Y. and Takenawa, T. (1998). Induction of filopodium formation by a WASP-related actin-depolymerizing protein N-WASP. *Nature* **391**, 93–96.

Milet, C. and Monsoro-Burq, A. H. (2012). Neural crest induction at the neural plate border in vertebrates. *Dev. Biol.* **366**, 22–33.

Miller, M. A. and Steele, R. E. (2000). Lemon encodes an unusual receptor protein-tyrosine kinase expressed during gametogenesis in Hydra. *Dev. Biol.* **224**, 286–298.

Minoux, M. and Rijli, F. M. (2010). Molecular mechanisms of cranial neural crest cell

migration and patterning in craniofacial development. *Development* **137**, 2605–2621.

Mitchell, B., Stubbs, J. L., Huisman, F., Taborek, P., Yu, C. and Kintner, C. (2009). The PCP Pathway Instructs the Planar Orientation of Ciliated Cells in the Xenopus Larval Skin. *Curr. Biol.* **19**, 924–929.

Mlodzik, M. (2015). *The Dishevelled Protein Family: Still Rather a Mystery After Over 20 Years of Molecular Studies*. 1st ed. Elsevier Inc.

Mogilner, A. (2009). Mathematics of cell motility: Have we got its number? *J. Math. Biol.* **58**, 105–134.

Molenaar, M., Van De Wetering, M., Oosterwegel, M., Peterson-Maduro, J., Godsave, S., Korinek, V., Roose, J., Destrée, O. and Clevers, H. (1996). XTcf-3 transcription factor mediates β-catenin-induced axis formation in Xenopus embryos. *Cell* **86**, 391–399.

Moore, R., Theveneau, E., Pozzi, S., Alexandre, P., Richardson, J., Merks, A., Parsons, M., Kashef, J., Linker, C. and Mayor, R. (2013). Par3 controls neural crest migration by promoting microtubule catastrophe during contact inhibition of locomotion. *Development* **140**, 4763–4775.

Moran, M. F., Koch, C. A., Sadowski, I. and Pawson, T. (1988). Mutational analysis of a phosphotransfer motif essential for v-fps tyrosine kinase activity. *Oncogene* **3**, 665–672.

Moriyoshi, K., Richards, L. J., Akazawa, C., Leary, D. D. M. O. and Nakanishi, S. (1996). Using Adenoviral Gene Transfer of Membrane-Targeted GFP. *Neuron* **16**, 255–260.

Mossie, K., Jallal, B., Alves, F., Sures, I., Plowman, G. D. and Ullrich, A. (1995). Colon carcinoma kinase-4 defines a new subclass of the receptor tyrosine kinase family. *Oncogene* **11**, 2179–2184.

Mullis, K., Faloona, F., Scharf, S., Saiki, R., Horn, G. and Erlich, H. (1986). Specific enzymatic amplification of DNA in vitro: The polymerase chain reaction. *Cold Spring Harb. Symp. Quant Biol* **51**, 263–273.

Na, H.-W., Shin, W.-S., Ludwig, A. and Lee, S.-T. (2012). The cytosolic domain of protein-tyrosine kinase 7 (PTK7), generated from sequential cleavage by a disintegrin and metalloprotease 17 (ADAM17) and γ-secretase, enhances cell proliferation and migration in colon cancer cells. *J. Biol. Chem.* **287**, 25001–25009.

Nakaya, M. A., Habas, R., Biris, K., Dunty, W. C., Kato, Y., He, X. and Yamaguchi, T. P. (2004). Identification and comparative expression analyses of Daam genes in mouse and Xenopus. *Gene Expr. Patterns* **5**, 97–105.

Nguyen, L. K., Kholodenko, B. N. and von Kriegsheim, A. (2016). Rac1 and RhoA:

Networks, loops and bistability. *Small GTPases* **0**, 1–6.

Nieuwkoop, P. D. and Faber, J. (1994). *Normal Table of Xenopus laevis (Daudin)*. New York: Garland Publishing Inc.

Nikolopoulou, E., Galea, G. L., Rolo, A., Greene, N. D. E. and Copp, A. J. (2017). Neural tube closure: cellular, molecular and biomechanical mechanisms. *Development* **144**, 552–566.

Nishita, M., Sa, K. Y., Nomachi, A., Kani, S., Sougawa, N., Ohta, Y., Takada, S., Kikuchi, A. and Minami, Y. (2006). Filopodia formation mediated by receptor tyrosine kinase Ror2 is required for Wnt5a-induced cell migration. *J. Cell Biol.* **175**, 555–562.

Nishita, M., Itsukushima, S., Nomachi, A., Endo, M., Wang, Z., Inaba, D., Qiao, S., Takada, S., Kikuchi, A. and Minami, Y. (2010). Ror2/Frizzled Complex Mediates Wnt5a-Induced AP-1 Activation by Regulating Dishevelled Polymerization. *Mol. Cell. Biol.* **30**, 3610–3619.

Nomachi, A., Nishita, M., Inaba, D., Enomoto, M., Hamasaki, M. and Minami, Y. (2008). Receptor tyrosine kinase Ror2 mediates Wnt5a-induced polarized cell migration by activating c-Jun N-terminal kinase via actin-binding protein filamin A. *J. Biol. Chem.* **283**, 27973–27981.

Ohta, Y., Hartwig, J. H. and Stossel, T. P. (2006). FilGAP, a Rho- and ROCK-regulated GAP for Rac binds filamin A to control actin remodelling. *Nat. Cell Biol.* **8**, 803–814.

Oishi, I., Suzuki, H., Onishi, N., Takada, R., Kani, S., Ohkawara, B., Koshida, I., Suzuki, K., Yamada, G., Schwabe, G. C., et al. (2003). The receptor tyrosine kinase Ror2 is involved in non-canonical Wnt5a/JNK signalling pathway. *Genes to Cells* **8**, 645–654.

Park, S.-K., Lee, H.-S. and Lee, S.-T. (1996). Characterization of the Human Full-Length PTK7 cDNA Encoding a Receptor Protein Tyrosine Kinase-Like Molecule Closely Related to Chick KLG. *J. Biochem.* **119**, 235–239.

Paterson, H. F., Self, A. J., Garrett, M. D., Just, I., Aktories, K. and Hall, A. (1990). Microinjection of recombinant p21rho induces rapid changes in cell morphology. *J Cell Biol* **111**, 1001–1007.

Peng, Y. and Axelrod, J. D. (2012). *Asymmetric Protein Localization in Planar Cell Polarity*. 1st ed. Elsevier Inc.

Peradziryi, H., Kaplan, N. A., Podleschny, M., Liu, X., Wehner, P., Borchers, A. and Tolwinski, N. S. (2011). PTK7/Otk interacts with Wnts and inhibits canonical Wnt signalling. *EMBO J.* **30**, 3729–3740.

Peradziryi, H., Tolwinski, N. S. and Borchers, A. (2012). The many roles of PTK7: a versatile regulator of cell-cell communication. *Arch. Biochem. Biophys.* **524**, 71–76.

Pla, P. and Monsoro-Burq, A. H. (2018). The neural border: Induction, specification and maturation of the territory that generates neural crest cells. *Dev. Biol.* **444**, S36–S46.

Podleschny, M., Grund, A., Berger, H., Rollwitz, E. and Borchers, A. (2015). A PTK7/Ror2 Co-Receptor Complex Affects Xenopus Neural Crest Migration. *PLoS One* **10**, e0145169.

Pollard, T. D. (2017). What We Know and Do Not Know About Actin. *Handb Exp Pharmacol* **235**, 331–347.

Pollard, T. D. and Borisy, G. G. (2003). Cellular motility driven by assembly and disassembly of actin filaments. *Cell* **112**, 453–465.

Prasad, M. S., Charney, R. M. and García-Castro, M. I. (2019). Specification and formation of the neural crest: Perspectives on lineage segregation. *Genesis* **57**, e23276.

Pukrop, T., Gradl, D., Henningfeld, K. A., Knöchel, W., Wedlich, D. and Kühl, M. (2001). Identification of Two Regulatory Elements within the High Mobility Group Box Transcription Factor XTCF-4. *J. Biol. Chem.*

Pulido, D., Campuzano, S., Koda, T., Modolell, J. and Barbacid, M. (1992). Dtrk, a Drosophila gene related to the trk family of neurotrophin receptors, encodes a novel class of neural cell adhesion molecule. *EMBO J.* **11**, 391–404.

Puppo, F., Thomé, V., Lhoumeau, A.-C., Cibois, M., Gangar, A., Lembo, F., Belotti, E., Marchetto, S., Lécine, P., Prébet, T., et al. (2011). Protein tyrosine kinase 7 has a conserved role in Wnt/β-catenin canonical signalling. *EMBO Rep.* **12**, 43–49.

Rabadán, M. A., Herrera, A., Fanlo, L., Usieto, S., Carmona-Fontaine, C., Barriga, E. H., Mayor, R., Pons, S. and Martí, E. (2016). Delamination of neural crest cells requires transient and reversible Wnt inhibition mediated by DACT1/2. *Development* **143**, 2194–2205.

Ren, X.-D., Kiosses, W. B. and Schwartz, M. A. (1999). Regulation of the small GTP-binding protein Rho.pdf. *EMBO J.* **18**, 578–585.

Ridley, A. J., Schwartz, M. a, Burridge, K., Firtel, R. a, Ginsberg, M. H., Borisy, G., Parsons, J. T. and Horwitz, A. R. (2003). Cell migration: integrating signals from front to back. *Science (80-.).* **302**, 1704–1709.

Riedl, J., Crevenna, A. H., Kessenbrock, K., Yu, J. H., Neukirchen, D., Bista, M., Bradke, F., Jenne, D., Holak, T. A., Werb, Z., et al. (2008). Lifeact: a versatile marker to visualize F-actin. *Nat. Methods* **5**, 605–7.

Roose, J., Molenaar, M., Peterson, J., Hurenkamp, J., Brantjes, H., Moerer, P., Van De Wetering, M., Destrée, O. and Clevers, H. (1998). The Xenopus Wnt effector XTcf-3 interacts with Groucho-related transcriptional repressors. *Nature* **395**, 608–

612.

Rothbächer, U., Laurent, M. N., Deardorff, M. A., Klein, P. S., Cho, K. W. and Fraser, S. E. (2000). Dishevelled phosphorylation, subcellular localization and multimerization regulate its role in early embryogenesis. *EMBO J.* **19**, 1010–1022.

Rouiller, I., Xu, X.-P., Amann, K. J., Egile, C., Nickell, S., Nicastro, D., Li, R., Pollard, T. D., Volkmann, N. and Hanein, D. (2008). The structural basis of actin filament branching by the Arp2/3 complex. *J. Cell Biol.* **180**, 887–895.

Rupp, R. A. Wx. embryos regulate the nuclear localization of Xm., Snider, L. and Weintraub, H. (1994). Xenopus embryos regulate the nuclear localization of XMyoD. *Genes Dev.* **8**, 1311–1323.

Russell, D. W. and Sambrook, J. (2001). *Molecular cloning: A laboratory manual*.

Saha, S., Bardelli, A., Buckhaults, P., Velculescu, V. E., Rago, C., St. Croix, B., Romans, K. E., Choti, M. A., Lengauer, C., Kinzler, K. W., et al. (2001). A phosphatase associated with metastasis of colorectal cancer. *Science (80-.).* **294**, 1343–1346.

Sato, A., Khadka, D. K., Liu, W., Bharti, R., Runnels, L. W., Dawid, I. B. and Habas, R. (2006). Profilin is an effector for Daam1 in non-canonical Wnt signaling and is required for vertebrate gastrulation. *Development* **133**, 4219–4231.

Sauka-Spengler, T. and Bronner-Fraser, M. (2008). A gene regulatory network orchestrates neural crest formation. *Nat. Rev. Mol. Cell Biol.* **9**, 557–568.

Scarpa, E., Szabó, A., Bibonne, A., Theveneau, E., Parsons, M. and Mayor, R. (2015). Cadherin Switch during EMT in Neural Crest Cells Leads to Contact Inhibition of Locomotion via Repolarization of Forces. *Dev. Cell* **34**, 421–434.

Schambony, A. and Wedlich, D. (2007). Wnt-5A/Ror2 Regulate Expression of XPAPC through an Alternative Noncanonical Signaling Pathway. *Dev. Cell* **12**, 779–792.

Schille, C., Bayerlová, M., Bleckmann, A. and Schambony, A. (2016). Ror2 signaling is required for local upregulation of GDF6 and activation of BMP signaling at the neural plate border. *Development* **143**, 3182–3194.

Schindelin, J., Arganda-Carreras, I., Frise, E., Kaynig, V., Longair, M., Pietzsch, T., Preibisch, S., Rueden, C., Saalfeld, S., Schmid, B., et al. (2012). Fiji: An open-source platform for biological-image analysis. *Nat. Methods* **9**, 676–682.

Schmidt, S. and Debant, A. (2014). Function and regulation of the Rho guanine nucleotide exchange factor Trio. *Small GTPases* **5**, e29769.

Schneider, C. A., Rasband, W. S. and Eliceiri, K. W. (2012). NIH Image to ImageJ: 25 years of image analysis. *Nat. Methods* **9**, 671–675.

Schwartz, M. A., Meredith, J. E. and Kiosses, W. B. (1998). An activated Rac mutant functions as a dominant negative for membrane ruffling. *Oncogene* **17**, 625–629.

Schwarz-Romond, T., Fiedler, M., Shibata, N., Butler, P. J. G., Kikuchi, A., Higuchi, Y. and Bienz, M. (2007). The DIX domain of Dishevelled confers Wnt signaling by dynamic polymerization. *Nat. Struct. Mol. Biol.* **14**, 484–492.

Seipel, K., Medley, Q. G., Kedersha, N. L., Zhang, X. A., O'Brien, S. P., Serra-Pages, C., Hemler, M. E. and Streuli, M. (1999). Trio amino-terminal guanine nucleotide exchange factor domain expression promotes actin cytoskeleton reorganization, cell migration and anchorage-independent cell growth. *J. Cell Sci.* **112**, 1825–34.

Sellers, J. R. (1991). Regulation of cytoplasmic and smooth muscle myosin. *Curr. Opin. Cell Biol.* **3**, 98–104.

Serra-Pagès, C., Kedersha, N. L., Fazikas, L., Medley, Q., Debant, a and Streuli, M. (1995). The LAR transmembrane protein tyrosine phosphatase and a coiled-coil LAR-interacting protein co-localize at focal adhesions. *EMBO J.* **14**, 2827–2838.

Sharma, M., Castro-Piedras, I., Simmons, G. E. and Pruitt, K. (2018). Dishevelled: A masterful conductor of complex Wnt signals. *Cell. Signal.* **47**, 52–64.

Shellard, A. and Mayor, R. (2019). Integrating chemical and mechanical signals in neural crest cell migration. *Curr. Opin. Genet. Dev.* **57**, 16–24.

Shellard, A., Trepat, X. and Mayor, R. (2018). Supracellular contraction at the rear of cell groups drives collective chemotaxis. *Science (80-.).* **362**, 339–343.

Shestopalov, I. A., Sinha, S. and Chen, J. K. (2007). Light-controlled gene silencing in zebrafish embryos. *Nat. Chem. Biol.* **3**, 650.

Shin, W.-S., Kwon, J., Lee, H. W., Kang, M. C., Na, H.-W., Lee, S.-T. and Park, J. H. (2013). Oncogenic role of protein tyrosine kinase 7 in esophageal squamous cell carcinoma. *Cancer Sci.* **104**, 1120–1126.

Shnitsar, I. (2009). The function of PTK7 during Xenopus neural crest migration.

Shnitsar, I. and Borchers, A. (2008). PTK7 recruits dsh to regulate neural crest migration. *Development* **135**, 4015–4024.

Shyamala, K., Yanduri, S., Girish, H. and Murgod, S. (2015). Neural crest: The fourth germ layer. *J. Oral Maxillofac. Pathol.* **19**, 221–229.

Sive, H. L., Grainger, R. M. and Harland, R. M. (2000). *Early Development of Xenopus laevis. A Laboratory Manual.*

Skruber, K., Read, T.-A. and Vitriol, E. A. (2018). Reconsidering an active role for G-actin in cytoskeletal regulation. *J. Cell Sci.* **131**, jcs203760.

Smith, W. C. and Harland, R. M. (1991). Injected Xwnt-8 RNA acts early in Xenopus embryos to promote formation of a vegetal dorsalizing center. *Cell* **67**, 753–765.

Sokol, S. Y. (1996). Analysis of Dishevelled signalling pathways during Xenopus development. *Curr. Biol.* **6**, 1456–1467.

Steinhart, Z. and Angers, S. (2018). Wnt signaling in development and tissue

homeostasis. *Development* **145**, dev146589.

Stramer, B. and Mayor, R. (2017). Mechanisms and in vivo functions of contact inhibition of locomotion. *Nat. Rev. Mol. Cell Biol.* **18**, 43–55.

Stricker, S., Rauschenberger, V. and Schambony, A. (2017). *ROR-Family Receptor Tyrosine Kinases*. 1st ed. Elsevier Inc.

Struhl, G., Casal, J. and Lawrence, P. A. (2012). Dissecting the molecular bridges that mediate the function of Frizzled in planar cell polarity. *Development* **139**, 3665–3674.

Strutt, D. I. (2001). Asymmetric localization of frizzled and the establishment of cell polarity in the Drosophila wing. *Mol. Cell* **7**, 367–375.

Strutt, H. and Strutt, D. (2008). Differential Stability of Flamingo Protein Complexes Underlies the Establishment of Planar Polarity. *Curr. Biol.* **18**, 1555–1564.

Stuhlmiller, T. J. and García-Castro, M. I. (2012). Current perspectives of the signaling pathways directing neural crest induction. *Cell. Mol. Life Sci.* **69**, 3715–3737.

Suzuki, T., Fujikura, K., Higashiyama, T. and Takata, K. (1997). DNA staining for fluorescence and laser confocal microscopy. *J. Histochem. Cytochem.* **45**, 49–53.

Szabó, A. and Mayor, R. (2018). Mechanisms of neural crest migration. *Annu. Rev. Genet.* **52**, 43–63.

Tamai, K., Zeng, X., Liu, C., Zhang, X., Harada, Y., Chang, Z. and He, X. (2004). A Mechanism for Wnt Coreceptor Activation. *Mol. Cell* **13**, 149–156.

Taneyhill, L. A. and Schiffmacher, A. T. (2017). Should I stay or should I go? Cadherin function and regulation in the neural crest. *Genesis* **55**, 1–21.

Tauriello, D. V. F., Jordens, I., Kirchner, K., Slootstra, J. W., Kruitwagen, T., Bouwman, B. A. M., Noutsou, M., Rudiger, S. G. D., Schwamborn, K., Schambony, A., et al. (2012). Wnt/β-catenin signaling requires interaction of the Dishevelled DEP domain and C terminus with a discontinuous motif in Frizzled. *Proc. Natl. Acad. Sci.* **109**, E812–E820.

Theveneau, E. and Mayor, R. (2012a). Neural crest migration: interplay between chemorepellents, chemoattractants, contact inhibition, epithelial-mesenchymal transition, and collective cell migration. *Wiley Interdiscip. Rev. Dev. Biol.* **1**, 435–445.

Theveneau, E. and Mayor, R. (2012b). Neural crest delamination and migration: from epithelium-to-mesenchyme transition to collective cell migration. *Dev. Biol.* **366**, 34–54.

Theveneau, E., Marchant, L., Kuriyama, S., Gull, M., Moepps, B., Parsons, M. and Mayor, R. (2010). Collective chemotaxis requires contact-dependent cell polarity. *Dev. Cell* **19**, 39–53.

Tortelote, G. G., Reis, R. R., de Almeida Mendes, F. and Abreu, J. G. (2017). Complexity of the Wnt/β‐catenin pathway: Searching for an activation model. *Cell. Signal.* **40**, 30–43.

Totsukawa, G., Yamakita, Y., Yamashiro, S., Hartshorne, D. J., Sasaki, Y. and Matsumura, F. (2000). Distinct roles of ROCK (Rho-kinase) and MLCK in spatial regulation of MLC phosphorylation for assembly of stress fibers and focal adhesions in 3T3 fibroblasts. *J. Cell Biol.* **150**, 797–806.

Towbin, H., Staehelin, T. and Gordon, J. (1979). Electrophoretic transfer of proteins from polyacrylamide gels to nitrocellulose sheets: procedure and some applications. *Proc. Natl. Acad. Sci.* **76**, 4350–4354.

Tree, D. R. P., Shulman, J. M., Rousset, R., Scott, M. P., Gubb, D. and Axelrod, J. D. (2002). Prickle mediates feedback amplification to generate asymmetric planar cell polarity signaling. *Cell* **109**, 371–381.

Turner, D. L. and Weintraub, H. (1994). Expression of achaete-scute homolog 3 in Xenopus embryos converts ectodermal cells to a neural fate. *Genes Dev.* **8**, 1434–1447.

Unterseher, F., Hefele, J. A., Giehl, K., De Robertis, E. M., Wedlich, D. and Schambony, A. (2004). Paraxial protocadherin coordinates cell polarity during convergent extension via Rho A and JNK. *EMBO J.* **23**, 3259–69.

Usui, T., Shima, Y., Shimada, Y., Hirano, S., Burgess, R. W., Schwarz, T. L., Takeichi, M. and Uemura, T. (1999). Flamingo, a seven-pass transmembrane cadherin, regulates planar cell polarity under the control of Frizzled. *Cell* **98**, 585–595.

van Rijssel, J. and van Buul, J. D. (2012). The many faces of the guanine-nucleotide exchange factor trio. *Cell Adhes. Migr.* **6**, 482–487.

Vidali, L., Chen, F., Cicchetti, G., Ohta, Y. and J., K. D. (2006). Rac1-null Mouse Embryonic Fibroblasts Are Motile and Respond to Platelet-derived Growth Factor. *Mol. Biol. Cell* **17**, 2377–2390.

Vincente-Manzanares, M., Ma, X., Adelstein, R. S. and Horwitz, A. R. (2009). Non-muscle myosin II takes centre stage in cell adhesion and migration. *Nat Rev Mol Cell Biol.* **10**, 778–790.

Wallingford, J. B. (2012). Planar cell polarity and the developmental control of cell behavior in vertebrate embryos. *Annu. Rev. Cell Dev. Biol.* **28**, 627–653.

Wallingford, J. B. and Habas, R. (2005). The developmental biology of Dishevelled: an enigmatic protein governing cell fate and cell polarity. *Development* **132**, 4421–4436.

Wallingford, J. B., Rowning, B. A., Vogeli, K. M., Rothbächer, U., Fraser, S. E. and

Harland, R. M. (2000). Dishevelled controls cell polarity during Xenopus gastrulation. *Nature* **405**, 81–85.

Wang, Y.-M., Wu, Z., Liu, S.-J. and Chu, X. (2015a). Structure-Switching Aptamer Triggering Hybridization Chain Reaction on the Cell Surface for Activatable Theranostics. *Anal. Chem.* **87**, 6470–6474.

Wang, M., De Marco, P., Merello, E., Drapeau, P., Capra, V. and Kibar, Z. (2015b). Role of the Planar Cell Polarity Gene Protein Tyrosine Kinase 7 in Neural Tube Defects in Humans. *Birth Defects Res A Clin Mol Teratol* **103**, 1021–1027.

Wang, L., Xiao, Y., Tian, T., Jin, L., Lei, Y., Finnell, R. H. and Ren, A. (2018). Digenic variants of planar cell polarity genes in human neural tube defect patients. *Mol. Genet. Metab.*

Watanabe, N., Madaule, P., Reid, T., Ishizaki, T., Watanabe, G., Kakizuka, A., Saito, Y., Nakao, K., Jockusch, B. M. and Narumiya, S. (1997). p140mDia, a mammalian homolog of Drosophila diaphanous, is a target protein for Rho small GTPase and is a ligand for profilin. *EMBO J.* **16**, 3044–3056.

Wehner, P., Shnitsar, I., Urlaub, H. and Borchers, A. (2011). RACK1 is a novel interaction partner of PTK7 that is required for neural tube closure. *Development* **138**, 1321–1327.

Williams, M., Yen, W., Lu, X. and Sutherland, A. (2014). Distinct apical and basolateral mechanisms drive planar cell polarity-dependent convergent extension of the mouse neural plate. *Dev. Cell* **29**, 34–46.

Winberg, M. L., Tamagnone, L., Bai, J., Comoglio, P. M., Montell, D. and Goodman, C. S. (2001). The transmembrane protein off-track associates with plexins and functions downstream of semaphorin signaling during axon guidance. *Neuron* **32**, 53–62.

Winning, R. S., Shea, L. J., Marcus, S. J. and Sargent, T. D. (1991). Developmental regulation of transcription factor AP-2 during Xenopus laevis embryogenesis. *Nucleic Acids Res.* **19**, 3709–3714.

Winston, J. T., Strack, P., Beer-Romero, P., Chu, C. Y., Elledge, S. J. and Harper, J. W. (1999). The SCFbeta-TRCP-ubiquitin ligase complex associates specifically with phosphorylated destruction motifs in Ikappa B alpha and beta-catenin and stimulates Ikappa Balpha ubiquitination in vitro. *Genes Dev.* **13**, 270–283.

Witte, F., Bernatik, O., Kirchner, K., Masek, J., Mahl, A., Krejci, P., Mundlos, S., Schambony, A., Bryja, V. and Stricker, S. (2010). Negative regulation of Wnt signaling mediated by CK1-phosphorylated Dishevelled via Ror2. *FASEB J.* **24**, 2417–26.

Wong, H.-C., Bourdelas, A., Krauss, A., Lee, H.-J., Shao, Y., Wu, D., Mlodzik, M.,

Shi, D.-L. and Zheng, J. (2003). Direct Binding of the PDZ Domain of Dishevelled to a Conserved Internal Sequence in the C-Terminal Region of Frizzled. *Mol. Cell* **12**, 1251–1260.

Wu, J. and Mlodzik, M. (2008). The Frizzled Extracellular Domain Is a Ligand for Van Gogh/Stbm during Nonautonomous Planar Cell Polarity Signaling. *Dev. Cell* **15**, 462–469.

Wu, Y. I., Frey, D., Lungu, O. I., Jaehrig, A., Schlichting, I., Kuhlman, B. and Hahn, K. M. (2009). A genetically encoded photoactivatable Rac controls the motility of living cells. *Nature* **461**, 104–108.

Wu, X., Yan, T., Hao, L. and Zhu, Y. (2019). Wnt5a induces ROR1 and ROR2 to activate RhoA in esophageal squamous cell carcinoma cells. *Cancer Manag. Res.* **11**, 2803–2815.

Xu, B., Santos, S. A. A. and Hinton, B. T. (2018). Protein tyrosine kinase 7 regulates extracellular matrix integrity and mesenchymal intracellular RAC1 and myosin II activities during Wolffian duct morphogenesis. *Dev. Biol.* **438**, 33–43.

Yamamoto, H., Yoo, S. K., Nishita, M., Kikuchi, A. and Minami, Y. (2007). Wnt5a modulates glycogen synthase kinase 3 to induce phosphorylation of receptor tyrosine kinase Ror2. *Genes to Cells* **12**, 1215–1223.

Yamanaka, H., Moriguchi, T., Masuyama, N., Kusakabe, M., Hanafusa, H., Takada, R., Takada, S. and Nishida, E. (2002). JNK functions in the non-canonical Wnt pathway to regulate convergent extension movements in vertebrates. *EMBO Rep.* **3**, 69–75.

Yanagawa, S. I., Van Leeuwen, F., Wodarz, A., Klingensmith, J. and Nusse, R. (1995). The dishevelled protein is modified by wingless signaling in Drosophila. *Genes Dev.* **9**, 1087–1095.

Yang, Y. and Mlodzik, M. (2015). Wnt-Frizzled/Planar Cell Polarity Signaling: Cellular Orientation by Facing the Wind (Wnt). *Annu. Rev. Cell Dev. Biol.* **31**, 623–646.

Zeng, X., Tamai, K., Doble, B., Li, S., Huang, H., Habas, R., Okamura, H., Woodgett, J. and He, X. (2005). A dual-kinase mechanism for Wnt co-receptor phosphorylation and activation. *Nature* **438**, 873–877.

Zeng, X., Huang, H., Tamai, K., Zhang, X., Harada, Y., Yokota, C., Almeida, K., Wang, J., Doble, B., Woodgett, J., et al. (2008). Initiation of Wnt signaling: control of Wnt coreceptor Lrp6 phosphorylation/activation via frizzled, dishevelled and axin functions. *Development* **135**, 367–375.

Zenke, F. T., Krendel, M., DerMardirossian, C., King, C. C., Bohl, B. P. and Bokoch, G. M. (2004). p21-activated Kinase 1 Phosphorylates and Regulates 14-3-3 Binding to GEF-H1, a Microtubule-localized Rho Exchange Factor. *J. Biol. Chem.* **279**,

18392–18400.

Danksagung

An dieser Stelle möchte ich mich bei allen bedanken, die mich während meiner Doktorzeit unterstützt haben.

Zunächst möchte ich mich bei Prof. Dr. Annette Borchers für die Aufnahme in ihrer Arbeitsgruppe bedanken. Besonders bedanken möchte ich mich dabei für die Betreuung und Beratung während dieser Zeit.

Ebenfalls möchte ich mich bedanken bei Prof. Dr. Ralf Jacob, für die Bereitschaft das Zweitgutachten zu übernehmen, und bei Prof. Dr. Monika Hassel und Prof. Dr. Christian Helker, für die freundliche Einwilligung Mitglieder meiner Prüfungskommission zu sein.

Großen Dank gilt auch den jetzigen und ehemaligen Mitgliedern der AG Borchers, Barbara, Ingrid, Melanie und Christiane. Aber besonders möchte ich mich bei Hanna, Marlen, Janina, Elisabeth und Marie für die guten Ratschläge und Hilfe und vor allem für die Zeit im und außerhalb des Labors bedanken.

Danke auch an Prof. Dr. Klaudia Giehl und Marisa Heipel für die Hilfe und Anmerkungen bei den GTPase assays.

Zuletzt möchte ich mich noch bei meiner Familie insbesondere bei meiner Mutter und meiner Schwester für ihre Unterstützung, Geduld und Verständnis während dieser Zeit bedanken.

Lebenslauf

Die Seite 95 (Lebenslauf) enthalten persönliche Daten. Sie sind deshalb nicht Bestandteil der Online-Veröffentlichung.

Erklärung

Hiermit versichere ich, dass ich die Dissertation „PTK7 signaling complexes in neural crest cell migration“ selbstständig verfasst und keine anderen als die angegebenen Hilfsmittel genutzt habe.
Die Dissertation wurde in der jetzigen oder einer ähnlichen Form noch bei keiner anderen Hochschule eingereicht und hat noch keinen sonstigen Prüfungszwecken gedient.

Marburg, den 09.08.2019 _____

Anita Grund